Numerical Investigation of Thermal Energy Storage (TES) System for Low and High-Temperature Applications

By

Tewodros Ayenew Esckemech

Office of Graduate Studies

Adama Science and Technology University

July, 2020

Adama, Ethiopia

Numerical Investigation of Thermal Energy Storage (TES) System for Low and High-Temperature Applications

By

Tewodros Ayenew Esckemech

Advisor: Dr. Dawit Gudeta (Assistant Professor)

A Thesis Submitted to Department of Thermal and Aerospace Engineering

School of Mechanical, Chemical and Materials Engineering

Office of Graduate Studies

Adama Science and Technology University

July, 2020

Adama, Ethiopia

DECLARATION

I hereby declare that this M.Sc. thesis titled "**Numerical Investigation of Thermal Energy Storage (TES) System for Low and High-Temperature Applications**" is my authentic work and that all sources of materials used for this thesis have been duly acknowledged. This thesis has been submitted in partial fulfillment of the requirements of the degree of Master of Science in Thermal Engineering under the supervision and guidance of Dr. Dawit Gudeta, Assistant Professor of Thermal and Aerospace Engineering at Adama Science and Technology University.

I solemnly declare that this thesis is not submitted to any other institution anywhere for the award of any academic degree, diploma, or certificate. All relevant resource information used in this paper has been properly admitted.

Tewodros Ayenew	______________________	__________________
Candidate	Signature	Date

This is to certify that the above statement made by the candidate is correct to the best of my knowledge and belief. This thesis has been submitted for examination with my approval.

Dr. Dawit Gudeta	____________________	_________________
Advisor	Signature	Date

APPROVAL PAGE

We, the undersigned members of the Board of Examiners of the final open defense by Tewodros Ayenew Esckemech have read and evaluated his thesis entitled *"***Numerical Investigation of Thermal Energy Storage (TES) System for Low and High-Temperature Applications***"* and examined the candidate. Therefore, this is to certify that the thesis has been accepted in partial fulfillment of the requirement of the Degree of Masters of Science in Thermal Engineering.

Name	Signature	Date
______________________	______________________	____________________
Name of Student		
______________________	______________________	____________________
Advisor		
______________________	______________________	____________________
External Examiner		
______________________	______________________	____________________
Internal Examiner		
______________________	______________________	____________________
Chairperson		
______________________	______________________	____________________
Head of Department		
______________________	______________________	____________________
School Dean		
______________________	______________________	____________________
Post graduate Dean		

Dedicated

To

People Who Died by COVID-19 Pandemic

# ACKNOWLEDGMENT

First and foremost, I praise the almighty God for his grace to do this work, blessings, wisdom, protection, and help me throughout my life. Then, I would like to express my sincere gratitude to Dr. Dawit Gudeta, the thesis advisor, for his unlimited support, encouragement, constructive comment, and unreserved guidance on the critical issues of the study. I would like to thank Dr. Addisu Bekele for sharing his academic experience, knowledge and he has been an enormous resource to me in all aspects of my academic life during my master's study. Heartfelt thanks also go to my friends for their willingness in providing and supporting me financially and their encouragement and constructive suggestion on the subject matter of the study.

I extend my deep gratitude to my best friend Seyoum Getachew for his willingness in providing and supporting me financially to accomplish this study. Without him I would have never been able to achieve my dream and thanks for his support, always backing me up.

Finally, I must express my very profound gratitude to my parents for providing me with unfailing support, continuous encouragement and all my ways have been prosperous by their prayer and support.

ABSTRACT

Energy is the pillar of all day to day human activity in the world and it is a dominant factor in a country's economy. Fossil fuels have served and fulfilled all human energy needs for a long era, but fossil fuels price is increased. Among several energy sources, solar energy has been identified to take the role of fossil fuels. However, the intermittent and fluctuating nature of solar radiation has been the main obstacle for the development and promotion of this renewable energy source. Integrating Thermal Energy Storage (TES) system in any solar thermal application has become the main solution to tackle the above-mentioned issue. TES system is a temporary storing of thermal energy in the form of hot or cold substance at low or high-temperatures for later utilization of the harvested solar energy. The aim of this study is to store (7) and (15) MJ amount of heat energy by investigating the performance analysis of the solar TES system for low and high-temperature applications. 3-D Multiphysics TES model is developed to investigate transient conjugate heat transfer between the HTF and the storage material. During the investigation paraffin wax and concrete are used as a storage material for low and high-temperature TES models, respectively. The governing equations involved in the developed model are solved by the help of COMSOL Multiphysics 4.3a commercial software. In addition to the major objective optimization of the number of HTF tubes and heat transfer, an enhancement technique is also applied in this study. A 2D TES model is developed to optimize the number of HTF tubes, the performance is compared by varying number of charging/discharging tubes (13, 17, 21, 25, and 29) and finally, 21 and 25 tubes are found to be in the configuration for both models. Based on the results obtained, a 9.8 and 15.06 MJ of heat energy is stored to fulfill the energy demand of 66 L hot water per day at 50 ℃ and produce saturated steams at steam power plant, respectively. Hence, the developed TES model has achieved the required amount of heat energy for low and high-temperature applications. Numerical investigations for intermediate temperature application could be recommended in future work.

KEY WORDS: Thermal energy storage, Solar energy, Optimization, Heat transfer fluid, Low-temperature application, High-temperature application.

TABLE OF CONTENTS

Contents **Page**

TABLE OF FIGURES

Figure **Page**

LIST OF TABLES

Table **Page**

NOMENCLATURE

A_{mush}	: Mushy zone constant
C_p	: Specific heat capacity at constant pressure (kJ/kgK)
$\vec{F}$	: Body force (N/m^3)
g	: Acceleration due to gravity (m/s^2)
H	: Enthalpy (kJ/kg)
I_B	: Daily beam solar radiation (kJ/m^{2}day)
I_B^*	: Hourly beam solar radiation (kJ/m^{2}hr.)
I_D	: Daily diffuse solar radiation (kJ/m^{2}day)
I_D^*	: Hourly diffuse solar radiation (kJ/m^{2}hr.)
I_G	: Daily global solar radiation (kJ/m^{2}day)
I_G^*	: Hourly global solar radiation (kJ/m^{2}hr.)
I_o	: Extraterrestrial solar radiation (W/m^2)
I_{SC}	: Solar constant (W/m^2)
k_f	: Thermal conductivity of the heat transfer fluid (W/mK)
k_s	: Thermal conductivity of the storage material (W/mK)
L	: Length of the storage bed (m)
L_F	: Latent heat of fusion (kJ/kg)
m	: Mass of the storage (kg)
N_H	: Day time duration (hr.)
$Q_{S,C}$	: Sensible energy stored (MJ)
$Q_{L,C}$	: Sensible energy stored (MJ)
$Q_{T,C}$	: Total energy stored (MJ)
Q_u	: Useful heat gain (W)
R_B	: Beam radiation factor
S	: Solar radiation heat flux (W/m^2)
$\vec{S}$	: Darcy law's source term (N/m^3)
T	: Temperature (K)
T_m	: Melting temperature (K)
T_{m1}	: Solidus temperature (K)

T_{m2}	: Liquids temperature (K)
t	: Time (s)
V_s	: Volume of the storage (m^3)
$\vec{v}$	: Velocity of the fluid (m/s)

GREEK SYMBOLS

ρ	: Density (kg/m^3)	Δ	: Change
ω	: Hour angle (°)	∇	: Gradient operator
μ	: Viscosity ($N.s/m^2$)	δ	: Declination angle (°)
ϕ	: Latitude angle (°)	β_a	: Surface slope angle (°)
λ	: Liquid fraction	η	: Efficiency (%)
ϵ	: Epsilon variant	β	: Thermal expansion (1/K)

ABBREVIATIONS

CFD	: Computational Fluid Dynamics
CSP	: Concentrated Solar Power
DSG	: Direct steam generation
FEM	: Finite element method
FPC	: Flat plate collector
HTF	: Heat Transfer Fluid
LHS	: Latent Heat Storage
LHTES	: Latent heat thermal energy storage
NGO	: Non-governmental organization
PCM	: Phase Change Material
PTC	: Parabolic Trough Collector
SHS	: Sensible Heat Storage
SHTES	: Sensible heat thermal energy storage
TES	: Thermal Energy Storage

CHAPTER ONE

INTRODUCTION

This chapter explains the general background, statement of the problem, objectives, significance, scope, and limitation of the present study. The general concept of TES systems and organization of the study is also included in this chapter, and then each section will be briefly illustrated below.

1.1 Background of the study

Energy is the pillar of all day to day human activity in the world and it is a dominant factor in a country's economy. Nowadays, energy demand has been increased due to the high energy consumption in different areas such as; household, transportation, industry, electricity generation, etc. This energy demand is expected to rise by approximately 1.5-3 times in the world by 2050 **(Dinçer & Zamfirescu, 2012)**. Fossil fuels have served and fulfilled all human energy needs for a long era, but the price of fossil fuels is increased in recent years and it is expected to continue increasing in the future; because energy demand is increasing while fossil fuels in reserves are decreasing. This is the main difficulty across the world especially for developing countries like Ethiopia.

A developing country especially in most parts of Africa, energy facility is characterized by highly dependence on traditional biomass fuels because of poor energy infrastructure. Many researches concerned about 2.5 billion people in developing countries dependent on biomass energy sources at the present, such as fuel wood, charcoal, agricultural waste, and animal dung, to meet their domestic energy demands. Similarly, forecast more than 2.7 billion people will still depend on these traditional fuels by 2030 **(Kaygusuz, 2012)**. Biomass is the fourth largest energy source in the world and the first in developing countries. It representing 14% and 35%, respectively of primary energy, from which 80% of this is consumed as firewood, mainly in the rural household **(Hall *et al.,* 1992)**. Take an example Ethiopia is the third largest user of traditional fuels in the world with 91 % of the population dependent on traditional biomass like fuel wood and dung to meet household energy demand. The remaining energy supply was petroleum about 7% of total primary energy and electricity accounts for only 2% of total energy use (**Mondal *et al.,* 2018**)**.** Most power production industries also currently consume conventional fuels and generally almost 80% of global energy consumption from conventional energy sources **(Mekhilef *et al.*, 2011)**. The rapid utilization of fossil fuels also another problem in this day because; highly increase in the emission of pollutant gases from the burning of those fuels is leads to a health problem. Consequently, the world was currently towards another alternative means of getting their energy demand. Therefore, renewable energies such as; solar energy, hydropower, wind energy, geothermal energy, and tidal energy are expected to play the major role for energy supply soon and those energies must be developed to take the role of fossil fuels. From those renewable energies, solar energy is clean and the most available renewable source of energy and it is the origin of all known forms of energy. According to the international energy agency it has estimated that solar power will produce 21% of the world's electricity by 2050 **(Al-Maghalseh, 2014)**.

For example, Ethiopia has a great potential for solar energy as it receives solar irradiation of 5-7 kWh/m^2 depending on the location and the season. The values vary with the seasons, ranging from 4.55 to 5.55 kWh/m^2/day, and over space ranging from 4.25 kWh/m^2/day in the extreme Western lowlands to 6.25 kWh/m^2/day in Adigrat area and generally received averages of 5.2 kWh/m^2/day solar radiation in Ethiopia **(Khan & Singh, 2017)**. Nevertheless, solar energy systems can operate only for a few hours during sunshine hours in summer days and much fewer hours during winter/rainy days and cannot operate at night time. So, there is an obstacle for the development and promotion of solar energy, due to the intermittent and fluctuating nature of solar radiation. To tackle this problem design of a robust Thermal Energy Storage (TES) system is mandatory for efficiently utilized the harvested solar energy during the absence of solar radiation. There is a limitation also happen in the present TES system regarding to the time taken to completely charge the system. Hence, the present study enhances the heat transfer rate to reduce the charging time.

1.2 Concept of thermal energy storage (TES) systems

Thermal energy storage (TES) can be defined as the temporary storing of thermal energy in the form of hot or cold substance at high or low temperatures for later utilization. The thermal energy storage (TES) system is considered the most important and advanced energy technologies in recent times for efficiently utilized the harvested solar energy. Which stores energy by cooling, heating, melting, solidifying, or vaporizing a storage material, and then the stored energy can be used during the absence of solar radiation. TES system recently, increasing attention has been paid to the utilization of this essential for cooling, heating, and power generation applications. It is a very important technology applied in many engineering applications **(Hasnain, 1998a)**. For example, among the practical problems involved in solar energy systems is the need for an effective means of excess heat collected during periods of bright sunshine duration. Then it can be stored, preserved, and later released for utilization during the night or other periods by integrated TES system. Similar problems arise from the production of power by solar energy in concentrated solar power (CSP) plants due to the discontinuous flow of solar energy. Thermal energy storage can also be applied in most types of buildings where heating needs are significant and domestic water heating application allows heat storage to be competitive with other forms of heating.

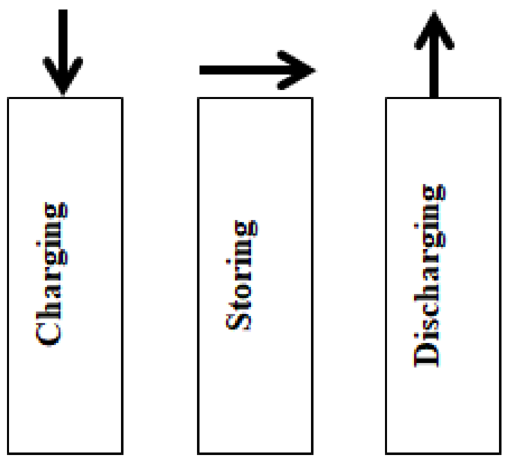

Fig.1.1 General processes of TES systems

The technology of thermal energy storage has been developed to a point where it can have a significant effect on modern life. With the advent of the industrial revolution, thermal energy storage introduced as a by-product of energy production. Heat storage at power plants is typically in the form of steam or hot water. Other materials such as oils having a very high boiling point have been suggested as heat storage substances for cooking utilities in recent time. Similarly, materials that have a high heat of fusion at high temperatures have also been suggested for this application **(Hasnain, 1998a)**. Generally, for solar heated applications, thermal energy storage is the most promising technology in this day, and there is various storage materials that has used for this technology. Fig.1.1 illustrated the basic process for the thermal energy storage (TES) system which is charging, storing, and discharging process. Most of the researchers agreed, there are three main categories of thermal energy storage systems as shown in Fig.1.2, based on their storing mechanism of thermal energy. These are sensible heat thermal energy storage systems, latent heat thermal energy storage systems, and thermochemical thermal energy storage systems. Sensible thermal energy storage systems are stored heat energy by raising the temperature of a solid or liquid using the heat capacity and the change in temperature of the material during the process of charging and discharging. The amount of stored energy depends on the specific heat of the medium, the amount of storage material, and the temperature change. The other TES system that uses in a various solar thermal application is the latent heat thermal energy storage system (LHTES) which is the amount of heat absorbed or released during the phase change of the material (latent heat).

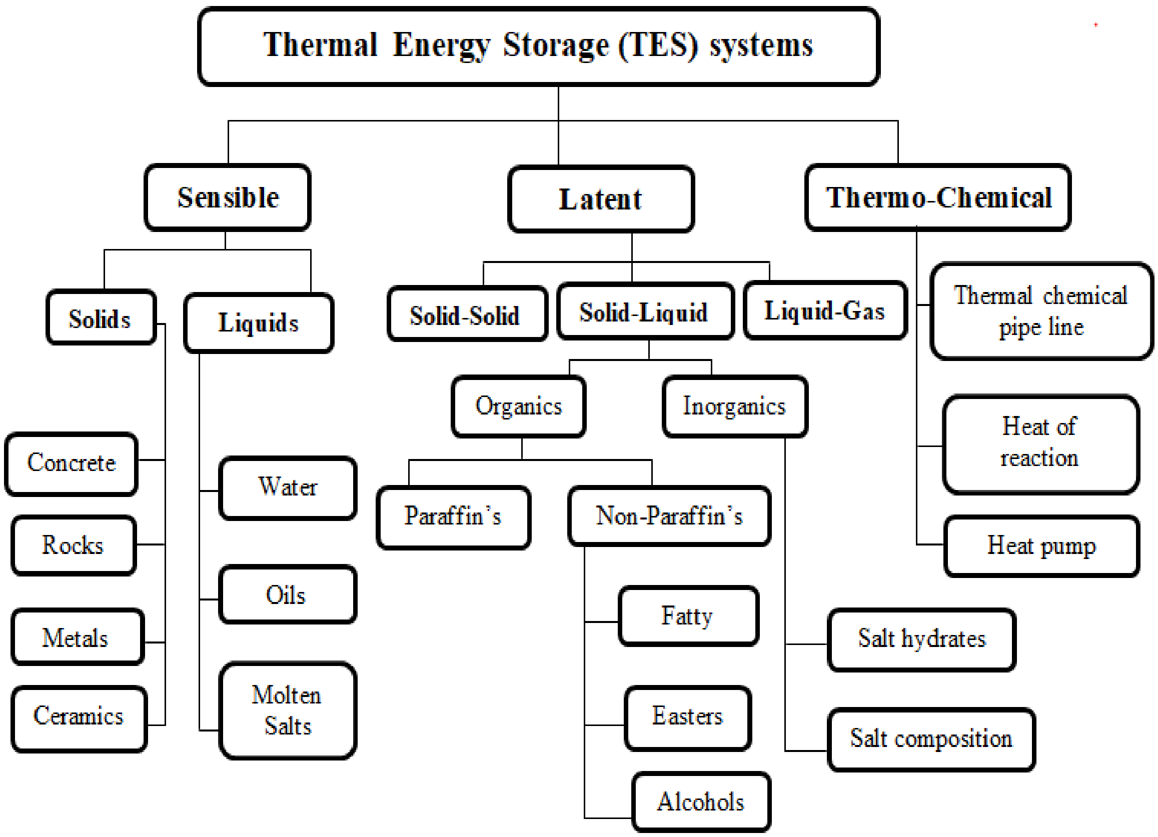

Fig.1.2 Category of TES systems with its storage material

Now, the present investigation is concerned with two of them which are both sensible and latent heat thermal energy storage (TES) systems used to store heat energy for low and high-temperature applications.

1.3 Statement of the problem

Fossil fuels have served and fulfilled all human energy needs for a long era. However, fossil fuel price is increasing, and the emission of pollutant gases from the burning of those fuels are the main problem for developing countries like Ethiopia. Take an example Ethiopia is the third largest user of traditional fuels for household energy use in the world with 91 % of the population dependent on traditional biomass fuels. Therefore, renewable energies such as solar energy, hydropower, wind energy, geothermal energy, and tidal energy are expected to take the role of fossil fuels. Among the various renewable energies, solar energy is clean, the most available, safe, and sustainable renewable source of energy. Nevertheless, the solar energy systems can operate only for a few hours during summer days and much fewer hours during winter/rainy days and it cannot operate at night time.

Therefore, there is an obstacle to the development and promotion of solar energy, mainly due to a lack of storage systems for various solar energy systems. To tackle the above-mentioned problem, build thermal energy storage (TES) systems are mandatory for effectively utilize the harvested solar energy during the discontinuous supply of solar radiation. In this research, an investigation of the performance analysis of the TES system for low and high-temperature applications (both sensible and latent heat energy storage) studied in-depth. 3-D Multiphysics model is developed to investigate a transient conjugate heat transfer between the HTF and the storage material by utilizing FEM-based solver COMSOL Multi-Physics 4.3a commercial software. Most of the existing TES system is designed based on a single shell-tube storage bed type model and it takes long charging time. Hence, the heat transfer enhancement technique is applied by embedding of multi-HTF tubes between the HTF and the storage material leads to reduce the charging time in the present TES model.

1.4 Objectives of the study

The general and specific objectives of this research are illustrated as follows.

1.4.1 General objective

The general objective of this study is to conduct a numerical investigation on the performance analysis of thermal energy storage systems for low and high-temperature applications (both sensible and latent heat storage) are studied in-depth for implementing solar renewable energy.

1.4.2 Specific objectives

The specific objectives are:

- ✓ Selecting the appropriate TES materials for low and high-temperature range.
- ✓ Optimizing the number of HTF tubes to reduce the charging time.
- ✓ Selecting the effective geometrical configuration of the TES model with appropriate cylinder orientation.
- ✓ Validating the result with previous published experimental and numerical work.
- ✓ Studying the various performance parameters of the TES model such as; charging/discharging time, liquid fraction, and total energy stored/released using FEM based solver COMSOL Multiphysics 4.3a software.
- ✓ Studying the heat transfer enhancement technique applied in the TES model by embedding the multi-HTF tubes on the storage bed.

1.5 Significance of the study

The significance of developing solar TES systems for low and high-temperature applications will be enabled to efficiently utilize the harvested solar renewable energy during the absence of solar radiation, as a result, minimize fossil fuel dependency and emission of gasses. This study helps to provide consistency between the energy supply and demand for various solar thermal applications. This study will give detailed information about which storage material will be used for appropriate temperature range, classification of thermal energy storage systems, and in what application could use this storage. To introduce the TES system integrated with varying solar thermal applications. After implementing the study, the developed TES system is integrated for domestic water heating application and steam generation purposes in concentrated solar power (CSP) plants suitable to work continuously.

1.6 Scope and limitations of the study

This study focuses on theoretical as well as numerical investigation of the performance analysis of TES systems. Sizing of the developed TES model, study the performance parameters such as; charging and discharging time, temperature variation on the developed model, and amount of heat energy stored/released with the help of COMSOL Multiphysics 4.3a commercial software. The present study begins with a comprehensive literature review tracing on the detailed background of TES systems with its varying application. Developed a mathematical model to validate against the previous patented experimental study on similar storage material was used and study the application of integrated this TES system i.e., for domestic water heating application and steam generation purpose in concentrated solar power (CSP) plants. This study also examines the optimization of the number of HTF tubes and heat transfer enhancement using embedding of multi-HTF tubes between storage material and the HTF in the developed TES model.

The present numerical study is considered based on a laminar flow regime with significant use of a low HTF flow rate. However, if the study is extended to a turbulent flow regime it may be several advantages achieved to enhance the heat transfer rate.

1.7 Organization of the study

The structure of this study is categorized into seven chapters preceded by the introduction of the research which shortly describes the summary of the whole work and a brief description of the content of each of the chapter is provided below:

Chapter – 1: introduces about the present study beginning by describing the background of the work, the general concept of thermal energy storage systems, statement of the problem, objectives of the study, significance of the study, scope, and limitations of the study are presented in this chapter.

Chapter – 2: a detailed review of related literature on various aspects of TES systems from books, journals, and different websites is offered. These aspects are to bring the background of TES systems, classification of the TES system, a brief study on the type of solar collector and thermal performance enhancement mechanism are presented. Additionally, the local research papers about the TES system are also presented and finally based on the summary of the literature survey objectives of the present study are framed.

Chapter – 3: the proposed methodology of the study, data collection and data analysis, research design, and the calculated available solar radiation by the given metrological data are presented in this chapter.

Chapter 4 and **Chapter 5:** in this two chapter's description of the system, sizing of thermal energy storage with a physical model, mathematical formulation with governing equation, initial and boundary condition, mesh generation and evaluation of performance parameters to both thermal energy storage system for low and high-temperature application are briefly presented.

Chapter – 6: the result and discussion obtained from the developed numerical model in both cases during charging and discharging processes are presented. The main performance parameters for the TES model are also briefly discussed in this chapter.

Chapter – 7: in the final chapter it draws the major conclusion arrived from the given numerical studies of thermal energy storage systems. Recommendation and scope for future work are also given in this chapter.

CHAPTER TWO

LITERATURE REVIEW

This chapter presents the review of previous studies regarding on the thermal energy storage systems, classification of TES systems, storage materials, and performance enhancement mechanisms of the TES system. Previous local studies on the TES system and literature summary with the research gap also included in this chapter. Generally, a review of several patented research studies regarding the TES system briefly described in the following section.

2.1 Background of thermal energy storage systems

The history of the TES system began earlier back to the twentieth century when people used heat storage and cooling processes in the caves and mountains to stay cool in the summer and keep warm in the winter. Next to this, in 1960 the US began the seasonal thermal energy storage system. Similarly, the study of the thermal energy storage system began in the late 1970s, and between 1976 and 1992 the solar energy storage system was developed in Europe **(Qi *et al.*, 2008)** and **(Heller, 2000)**. Nowadays, a thermal energy storage system is an attractive type of energy storage technology used in different thermal applications such as; heating, cooling, and power generation applications. The emphasis on the applicability of thermal energy storage technology also researched and spread widely in the future because this technology helps to reduce fossil fuel consumption and to minimize global warming in the world. Several researchers explain the whole background of thermal energy storage (TES) systems on its; application area, storing mechanism and thermal performance, some of them are given below.

Cabeza *et al.*, (2003) were suggested about the history of TES systems on the review paper, that was thermal energy storage in general, had been the main topic in research for the last 20 years, but although the information is quantitatively enormous, it is also spread widely in the future. The commercial utilization of TES systems in different temperature ranges began seeing a major increase decade ago stated by **(Wu & Zhao, 2011)**. The history of thermal energy storage and different techniques adopted for thermal energy storage systems and three aspects such as storage methods, classifications, and applications were carried out by (**Chavan *et al.*, 2015**) on the review paper. Both authors describe the history of a thermal energy storage system and given a suggestion for the present day. Thermal energy storage system has mandatory for utilization of harvesting solar heat energy integrated into different solar thermal application.

Alva *et al.*, (2018) recently reviewed a general description of thermal energy storage systems with a brief explanation. During the reviewed wide scope of thermal energy storage field briefly discussed. The role of TES in the contexts of different thermal energy sources and explained how TES used for un-necessitates burning of fossil fuel, solar power generation, building thermal comfort, and other niche applications of TES was also explained. This paper has given guidelines for the design of the thermal energy storage (TES) system with appropriate heat storage material for the present study.

2.2 Classification of thermal energy storage (TES) systems

Depending on various criteria there are different classifications of thermal energy storage systems. **Ataer, (2006)** listed the criteria, which determine the selection of thermal energy storage methods as follows.

- ✓ The temperature range over which the storage has to operate.
- ✓ The capacity of the storage.
- ✓ Heat losses from the storage must be kept to a minimum.
- ✓ The charging and discharging rate.
- ✓ The cost of the storage unit is some of the criteria to select the appropriate thermal energy storage methods, so, this study has been done based on the above criteria.

The classification of the thermal energy storage system can be described depending on such characteristics **(Sarbu & Sebarchievici, 2018)**; capacity of the system, the discharged power, efficiency, storage period, charging and discharging time and cost of the system are some of the characteristics to determine the type of thermal energy storage system.

Hasnain, (1998) has classified as thermal energy storage systems based on the time length of stored the heat energy, it can be divided into “short term” and “long term” thermal energy storage systems. **Hasnain, (1998)** on another study has also classified thermal storage systems based on the temperature level of stored thermal energy criterion; it can be divided into “heat storage” and “cold storage” systems. **Sharma *et al.*, (2009)** classified thermal energy storage systems based on the state of energy storage material; it can be divided into sensible heat storage, latent heat storage, and thermochemical heat storage. Most researchers agreed on the classification of TES systems are based on the above classification as shown in Fig.2.1. The present study also depends on this classification; concerned mainly sensible and latent TES system.

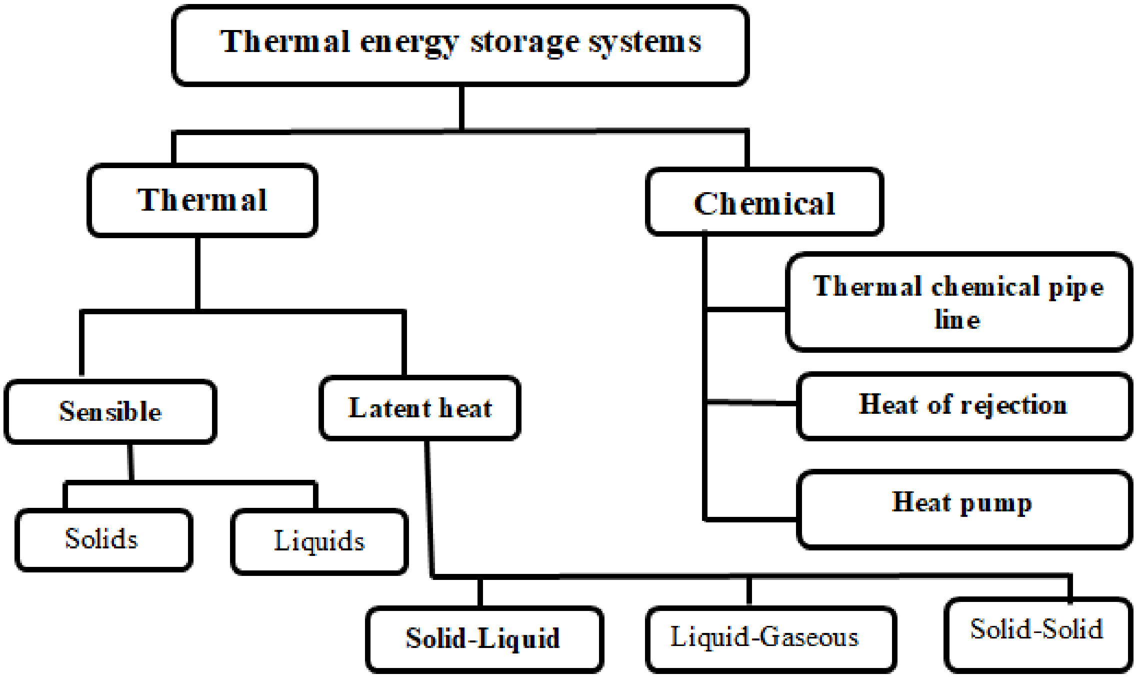

Fig.2.1 Classification of thermal energy storage for solar energy (**Sharma *et al.*, 2009**)

Alva *et al.*, (2018) was also grouped thermal energy storage systems based on operating temperature range that means depending on the melting point of storage materials into:

- ✓ Cold thermal energy storage systems (< 20 ℃)
- ✓ Low-temperature thermal energy storage systems (20 – 100 ℃)
- ✓ Medium-temperature thermal energy storage systems (100 – 250 ℃)
- ✓ High-temperature thermal energy storage systems (> 250 ℃)

➢ The **Alva *et al.*, (2018**) classification are the main guidelines for the present study, so according to this classification the present study conducted on a thermal energy storage system for low and high-temperature applications and briefly illustrated with different previous studies as follows:

2.2.1 TES systems for low-temperature application

A. Sensible heat storage

Sensible heat storage is one of the most widely used thermal energy storage mechanism, which consists of accumulating thermal energy in a solid or liquid medium whose temperature then rises. Sensible heat storage (SHS) system utilizes the heat capacity and the change in temperature of the storage material during the charging and discharging process. According to (**Stutz *et al.*, 2017)** the amount of heat stored depends on the specific heat of the medium, the temperature change, and the amount of the storage material. Integrated sensible heat storage for low-temperature applications mainly concerns with the domestic water heating system at the individual scale, district heating at the large scale, and thermal comfort for buildings.

Dincer *et al.*, (1997) studied sensible heat energy storage systems and their performance evaluation techniques. A detailed investigation is presented on the availability of SHS techniques for solar thermal applications, selection criteria for SHS systems, the economics of SHS systems, the main issues in evaluating SHS systems, the viability of SHS systems, the environmental impacts of SHS systems and criteria for SHS feasibility studies, as well as energy-saving options.

Duffie and Beckman, (2013) conducted one of the sensible heat storage systems, which is a basic theoretical introduction for the water is used as a thermal energy storage material in various solar thermal energy storage systems as well as analytical models for the water storage stratification.

Pinel *et al.*, (2011) investigated seasonal sensible thermal energy storage for residential applications. The characteristics of sensible thermal energy storage material such as; low cost, high specific heat capacity, good compatibility with its containment, and long-term stability under thermal cycling also studied. Finally, the study concludes that water is the best choice for sensible thermal energy storage material due to several advantages. Which is water has a larger operating temperature range, it is inexpensive, easy to handle, noncombustible, and widely available. It also used for both short-term and long-term thermal energy storage material due to its relatively high specific heat and high rates of charge and discharge.

- ➢ The most widely used sensible TES material for low-temperature application in liquid media is water due to:
  - ✓ It is abundant and inexpensive.
  - ✓ It can be easily stored in all kinds of containers.

- ✓ It can be easy to handle, non-toxic, and noncombustible.
- ✓ It is easily mixable with additives
- ❖ However, it is corrosive, has high vapor pressures and low volumetric energy density.

Rock and bricks are also another sensible TES material for low temperatures application in solid media due to the economic point of view.

B. Latent heat storage

Latent heat storage also another main storage mechanism in TES systems which involves the heat absorbed or released when a material changes from one physical state to another with phase change material. Latent heat storage system stored heat in the form of heat of fusion (solid-liquid transition), the heat of vaporization (liquid-vapor), or heat of solid-solid crystalline phase transformation. These storage mechanisms store heat in the form of latent heat during a constant temperature process, usually; the solid-liquid phase change is used in many TES systems. PCMs can be used for low-temperature solar thermal applications such as water heating, baking, and drying processes that should have a melting temperature in the range of 45 to 90 ℃ **(Rathod & Banerjee, 2014)**. Paraffin can be widely used as a thermal energy storage material for such applications because they are available at a reasonable cost with moderate latent heat storage density and a wide range of melting temperatures.

Da Cunha *et al.*, (2016) reviewed thermal energy storage for low and medium temperature application with phase change materials. The study presented a comprehensive review of PCMs melting temperature range between 0 and 250 ℃, and the most appropriate thermo-physical properties of the materials. From the study, organic compounds and salt hydrates seem more promising materials below 100 ℃. However, phase segregation and sub-cooling is the dominant factor in this PCMs. Additionally, the paper also reported indirect latent heat storage containers and systems suitable for integration with various heating and cooling process networks.

Xue, (2016) investigated on the domestic solar water heater integrated with PCMs as a storage material. Comparison between the thermal performances of the domestic solar water heater with phase change energy storage to that of traditional water-in-glass evacuated tube solar water heaters with an identical collector area also performed. Domestic solar water heater with PCM performs more efficiency with a constant flow rate than under the condition of exposure.

Finally, the study concluded that solar water heaters had high-temperature properties because of PCMs, so PCMs were promising use in solar heating applications.

Pielichowska & Pielichowski, (2014) investigated different groups of storage materials including; inorganic systems (salt and salt hydrates), organic compounds such as paraffin's or fatty acids, and polymeric materials. Paraffin's constitute broadly used solid-liquid phase change material, possess a high latent heat storage capacity over a narrow temperature range, and are considered as non-toxic and ecologically harmless from those groups of storage material. Paraffin's between C5 and C15 are liquids with the higher analogs being waxy solids with melting temperatures ranging from 23 to 67 ℃ and select an appropriate storage material for specific latent heat thermal energy storage application.

Dutta *et al.*, (2008) studied a paraffin wax encapsulated in the annulus of two coaxial circular cylinders under variable heat fluxes both experimentally and numerically. During experimental work, they used a hollow adiabatic steel cylinder, an internal pipe that was placed coaxially and horizontally with the outer cylinder, and thermocouples were placed in the radial direction in the annulus to record the temperature. For the numerical work, they used a 2D unsteady state numerical model and selected the annulus gap between the inner cylinder and outer cylinder. Finally, the study verified their numerical model with their experimental findings and obtained a good agreement between their predicted and experimental results.

Diarce *et al.*, (2015) was studied new binary eutectic mixtures of sugar alcohols for thermal energy storage in the 50-90 ℃ temperature range. Three new binary mixtures of sugar alcohols composed of erythritol and xylitol, erythritol and sorbitol, and xylitol and sorbitol were studied. Equilibrium temperatures and melting enthalpies obtained from simulations were in good agreement with experimental results. Therefore, the method could be used for the prediction of new PCMs made of binary eutectic mixtures. The importance of considering the specific heat capacity difference between the solid and liquid phases to correctly predict melting enthalpies of the mixtures was highlighted.

Farid *et al.*, (2004) reviewed on latent heat energy storage materials or PCMs and its applications. From those storage materials, hydrated salts are attractive materials used for in thermal energy storage system, due to their high volumetric storage density (350 MJ/m^3), relatively high thermal conductivity (0.5 W/m℃) and moderate cost. Glauber salt (Na_2SO_4 and H_2O), which contains 44% Na_2SO_4 and 56% H_2O by weight has been studied. It has a melting temperature of about 32.4℃, a 254 kJ/kg (377 MJ/m^3) of latent heat energy and it is one of the cheapest materials that can be used for thermal energy storage. However, the problems of phase segregation and sub-cooling have limited its application.

Mosaffa *et al.*, (2012) studied an approximate analytical model for the solidification process in a shell and tube finned thermal energy storage system. A comparative study is presented for solidification of the PCM in a cylindrical shell and rectangular storages having the same volume and heat transfer surface area. The result showed for the two methods was a good agreement which, indicates that the PCM solidifies more quickly in the cylindrical shell storage than in rectangular storage. So, the PCMs used with a phase change temperature of 18–30 ℃ is preferred to meet the need for thermal comfort for building applications.

Colella *et al.*, (2012) numerically investigated by the application of computational fluid dynamics (CFD) to the design and characterization of a medium scale latent heat energy storage unit for district heating systems. The system has been designed for a comparison between traditional water storage systems and LHTES systems for district heating shell-and-tube LHTES with technical grade paraffin thermal energy storage material and water used as a heat transfer fluid (HTF). The final analysis of the investigations shows that latent heat storage units installed on the building heating network most promising than on the primary district heating network in terms of energy storage density.

Adine & Qarnia, (2009) studied numerically on analysis of a coupled solar collector latent heat storage unit using various PCMs for heating the water and developed a theoretical model to predict the thermal behavior and performance of a solar latent heat storage unit based on the energy equations. Conducted a series of numerical simulations were for three kinds of PCM (n-octadecane, Paraffin wax and Stearic acid), the finite volume approach was also developed to numerically evaluate the thermal performance of the LHS unit. Finally, the study concluded that the mass flow rate of the PCM, the number of tubes, and the flow rate of HTF in solar collector maximizes the efficiency of thermal energy.

Trp, (2005) investigated the heat transfer during technical grade paraffin melting and solidification in a shell-and-tube latent thermal energy storage unit during charging and discharging. An experimental and numerical investigation has been performed on transient forced convective heat transfer between the heat transfer fluid (HTF) and the tube wall, heat conduction through the wall, and solid-liquid phase change of the phase change material (PCM), based on the enthalpy formulation. Finally, both numerical predictions and experimental data showed good agreement for both paraffin non-isothermal melting and isothermal solidification.

Vyshak & Jilani, (2007) investigated the numerical analysis of latent heat thermal energy storage systems to study the effect of the shape of the latent heat storage system on the melting rate of the phase change material. The study performed a comparative study of the total melting time of a phase change material (PCM) packed in three containers with different geometric configurations such as a rectangular, cylindrical, and cylindrical shell. The result showed that shell and tube arrangement has a faster melting rate compared to rectangular latent heat storage for the same heat transfer area and volume.

Mahfuz *et al.*, (2014) worked both experimental and numerical investigation of a shell and tube latent heat storage using paraffin wax as PCM. The study carried out a parametric study to analyze the heat transfer behavior of the storage unit with different flow parameters and system dimensions and obtained a good agreement between numerical and experimental results. The result showed that the inlet temperature has a higher effect on the performance of the system than the mass flow rate of the heat transfer fluid, from this finally concluded that the inlet temperature of HTF has a great influence in solidification and melting of PCM whereas mass flow rate has small influences.

Wang *et al.*, (2013) numerically investigated the charging and discharging characteristics of a shell-and-tube phase change heat storage unit to study the effect of inlet temperature and mass flow rate of HTF on the thermal performance of shell and tube latent heat storage system. The study finally concluded from the obtained result was the inlet temperature of the HTF had more effect on thermal energy storing capacity and melting rate than the mass flow rate.

- From the above literature survey, paraffin wax is the best promising thermal energy storage material for low-temperature application because:
    - ✓ It economically viable and repeated cycling across the solid-liquid phase transition.
    - ✓ It possesses a high latent heat storage capacity over a narrow temperature range.
    - ✓ It has chemically stable, non-toxic, non-corrosive, and ecologically harmless.
    - ✓ Paraffin waxes exhibit moderate TES density based on molar mass.
    - ✓ Paraffin's between C5 and C15 are liquids with the higher analogs being waxy solids with melting temperatures ranging from 23 to 67 ℃.
    - ✓ It has also no sub-cooling effects during the solidification process.

One of TES systems integrated for low-temperature application is solar heating purpose or domestic water heating systems integrated with thermal energy storage system as shown in Fig 2.2. Since the above summary in this study also paraffin used as a storage material integrated for the domestic water heating system during the investigation.

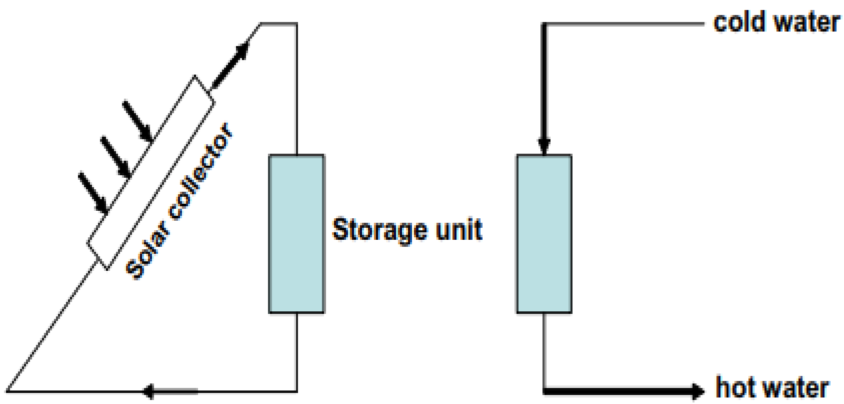

Fig.2.2 TES integrated for solar water heating system **(El Qarnia, 2009)**

2.2.2 TES systems for high-temperature application

Thermal energy storage (TES) systems for high-temperature applications mainly concerned with steam generation in concentrated solar power (CSP) plants. **Alva *et al.*, (2017)** and **Medrano *et al.*, (2010)** have investigated the thermal energy storage materials and systems for solar energy applications. Investigated different thermal energy storage materials both sensible and latent heat storage materials; steam, mineral oil, metals, earth materials, molten salts, organic and inorganic material, etc. From the investigation molten salts (especially the nitrates) are currently the most attractive thermal energy storage materials in CSP plants which, are cheap, giving them high energy storage density, lower vapor pressure than water and are capable of operating at high temperatures in the liquid form up to 400 ℃. This permits to improve the efficiency of the Rankine cycle at high temperatures in the plant.

A. Sensible heat storage

High-temperature sensible thermal energy storage (STES) improves the dispatchability of a concentrating solar power (CSP) plant. **Liu *et al.*, (2016)** reviewed a concentrating solar power plant and new developments in high-temperature thermal energy storage technologies. The study provided a comprehensive summary of CSP plants both in operation and under construction. It covers the available technologies for the receiver, thermal energy storage, power block, and heat transfer fluid**.**

Alonso *et al.*, (2016) developed on a concept of thermal energy storage (TES) systems in concrete as solid media for sensible heat storage are proposed to improve the cost and efficiency of solar thermal electricity plants. A new cement-based mix that could conduct and store heat at high temperatures, with the temperature range 290-550 ℃, making it suitable for a thermal energy storage system in solar power plants.

Bauer *et al.*, (2013) studied thermo-physical properties, metallic corrosion, and thermal decomposition processes of solar salt for sensible thermal energy storage (TES) systems in the temperature range from 250 ℃ to 550 ℃. The study utilized a mixture of 60% sodium nitrate ($NaNO_3$) and 40% potassium nitrate (KNO_3) solar salt for concentrating solar power applications during the study. Finally, the study concluded that reliable thermophysical properties were important for the modeling and dimensioning of molten salt storage systems and to handle molten salt in TES systems. It is also mandatory to understand the corrosion behavior of the storage tank.

Gokon *et al.*, (2008) investigated for high-temperature thermal energy storage by using composite materials of molten alkali-carbonate/MgO-ceramics are examined as thermal storage media in a tubular reformer using a double-walled reactor tube of a laboratory scale. Composite materials used were Na_2CO_3, K_2CO_3, and Li_2CO_3 with magnesia are tested as thermal energy storage media. Finally, the study decided from the experimental result after a heat-discharge test that a composite with a higher melting point is feasible for use as a thermal storage medium in the double-walled reactor for high-temperature application.

One of the applications of a high-temperature thermal energy storage system is it integrated into solar power plants used for continuous power production as shown in Fig.2.3. Nowadays, most thermal power plants integrated sensible storage material is used as a storage material to store heat energy.

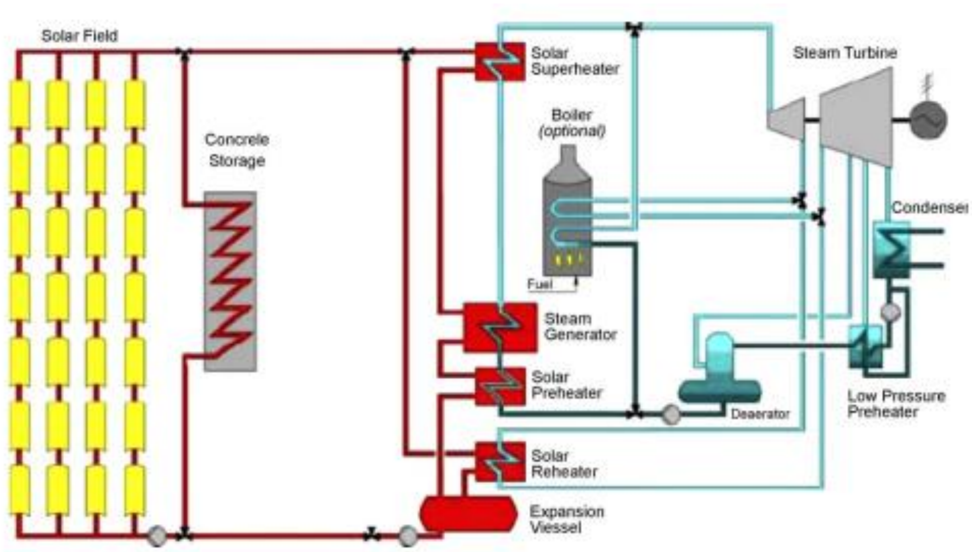

Fig.2.3 High-temperature TES integrated into a solar power plant **(Medrano *et al.*, 2010)**

Singh & Sørensen, (2017) carried out a numerical investigation on concrete based thermal energy storage for steam generation. The storage system consisted of a heat transfer fluid (HTF) flowing inside the heat exchanger tubes embedded in a cylindrical shape concrete configuration to store the temperature range of 350-390 ℃. The study also evaluated conjugate transient heat transfer between the two mediums; the HTF, and the concrete, similarly the performance of the storage system using finned heat exchanger tubes and thermal characteristics evaluated in the developed model. Finally, the developed model suitably proved the dynamic behavior of the concrete based thermal storage system and its sub-processes, and thus offers a suitable framework for future investigations leading to an easier and more economical solution.

B. Latent heat storage

Haillot *et al.*, (2011) identified the thermal behavior of eleven potential TES storage materials using differential scanning calorimetry analysis (DSC) to determine the main characteristics of these storage materials. After investigation, the study concludes that four materials show unsuitable characteristics for latent heat storage materials from the eleven selected materials due to degradation with temperature and due to a low decomposition temperature. The remaining seven materials are shown suitable for latent heat storage, also emphasizes the importance of the measurement conditions on the results.

Cárdenas & León, (2013) reviewed a series of PCMs, mainly inorganic salt compositions and metallic alloys, which could potentially be used as storage media in a high temperature (above 300°C) latent heat storage system. The study seeking to serve the reader as a comprehensive thermo-physical properties database to facilitate the material selection task for high-temperature applications. The study proposed a lot of performance enhancement techniques such as; using extended surface, dispersion of highly conductive particles within the PCM, etc. Several design considerations also considered aiming to provide a broad overview of the design of high-temperature latent heat based thermal energy storage systems.

Wu & Zhao, (2011) experimentally investigated in high-temperature TES systems by using porous materials such as metal foams and expanded graphite to enhance the heat transfer capability of PCMs. They were used $NaNO_3$ with 99% purity is selected as the PCM for the experimental investigation. The heat performances of metal foams and expanded graphite in high-temperature TES system experimentally investigated under the bottom and top heating conditions. During the experimental investigations, the results showed that the heat transfer rate can be enhanced through the addition of the porous materials by 2.5 times compared to that of pure $NaNO_3$ in the heating process from 250-300 ℃.

Wang *et al.*, (2006) developed and conducted a high-temperature phase-change storage heater with a series of experiments to test the heat charge and discharge performance of this kind of heater. In this investigation, an Al-Si alloy was used as a PCM to store thermal energy because of its high heat of fusion and thermal conductivity. The results show that; with a high heat of fusion and thermal conductivity, $AlSi_{12}$ is suitable to heat storage medium; the heat storage ratio of the heater is high and increases with increasing heating power, during the phase change process. The heater can also provide a stable heat discharge rate and meet the demand for thermal comfort indoors to some extent and the heater is economical for domestic space heating because of low operating costs.

Adinberg *et al.*, (2010) developed and tested the reflux heat transfer storage concept for producing high-temperature superheated steam in the temperature range of 350-400 ℃ with Zinc-Tin alloy metallic substance as a thermal storage medium which also serves as the phase change material. The experimental tests performed and produced satisfactory results in terms of thermal stability and compatibility of the utilized storage materials (Zn70Sn30).

Kenisarin, (2010) studied the developments of PCM's perspective for high-temperature TES systems and solar energy. Thermo-physical properties of potential heat storage salt compositions and metal alloys were studied on the review paper and, the compatibility of heat storage materials and constructional materials are presented. Finally, the paper concludes that hundreds of perspective compositions and materials had been found out based on inorganic salts and metal alloys for high-temperature thermal energy storage systems.

Wei *et al.*, (2018) reviewed material selection, innovation, and investigation of thermo-physical properties of PCM for high-temperature applications to give a helpful reference for the design of high-temperature phase-change TES systems. Evaluated the selection principles of PCMs on high-temperature thermal energy storage systems, summarized the thermo-physical property of high-temperature PCMs, and summarized a lot of heat transfer enhancement techniques as a potential alternative method to overcome poor thermal conductivity of PCM. Finally, the paper concludes that the selection of heat storage material was very important for the development of high-temperature TES systems used in CSP plant and molten salt useful PCMs for high-temperature applications.

Bellan *et al.*, (2015) investigated numerically on a latent heat thermal energy storage system, which consists of sodium nitrate ($NaNO_3$) filled spherical capsules in a cylindrical tank and the high-temperature synthetic oil as a heat transfer fluid used in CSP plant. The developed numerical model is validated using the reported experimental and numerical data and studied the influence of capsule size and the flow rate of heat transfer fluid (HTF) on the temperature distribution, fluid flow, melting and solidification of the system. Finally, the study concludes from the result, the heat transfer rate is increased, and eventually the charging/discharging time is decreased when the capsule size is decreased, or the HTF flow rate is increased.

Tehrani *et al.*, (2016) worked on the design and feasibility study of high-temperature shell and tube latent heat thermal energy storage system for solar thermal power plants in the 286-565℃ temperature range. The primary objective of the study is to evaluate the potential of the configuration for CSP plants. Finally, the study concluded that a proper design method of the storage configuration should simultaneously account for the effects of geometric parameters and the number of modules to achieve the highest amount of total stored/delivered energy with a minimum heat transfer surface area.

- From the above literature survey for high-temperature applications, concrete, and nitrate salt (KNO_3) are the most attractive sensible and latent heat TES material for high-temperature applications.
  - Due to its high specific heat capacity, good mechanical properties such as; compressive, tensile strength, high mechanical resistance to cyclic thermal loading, etc., and availability that means the concrete aggregates available everywhere cheaply. Because of this concrete thermal energy storage material is an adaptive technology that can be implemented in the Sunbelt countries.
  - Nitrate salts with a melting point above 250 ℃ are considered for latent heat storage and used as a PCM. However, choosing an appropriate salt with a melting point within the operational temperature range of TES can greatly enhance the volumetric thermal energy storage capacity. For example, in an operating range between 300 ℃ and 500 ℃, by choosing $LiNO_3$ (melting point: 250 ℃) only sensible heat can be used for thermal energy storage and it will give a volumetric storage capacity of around 440 MJ/m^3. But by choosing KNO_3 (melting point: 335 ℃) both sensible heat and latent heat can be used for thermal energy storage and it will give a volumetric storage capacity of around 935 MJ/m^3. Therefore when nitrate salt is required to fulfill thermal storage purposes, utilizing latent heat is a good option **(Alva *et al.*, 2018)**.

2.2.3 Classification of TES system based on storage concept

According to (**Dolado *et al.*, 2010)**, (**Liu *et al.*, 2016**) and (**González-roubaud *et al.*, 2017**) classified thermal energy storage systems based on storage concepts especially in the high-temperature application were classified into two main storage concepts. These are active and the passive storage systems; active storage systems the storage medium was circulated itself through a heat exchanger and heat transfer into the storage material is characterized by forced convection, they are also subdivided into direct and indirect storage systems. The passive storage systems are a dual-medium storage system that means the HTF and the storage material are different and the HTF used for charging and discharging the storage material.

i. Active direct storage systems

The principle of an active direct storage system is the heat transfer fluid (HTF) and the storage medium is the same that means the HTF serves also as the storage medium because the material is to achieve both a good HTF and good storage material characteristics at the same time. The advantages of this storage system are cost-effective, due to no need for expensive heat exchangers and the working temperatures can be higher improving the performance of the plant. For example, a molten salt used as an HTF and storage material at the same time eliminates the need for expensive heat exchangers.

One of the active direct storage systems is the two-tank direct storage system, one tank is used to store the hot HTF and the other one to store the HTF when it has been discharged and the HTF which directly stored in a hot tank is used to during the time of no solar radiation. The cooled HTF is pumped to another tank, to circulate again. The advantages of the two tanks direct storage system are the cold and heat storage materials are separated, reducing the risk of approach, and performed high working temperatures. However; the high cost of the heat exchanger to produce steam for the Rankine cycle, needs two tanks and a high risk of solidification of the storage fluid due to its high freezing temperature is limit its applicability.

ii. Active indirect storage systems

This group needs a second medium used for storing the heat and working with different HTF and storage medium. One of the active indirect storage systems is the two tanks indirect systems that work as the direct one but as the HTF fluid and the storage material are different it needs a heat exchanger between them. The advantages of two tank indirect storage systems are: the separation between cold and hot HTF and the storage material flows only between hot and cold tanks, not through the parabolic troughs and the disadvantages are the same as in the two tanks direct systems. The other active indirect storage systems are the single tank (thermocline) system, the cold and hot fluids are in the same tank but separated because of the density of the fluid, the hot fluid is at the top and the cold fluid at the bottom, as a result, this fluid stratification zone is known as the thermocline. There is also the need of a heat exchanger to transfer the heat energy between the HTF and the storage material, the HTF which arrives from the solar field passes through a heat exchanger, heating the thermal storage fluid media. The advantages of this concept are the decrease in the cost in front of the two-tank storage system. however, it is more difficult to separate the hot and cold HTF; in the case of using molten salts it is necessary to keep a minimum system temperature to avoid freezing and salt dissociation as they have high melting temperatures; the outlet temperature is high increasing losses in the solar field; the thermocline needs to be controlled with some method (complicated) and it is an inefficient power plant due to complex design of storage system thermodynamically point of view.

iii. Passive storage systems

A passive storage system is another storage concept that has both the HTF and the storage medium, the heat transfer medium passes through the storage only for charging or discharging the system, the storage medium itself does not circulate and these storage systems generally called dual-medium storage systems. Passive storage systems are mainly solid storage systems (concrete, castable materials, and PCM). In the case of using concrete as a storage material the advantages are the low cost of it; its high heat transfer rate due to good contact between concrete and piping; the facility of handling the material and the low degradation of heat transfer between the heat exchanger and the storage material. Another and very important thing on a passive energy storage system is the use of phase change materials (PCMs) as storage material and it is advantageous due to the improvement of storage ratio. The advantages of these storage systems are better to use PCM storage capacities; reduction of costs, compared with storage systems with the only PCM as storage media; and improve storage ratio, compared with systems with only sensible heat materials.

- Due to no need for two-tank systems (cost-effectiveness) and reliability, a passive storage system is applicable for this study. The operating principle is heat energy transferred from the solar field by the HTF to the PCMs and the PCMs contain a shell and tube heat exchanger to transfer the thermal energy from the HTF to the storage material.

2.3 Solar collectors for TES system

A solar collector is one of the major components integrated into a thermal energy storage system that converts solar radiant energy into thermal energy for various uses. Depending on the application of temperature range there are various types of solar collector have been applicable, but fundamentally grouped into two types of solar collectors;

1. **Non-concentrating solar collectors:** it is also known as stationary solar collectors; solar pond, flat plate collector, and evacuated tube collectors are also grouped under this type of solar collector. It has the same area for intercepting and absorbing solar radiation and no need for sun-tracking.
2. **Concentrating solar collectors:** this type of solar collector consists of; compound parabolic, linear Fresnel, parabolic trough, parabolic dish reflector, and heliostat field collector. This type of solar collector is the need of sun-tracking.

Due to the application of temperature range and simplicity of operation flat plate collector for low-temperature TES system and parabolic trough for high-temperature TES system are selected for the present study and briefly discussed below.

2.3.1 Flat plate solar collector

Flat plate collector was a main solar component and most efficient means of collecting solar energy for low-temperature applications such as; solar water heating, building heating, and air-conditioning. Flat plate solar collectors are; simple in design, with no need for tracking mechanism and usually consist of glazing covers, absorber plates, insulation layers, recuperating tubes, and other auxiliaries as shown in Fig 2.4. The flat-plate collectors can be designed for applications requiring energy delivery at temperatures ranging from ambient temperature up to 100 ℃ suggested by (**Janjai *et al.*, 2000**). The detailed analysis of a solar flat plate collector is a complex task, due to the high number of parameters affecting its performance but some relevant studies on the performance analysis of solar flat plate collectors that have been used for this study are illustrated below.

Gunjo *et al.*, (2017) investigated experimentally on the performance of a flat plate solar collector integrated for the solar water heating system. The study presented the effect of different operating parameters on the flat plate collector. The result showed that the thermal efficiency of the solar water heating system increases with ambient temperature, solar insolation, and the mass flow rate of water. CFD model of a flat plate solar collector also developed with a single riser tube and absorber plate at the steady-state condition to predict the outlet water and absorber plate temperature of the heating system with reasonable accuracy. Finally validated the CFD results with the experimental results and obtained a good agreement between their CFD model and experimental results.

Rangababu *et al.*, (2015) evaluated the performance of solar flat plate collectors in terms of thermal efficiency by developing a 3D model using ANSYS software to analyze the heat transfer phenomenon inside the riser of the solar flat plate collector. The evaluation was carried out numerically as well as experimentally and used two nano-fluids; Al_2O_3-water and CuO-water to improve the thermal performance of flat plate collectors. During the evaluations, the CuO based solar flat plate collector gives higher thermal collector efficiency compared to Al_2O_3 and water-based solar flat plate collector due to higher thermal conductivity. The study obtained a good agreement between the developed model and experimentally measured data then finally, concluded that the thermal efficiency of solar flat plate collectors could be improved by changing the working fluid.

Bouadila *et al.*, (2014) developed a combined energy and exergy optimization of flat plate solar collectors to determine the optimal performance and design parameters between solar to heat energy conversion systems. Absorber plate area, dimensions of solar collector, pipe diameter, mass flow rate, inlet, and outlet fluid temperature, etc., were considered as geometric and operating parameters in the analysis. Obtained the optimum values of the mass flow rate, the absorber plate area, and the maximum exergy efficiency with more accurate results and also obtained a good agreement between the developed model and the experimental measurements. Finally, the study concluded that the exergy was beneficial parameters in the design of solar collectors.

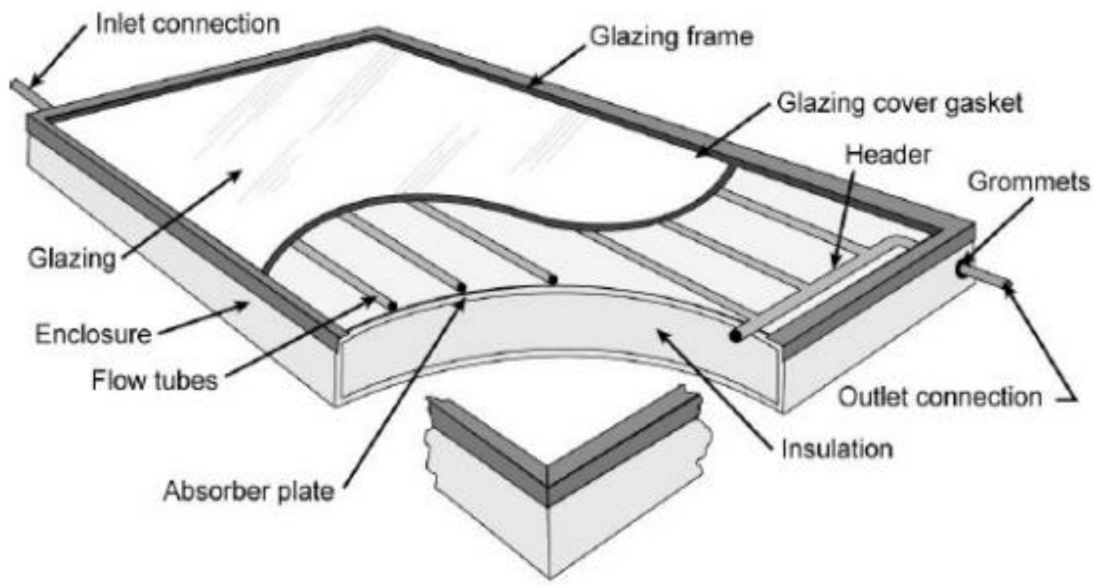

Fig.2.4 Cross-sectional view of FPC with basic component **(Bekele, 2007)**

Tagliafico *et al.*, (2014) simulated and analyzed the heat transfer phenomena in solar flat plate collectors with water flow using computational fluid dynamics (CFD) software. The mixed heat transfer modes of conduction, convection, and radiation between tube surface, glass cover, sidewalls, and insulating base of the collector as well as the mixed convective heat transfer in the circulating water inside the tube and conduction between the base and tube material were considered during those investigations. An experimental setup was built and an experiment performed to validate the CFD model and obtained a good agreement. Finally, conclude that the temperature was lower in the case for water flow than that of without flow due to the forced convection heat transfer.

2.3.2 Parabolic trough solar collector

Parabolic trough collector (PTC) is another type of solar collector used to deliver high temperatures with a good thermal performance for thermal energy applications. Parabolic trough collectors mainly light structures and low-cost technology systems for process heat application up to 400℃. It focuses direct solar radiation onto a focal line on the collector axis and a receiver tube with a fluid flowing inside that absorbs concentrated solar energy from the tube walls and raises its enthalpy is installed in this focal line as shown in Fig 2.5. Parabolic trough collector is mostly applicable in concentrated solar power (CSP) plants and heating in various industrial processes. This solar collector also used in the present study to delivering high temperatures to thermal energy storage systems for direct steam generation in CSP plants during the discontinuous and intermittent flow of solar intensity. The heat transfer and optical analysis of the parabolic trough collector are essential to optimize and understand its performance under different operating conditions. Therefore, numerous studies had been done about: application, construction, design, and modeling of this kind of collector integrated within CSP plants, and some of those studies are listed below.

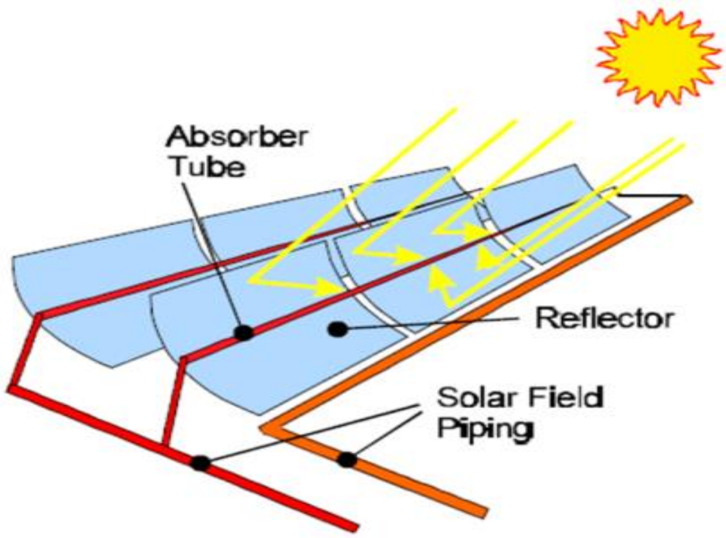

Fig.2.5 Typical view of parabolic trough collector (**Lüpfert *et al.*, (2000)**

García *et al.*, (2010) studied parabolic trough collectors and their application briefly; also presented a survey of systems that incorporate parabolic trough collectors could supply thermal energy up to 400 ℃, especially steam power cycles for electricity generation, including examples of each application. According to the study, there are currently several commercial collectors used for direct steam generation applications that have been successfully tested under real operating conditions. Nowadays typical aperture widths about 6 m, total lengths from 100 to 150 m, geometrical concentrating ratios between 20 and 30, and temperatures from 300 to 400 ℃ parabolic trough collectors were connected to steam power cycles both directly and indirectly.

Hachicha *et al.*, (2013) presented a mathematical formulation based on the finite volume method for parabolic trough collector a temperature ranges up to 400 ℃ to analyze a detailed numerical heat transfer model. Different elements of the receiver are discretized into several segments in both axial and azimuthal directions and energy balances were applied for each control volume. In the model and a set of algebraic equations are solved simultaneously using direct solvers. An optical model was also developed for calculating the non-uniform solar flux distribution around the receiver. Finally, determined the solar heat flux as a pre-processing task and coupled to the energy balance model as a boundary condition for the outer surface of the receiver.

Odeh *et al.*, (1998) determined the efficiency of parabolic trough collectors for the steam energy generation system. The developed model to study the thermal performance of a parabolic trough collector and the thermal losses from the collector is by using synthetic oil as the working fluid. Developed an efficiency equation for trough collectors used in a simulation model and evaluated the performance of direct steam generation collectors for different radiation conditions and different absorber tube sizes. Finally, conclude that the thermal losses from the trough collector were described in terms of absorber emissivity, absorber wall temperature, radiation level, and wind speed.

Theses *et al.*, (2011) performed a detailed one-dimensional numerical heat transfer analysis of a PTC by divided the receiver and envelope into several segments by applied mass and energy balance in each segment. Performed the partial differential equations in the discretized segment and the nonlinear algebraic equations were solved simultaneously. It also presented improvements either in the heat transfer correlations or irradiative heat transfer analysis as well. Validated the numerical model results compared with experimental data and also compared from other one-dimensional heat transfer models, finally, the result obtained that a better agreement in both cases.

Behar *et al.*, (2015) modeled the development, validation, and heat transfer of parabolic trough collector (PTC) implemented in Engineering Equation Solver to determine the performance of a parabolic trough solar collector's linear receiver. Studied briefly in all heat transfer and thermodynamic equations, optical properties, and parameters used in the model. The design and parameter study includes numerous charts showing a parabolic trough solar collector's linear receiver or heat collector element performance trends based on different design and parameter inputs. The model compared with experimental results and obtained a good agreement, finally suggested for further study about the heat collector element and trough improvements based on the design and parameter study.

Alguacil *et al.*, (2014) studied on parabolic trough collectors for direct steam generation applications with thermal oil as an HTF. The study developed temperatures higher than 400 ℃ due to operating by the second generation of parabolic troughs at, Abengoa solar power plant is assessing, it is the use of direct steam generation (DSG) inside parabolic troughs to achieve higher temperatures; the first stage heating up to 450 ℃ and the second stage heating up to 550 ℃.

- From the above literature survey due to the application of temperature range and simplicity of operation, flat plate collector, and parabolic trough collector are the most attractive type of solar collector. Therefore, the present study is taken those solar collectors used as solar energy collecting component to feed heat energy on TES systems for low temperature and high-temperature applications, respectively.

2.4 Storage media and heat transfer fluid (HTF)

This section contains the storage media and types of heat transfer fluid applicable for thermal energy storage systems. In the thermal energy storage system, especially sensible heat thermal energy storage heat will be stored in either solid or liquid media.

i. Storage media

There are two storage media is applicable in thermal energy storage system especially for sensible storage system used to store heat energy, which is solid and liquid storage media described as follows.

a. Solid Media

Solid media is one of the storage media in the storage system; usually it requires a heat transfer fluid (HTF) to exchange heat in TES systems. When very low heat capacity HTF used in the system like air, solid is the only storage material in that system. However, when the fluid is a liquid, its capacity is not negligible, and the system is called a dual storage system. An advantage of a dual storage system is the use of inexpensive solids such as rock, sand, or concrete for storage materials in conjunction with more expensive HTFs.

b. Liquid Media

Liquid media is another storage media used in TES systems, which maintain a natural thermal stratification (thermocline) because of density differences between hot and cold fluid. Due to the nature of density difference the hot fluid be supplied to the upper part of a storage system during charging and the cold fluid be extracted from the bottom part during discharging or using another mechanism to ensure that the fluid enters the storage at the appropriate level by its temperature (density) to avoid mixing this phenomenon is known as the thermocline.

ii. Heat transfer fluids (HTF)

Heat transfer fluids (HTF) is used to transfer thermal energy from the solar field collecting by the solar collector into the thermal energy storage system and a water storage tank for the water heating system or the heat exchanger for steam generation in CSP plants. The type and characteristics of HTF dictate the amount and the quality of energy that can be supplied to load and it must be compatible with the containment materials, storage media and be able to operate in the required temperature range. Thermal energy storage that operates at low and high-temperatures can use mainly water, thermal oil, molten salts, steam, air, etc., as heat transfer fluids (HTFs), and some of these are illustrated below.

Thermal oil: synthetic oil, most widely known as Therminol VP-1 brand name is used as an HTF in most CSP plants to avoid the high-pressure requirement and phase transition. It is highly flammable, hazardous to the environment if it should leak out of the system and this synthetic organic HTF can operate at high-temperature which is 400 °C used to collect and transport heat energy in most CSP plants.

Molten salt: it is non-toxic, non-flammable, has a low vapor pressure, and it is one of the most prominent heat transfer fluid as well as thermal energy storage mediums today. Different molten salt mixtures are available but they generally have similar heat transfer characteristics are solar salt, it is the most prominent type of molten salt for high-temperature application. It is a eutectic mixture of sodium nitrate (60% by weight) and potassium nitrate (40% by weight). It has a melting point of 238 ℃ and an operative temperature range of between 260 and 567℃.

Direct steam: it is another heat transfer fluid and that allows higher operational temperatures than possible with either molten salt or thermal oil. Theoretically, it is possible to achieve superheated temperatures, but the high operating pressures are a limiting factor why this is not always used as a heat transfer fluid.

Generally, the desirable properties of heat transfer fluids (HTFs) are listed below:

- ✓ High thermal conductivity
- ✓ High volumetric heat transfer capacity
- ✓ High boiling point
- ✓ Low viscosity for lowering pumping power
- ✓ Low price and easily available
- ✓ Low freezing point to reduce freezing problem which may clog the pipe
- ✓ Non-flammable and non-corrosiveness.

It is difficult to get HTF material that satisfies all of the above properties. Therefore, select the best-suited HTF in the present investigation by studying its effect on the system.

- ➢ Both the solid and liquid (during phase change) storage media are used in the present study in addition to this water and thermal oil are also selected as an HTF used for low and high-temperature thermal energy storage systems respectively. This is mainly due to the applicability of its working temperature range.

2.5 Thermal enhancement mechanism in the TES system

The development of proper thermal performance enhancement techniques must be required to design a cost-effective thermal energy storage system. **Liu *et al.*, (2012)** reviewed on thermal performance enhancement techniques for high-temperature phase-change thermal energy storage systems in CSP plants that were currently operating and under construction. During the study, various techniques employed to enhance the thermal performance of high-temperature phase-change thermal storage systems with melting temperatures above 300 ℃ had been reviewed and discussed.

Some of these various techniques were; by adding high conductive materials like graphite, extending heat transfer surface by fins and capsules, packing the phase change thermal storage system with multiple PCMs of different melting temperatures. Finally, the study concludes that sandwich configuration with graphite foil fins (up to 250 ℃) or aluminum fins (330 ℃) has proven to be promising to construct high-temperature phase-change thermal storage systems. There are a lot of studies were included in this section to enhance the thermal performance of thermal energy storage systems and from those enhancement techniques were listed as follows:

A. Enhancement using of extended heat transfer surfaces

Extension of heat transfer surface is one of the improvement techniques of the heat transfer rate because of reduces the distance for heat transport within the PCM in the form of using either capsules or finned tubes. Flexible capsules, usually plastic, are used for low-temperature PCM applications and fins usually graphite foil, aluminum, steel, and copper are arranged orthogonal to the axis of the heat transfer fluid pipes, namely sandwich design, are generally used to improve the heat transfer in the high-temperature storage system.

Jegadheeswaran & Pohekar, (2009) were great work on different performance enhancement techniques both experimentally and theoretically. According to the investigation, fins were a very promising heat transfer enhancing techniques focusing on lower temperature PCM materials (namely, paraffin), and they can be employed on either the PCM or HTF side and also studied on common fin arrangements in a latent heat storage system.

Bugaje, (1997) showed the effectiveness of fins in improving heat transfer rates, with fins performing better than star-shaped matrices and improving phase change times for both melting and freezing, with the effect more pronounced during solidification.

Agyenim *et al.*, (2009) worked on a comparison of heat transfer enhancement in medium-temperature thermal energy storage with a horizontal concentric tube exchanger using fins. Three experimental configurations, a control system with no heat transfer enhancement and systems augmented with circular and longitudinal fins have been studied. The experimental study also compared two practical heat transfer enhancement methods; circular finned and longitudinal finned systems with a control system with no heat transfer enhancement. The results presented to compare the system heat transfer characteristics using isotherm plots and temperature-time curves and satisfying longitudinal finned system.

B. Enhancement using highly conductive materials

Enhancement of thermal conductivity of thermal energy storage is a direct route of heat transfer improvement and focused on saturating high conductivity porous materials with PCM or dispersing highly conductive particles in the PCM. The heat transfer enhancement technique takes place within a PCM storage system by composing high thermal conducting material (sensible heat phase) into the PCM (latent heat phase). Graphite, aluminum, and copper are the most common materials used in such enhancement techniques incorporated with paraffin wax PCM latent heat storage systems.

Gunjo *et al.,* (2018) recently investigated on latent heat storage thermal conductivity enhancement mechanism by dispersed Cu, CuO, and Al_2O_3 nanoparticles in paraffin wax for solar thermal application. During the investigation addition of 5% of Cu, 5% of Al_2O_3 and 5% of CuO nanoparticles improved the melting rate by 10 times, 3.46 times and 2.25 times and the discharged rate by 8 times, 3 times and 1.7 times, respectively compared to the pure paraffin filled latent heat storage system.

Wu & Zhao, (2011) carried out both experimental and two-dimensional numerical analysis investigations on the solid/liquid phase change in which paraffin wax embedded in high porosity copper metal foams to enhance the heat transfer. The result compared to that of pure PCM sample, the effect of metal foam on solid/liquid phase change heat transfer is very significant and it can increase the overall heat transfer rate by 3-10 times (depending on the metal foam structures and materials) during the melting process. The result also showed that the use of metal foams can make the sample solidified much faster than pure PCM samples, evidenced by the solidification time being reduced by more than half.

C. Enhancement using multiple PCMs

Another heat transfer enhancement technique in thermal energy storage systems is by using multiple PCMs with different melting temperatures. In this type of enhancement technique, different PCMs containing different melting temperatures and those are connected in series. When employing multiple PCMs to enhance the thermal performance of latent heat storage systems, it is important to select the appropriate PCMs and relative proportions of the PCMs. The multiple PCMs in shell and tube units should be in the flow direction that the melting temperature decreases in the charging process and increases in the discharging process.

D. Enhancement using inserting of heat pipes

Embedding of the heat pipe is another thermal performance enhancement technique that can be used in thermal storage systems to serve as HTF tubes between the HTF and the thermal energy storage material.

Shabgard *et al.,* (2010) developed a thermal network model used to analyze heat transfer in a high-temperature latent heat thermal energy storage unit for solar thermal electricity generation. The impact of the number of heat pipes as well as their orientation relative to the HTF flow direction and the gravity vector in two distinct system configurations also investigated. Two storage configurations are considered; one with PCM surrounding a tube that conveys the heat transfer fluid, and the second with the PCM contained within a tube over which the heat transfer fluid flows. Both melting and solidification are simulated. Finally, it was demonstrated that adding heat pipes enhances thermal performance, which was quantified in terms of dimensionless heat pipe effectiveness.

Agyenim *et al.*, (2010) experimentally investigated heat transfer enhancement techniques in a medium temperature thermal energy storage system using a multi-tube heat transfer array energy storage system. The study analyzed the thermal characteristics in the systems using isothermal contour plots and temperature-time curves. The temperature gradients recorded in the axial direction for the control and multi-tube systems during the change of phase were respectively 2.5 and 3.5% that of the radial direction, indicating essentially a two-dimensional heat transfer in the PCM. The result showed that the multi-tube system improved the heat transfer rate during charging and produced a high output temperature.

- From the above section finally, conclude that there are various thermal performance enhancement techniques were given. However, those techniques have their side effects; for example, enhance by using extended heat transfer surface was reduces storage volume from PCM in a container. This affected the thermal storage capacity and those also more impact on improving the solidification rate than the melting rate. The second technique was enhancement by using multi-PCM, and this needs different phase change material then it leads to economic impact.
- To solve the above problem, enhance the heat transfer rate by using embedding of multi-HTF tubes or pipes between the HTF and the storage material is the best thermal performance enhancement technique apply in the thermal energy storage system. Similarly, inserting highly conductive material in the HTF tube also enhances the heat transfer rate especially for low thermal conductivity storage material. Due to this fact, the present study also applies this heat transfer enhancement technique in both developed TES storage model

2.6 Local researches on the thermal energy storage system

There are a few numbers of local research works investigated regarding thermal energy storage systems because of fewer policy decisions are applied to promote and implement solar renewable energy for different solar thermal applications. However, the present study included among some of these few related research works given below.

Tesfay *et al.*, (2014) investigated on solar-powered heat storage for injera baking application in Ethiopia. During the investigation heat storage is developed and tested by integrated with injera baking application at different places. Direct steam-based injera baking prototype developed and tested in Mekele University (Ethiopia) and the other baking mechanism heat storage with PCM based prototype was developed and tested at NTNU. Finally, the paper concludes that there is a possibility of injera baking in both cases, but included latent heat storage is used to increase sustainability for the injera baking mechanism.

Tesfay & Venkatesan, (2013) worked on CFD analysis of sensible thermal energy storage systems in solar thermal power plants. The material used during the investigation was concrete and solid NaCl sensible thermal energy storage material as a solid medium and parabolic trough solar collector. The design TES system produced 1MWe and the result showed by Gambit and fluent software simulation and finally, the study concluded that integrating sensible thermal energy storage can be used in a solar thermal power plant.

Yayeh, (2013) studied thermal energy storage systems by designing a solar thermal powered Injera baking system to made cooking indoor convenient and avoid the problems caused due to carbon inhalation and deforestation. The system consists of the primary concentrator (Scheffler), secondary reflector, and thermal energy storage system with the cooking (pan) assembly. The storage device involves a sensible heat storage mechanism with Hitec heat transfer salt as a storage medium. During the investigation, the study also determined the heat retention capacity of the thermal energy storage system from heating and cooling curves generated during modeling and simulation by ANSYS software.

Asefa, (2019) studied the performance analysis of PCMs (Erythritol) encapsulated by spherical capsules integrated into the solar vapor absorption refrigeration system for industrial application. The study developed a Python coding to solve a one-dimensional unsteady heat transfer phenomenon. The coupled partial differential equations of the spherical PCM and the heat transfer fluid were numerically solved using the finite difference method and the enthalpy approach. Finally, the study demonstrated that the time required to charge the PCM is lower than the discharging time mainly due to the natural convection inside the spherical capsule at the phase transition state. The liquid part creates natural convection on the interface of the sphere, which is directly related to the amount of liquid phase inside the capsule.

Kefa, (2019) performance analysis of concrete based thermal energy storage system by integrated a linear Fresnel collector for heat generation at the industrial process. A one-dimensional transient numerical model is developed for concrete thermal energy storage and solved using a finite difference scheme. Finally, the investigation concludes that the thermal energy storage can serve as a thermal battery for smoothing the output from the collector field and buffer storage in cloudy hours of the day.

2.7 Literature summary

In this chapter presented a detailed literature survey regarding the investigation of various TES systems for low and high-temperature applications with both sensible and latent heat storage. Extensive studies on types of solar collectors (flat plate solar collectors and parabolic trough solar collectors) and various thermal performance enhancement techniques implemented in the TES systems are also reviewed. The TES materials, storage concept, storage media, and heat transfer fluid (HTF) used in both low and high-temperature applications are briefly studied and included local studies relevant to TES systems. It is usually required to specify the major area of studies and its finding; therefore, Table 2.1 has summarized some literature major findings. Finally, it is observed from the literature review that thermal energy storage systems have been proved; it is reliable, economically viable, environmentally friendly, and generally useful to develop and promote strong solar thermal energy. Considering these facts, the present study targets an investigation of TES systems for low and high-temperature applications by developing a three-dimensional TES model with sensible and latent heat as a storage mechanism.

Table 2.1 Literature summary

Year	Authors	Major finding
2007	Vyshak & Jilani	Study the effect of the shape of the LHS system.

2009	Agyenim *et al.*	Fins were a very promising heat transfer enhancing techniques focusing on lower-temperature PCM materials.
2011	Pinel *et al.*	Water is the best sensible TES material for residential applications.
2011	Wu & Zhao	Carried out experimental analysis in the LHTES system to enhance heat transfer rate by embedding copper foams into a paraffin wax storage bed.
2012	Liu *et al.*	Reviewed on thermal performance enhancement techniques for high-temperature LHTES systems.
2013	Wang *et al.*	Study the effect of the inlet temperature of HTF on the thermal performance of the shell-tube LHS system.
2013	M. Tesfay & Venkatesan	A local paper worked on CFD analysis of concrete STES systems in solar thermal power plants and produced 1MWe.
2014	Rathod & Banerjee	Paraffin wax can be widely used LHTES material for low temperature solar thermal applications.
2016	Tehrani *et al.*	The highest amount of stored/delivered energy is achieved by a proper design method of the storage configuration.
2017	Singh & Sørensen	Carried out a numerical investigation on a concrete based TES system for steam generation.
2018	Alva *et al.*	Grouped TES systems based on the operating temperature range.
2018	Wei *et al.*	Evaluated the selection principles of PCMs on high-temperature thermal energy storage systems.

Additionally, the following concepts are briefly depicted in this study and used as a by-product during the investigation:

- ✓ Flat plate collectors and parabolic trough solar collectors are used as solar radiation collecting elements for low and high-temperature applications respectively.
- ✓ Paraffin wax, water, concrete, and nitrate salt (KNO_3) is selected as a storage material to use in the developed TES model.

- ✓ Embedding of a multi-HTF tube between the storage material and the heat transfer fluid was used as a thermal enhancement technique.
- ✓ Water and thermal oil used as a heat transfer fluid.
- ✓ A passive storage concept with a shell-tube regenerative heat exchanger type storage configuration is used during the investigation.

2.8 Research gaps

The literature reviewed still has a wide range of gaps that are to be addressed in the upcoming years with a focused dedication to enhancing the concept of the TES system to bridge a gap between the present and past research. Although a lot of efforts made to develop the TES systems integrated for different thermal applications, the following areas still demand the attention of the researchers.

- ➢ Several researchers developed a lot of storage models to study the performance characteristics of the TES system. However, the majority of the developed TES models were based on a single shell and tube heat exchanger type TES model. Enhancing of TES system using embedding of multi-HTF tubes between the HTF and the storage material rarely investigated.
- ➢ It is understood from the literature survey that most of the research work on the TES model is concerned with either sensible heat storage systems or latent heat storage systems with a specific temperature range.
- ➢ The other is time take to reach phase transition temperature for a latent heat thermal energy storage system. But up to the phase change transition temperature; it is the sensible heat storage system. Therefore, a system must design which will work as both a sensible and latent heat storage unit, called a multi-functional storage unit.

Considering these facts, the present work aims to fill the above-mentioned gaps by developed efficient thermal energy storage systems integrated for low and high-temperature applications, with enhancing the thermal performance of the developed TES system.

CHAPTER THREE

METHODOLOGY

This chapter introduces the method employed and details numerical expressions of the overall modeled TES system considered, to achieve the objective of the research which is mentioned in chapter one. Sources of data and methods of gathering those data, research design method, and calculation of the available solar radiation thought the year using the given metrological data also presented in this chapter.

3.1 Proposed methodology

The schematic diagram of the conceptual framework of the applied methodologies so-called proposed methodology is as shown in Fig. 3.1.

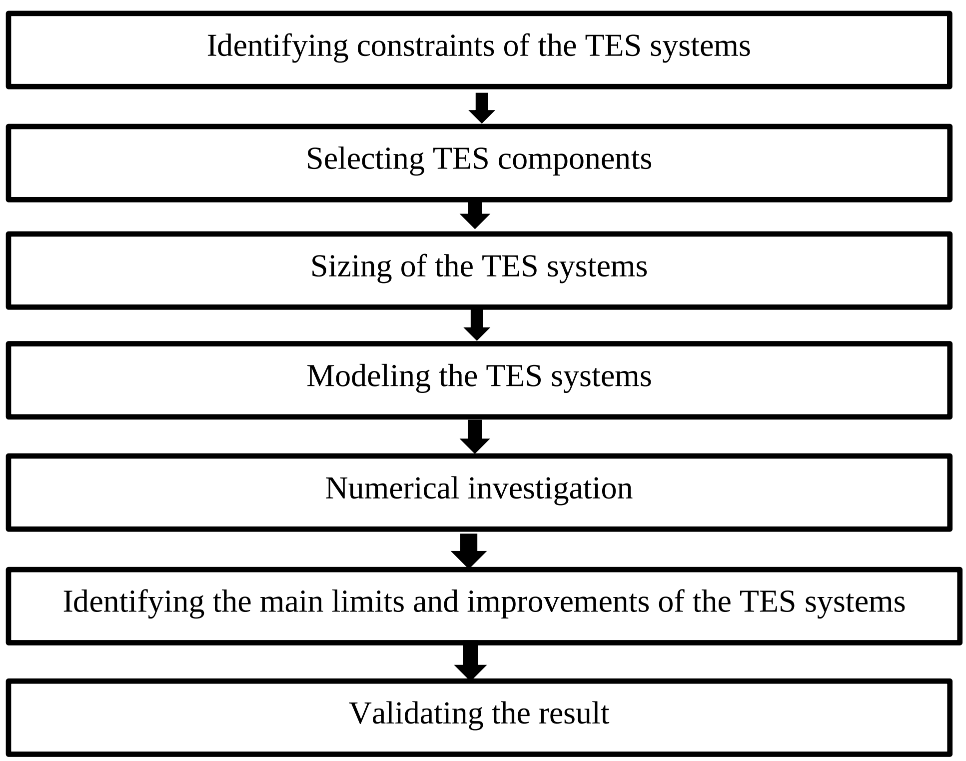

Fig.3.1 A proposed methodology for the present study

3.2 Data collection and data analysis

Data has been collected from both primary and secondary sources in the present study. The primary data sources would be taken by direct measure temperature, charging, and discharging time from previous thermal energy storage systems developed by local researchers for different applications. Secondary sources of data include; reference books, journals, kinds of literature, internet, etc., and Ethiopian energy status from the Ethiopian energy sector was being collected in this investigation. Reviewed some literature papers or previous patented work regarding the TES system also performed for this study to gathering brief information about thermal energy storage materials on its classification, applications, and performance enhancement mechanism from those papers. The appropriate storage material for a given sensible and latent heat thermal energy storage system for both low and high-temperature range is identifying from the literature.

3.3 Research design

The method uses to do this thesis is theoretically as well as numerical approaches. The software that has been used for the present study was COMSOL Multi-physics 4.3a commercial software, and M.S office 2019. Mathematical modeling implemented to study the TES performance parameters such as charging and discharging time, liquid fraction, stored/released energy numerically. A 2D model is developed to optimize the number of HTF tubes with a theoretical approach. The result of TES systems obtained from the simulation is also validated with the previous experimental as well as numerical study. Related literature obtained from academic literature, articles, websites, etc., were studied to gain brief information about the study and used as a bridge to achieve the objective of the present research. The study would also do based on hypothesis and hypothesis testing and both qualitative and quantitative research design techniques will be used.

3.4 Estimation of available solar radiation within the climatic condition

Solar radiation data is necessary for any solar energy conversion device design and to determine the level of solar radiation for the given location and the amount of energy available at the collector surface. So, in this investigation also solar radiation data collected from Meteorology are required for evaluating the available amount of heat energy used as an input in the TES system. The present investigation is performed on one of the tropical characterized climatic conditions which are located at Adama within a monthly average temperature range of 20.1℃ (December) and 24.1℃ (March) as shown in Table 3.1; it has a high intensity of solar radiation. So, in this paper five years of average climatic conditions of Adama are used to analyze different parameters.

Table 3.1 Monthly average annual climatic condition of Adama (**Ethiopia National Meteorology Agency**)

Temperature (℃)	Month											
	Jan	Feb	Mar	Apr	May	Jun	Jul	Aug	Sep	Oct	Nov	Dec
Min	13.3	15.7	17.2	17.0	17.2	17.1	16.7	16.6	15.9	15.6	14.9	13.6
Max	27.6	29.3	31.1	30.7	30.2	29.8	29.2	27.1	28.2	28.8	27.8	26.6
Average	20.4	22.5	24.1	23.9	23.7	23.5	22.9	21.9	22.0	22.2	21.3	20.1
Wind speed (m/s)	3.5	2.7	3.2	3.5	3.1	2.8	3.1	2.7	2.8	3.4	4.3	3.5

This data can be derived from satellite imagery, where models of surface and cloud reflectivity allow the solar radiation at ground level to be estimated with reasonable accuracy. The solar thermal energy system requires accurate estimates of direct beam irradiation data to perform numerical simulation and succeeding economic evaluation tasks for the different solar collectors. The purpose of study this section is therefore to use the available sources of solar irradiation data, which is found from National Meteorological Agency to arrive at a good estimate of the solar resource at Adama city, in such a way that subsequent modeling can predict the solar collector system output with some confidence. in the present study, an empirical model is used to predict and estimate solar radiation. Because there is a scarcity of trustworthy solar radiation data in the given location and also these models use climatological parameters of the location under study. Among which sunshine hours are the most widely and commonly used climatological parameters for this study.

3.4.1 Calculation of extraterrestrial solar radiation

Extraterrestrial solar radiation (I_O) is simply the solar radiation outside of the earth's atmosphere which is found from the sun's position in the sky as seen from the earth as a function of the day of the year and of the time of the day. Calculating each day of the year, the day time duration, global daily solar radiation (I_G) on a horizontal surface and, global daily solar irradiance received by a horizontal surface at the upper limit of earth atmosphere (I_O), which is known as extraterrestrial. The main thing in the calculation of extraterrestrial solar radiation is determining of incident solar radiation; initially by finding out solar hour angle (ω_{sr}) from the solar time equation. Solar time is a time based on the apparent angular motion of the sun across the sky with solar noon which the sun crosses the meridian of the observer and it is given by (**Duffie and Beckman, 2013**):

Solar time = Standard time + $4(L_{st} - L_{loc})$ + E 3.1

where: L_{st}- represents standard meridian for the local time zone, in degrees ($0° \leq L_{st} \leq 360°$) L_{loc}- represents longitude of the location in the equation, in degrees ($0° \leq L_{loc} \leq 360°$) and E- is the equation of time (in minutes), and is given by:

E = 229.2 (0.000075+ 0.001868 $\cos B$ – 0.032077 $\sin B$ – 0.014615 $\cos 2B$ – 0.014615 $\sin 2B$) 3.2

B = (n - 1)* $\frac{360}{365}$ 3.3

where: n- is the nth day of the year, thus $1 \leq n \leq 365$

The position of a location on the earth's surface is defined by the coordinate's latitude and meridian or longitude angles. Depending on the orientation of the inclined surface, the the expression for the basic sun-earth Angles is obtained as:

Hour angle, ω (^{0}): it is the angular displacement of the sun towards east or west of the local meridian due to rotation of the earth on its axis at 15^0 per hour. The value is negative in the morning and positive in the afternoon, and it is given by (**Duffie and Beckman, 2013**):

ω = (Solar time - 12)*15 3.4

Declination angle, $\boldsymbol{\delta}$ (^{0}): is the angular position of the sun at solar noon (i.e., when the sun is on the local meridian) concerning the plane of the equator, north positive; $-23.45^0 \leq \delta \leq 23.45^0$ and is given by (**Duffie and Beckman, 2013**):

$$\delta = 23.45 * \sin\left(\frac{360}{365}(284 + n)\right) \quad 3.5$$

Representative Day of each month in the year and the value of the declination angle on its day can be obtained by Table 3.1.

The zenith angle, $\boldsymbol{\theta_Z}$ (^{0}): is the angle between the vertical and the line to the sun that is the angle of incidence of beam radiation on a horizontal surface, which is given by the equation:

$$\cos\theta_Z = \cos\phi\cos\delta\cos\omega + \sin\phi\sin\delta \quad 3.6$$

where: ϕ is the latitude angle and it is equal to 8.557^0 for Adama location.

The angle of incidence, $\boldsymbol{\theta_i}$ (^{0}): it is the angle between the sun's ray incident on the plane surface (collector) and normal to that surface. The relationship between the angle of incidence θ_i and the other angles is given by (**Duffie and Beckman, 2013**):

$$\cos\theta_i = \sin\delta\sin\phi\cos\beta - \sin\delta\cos\phi\sin\beta\cos\gamma + \cos\delta\cos\phi\cos\beta\cos\omega + \cos\delta\sin\phi\sin\beta\cos\gamma\cos\omega + \cos\delta\sin\beta\sin\gamma\sin\omega \quad 3.7$$

where: β is the slope or tilt angle which is defined as the angle between the inclined plane surface and the horizontal, and γ is surface azimuth angle which is the angle in the horizontal plane, between the line due south and the horizontal projection of the normal to the inclined plane surface. At sunrise, the sun's ray is parallel to the horizontal surface, hence $\theta_i = \theta_Z = 90^0$ the solar hour angle magnitude, ω_{sr} is calculated as follows:

$$\omega_{sr} = \cos^{-1}(-\tan\phi\tan\delta) \quad 3.8$$

Since 15^0 of hour angle is equivalent to one-hour duration, so the duration of the day time, N_H (hr.) is given by:

$$N_H = \frac{2}{15}\omega_{sr} \quad 3.9$$

Table 3.2 Recommended average days for months in the year (**Duffie and Beckman, 2013**)

Month	n for i^{th} Day of the Month	For the average Day of the Month		
		Date	n, Day of the Year	δ , Declination
January	*i*	17	17	-20.9
February	31 + *i*	16	47	-13.0
March	59 + *i*	16	75	-2.4
April	90 + *i*	15	105	9.4
May	120 + *i*	15	135	18.8
June	151 + *i*	11	162	23.1
July	181 + *i*	17	198	21.2
August	212 + *i*	16	228	13.5
September	243 + *i*	15	258	2.2
October	273 + *i*	15	288	-9.6
November	304 + *i*	14	318	-18.9
December	334 + *i*	10	344	-23.0

The global daily solar irradiance received by a horizontal surface at the upper limit of earth atmosphere (expressed in J/m^{2}day), is calculated as follows (**Duffie and Beckman, 2013**):

$$I_O = \frac{24*3600}{\pi} I_{SC} \left[1 + 0.033 \cos\left(\frac{360n}{365}\right)\right] * [\cos\phi \cos\delta \sin\omega_{\mathbf{sr}} + \pi \frac{\omega_{\mathbf{sr}}}{180} \sin\phi \sin\delta] \qquad 3.10$$

where: I_{SC} is the solar constant, which is equal to 1367 W/m^2

3.4.2 Calculation of monthly average daily global radiation on a horizontal surface

Global solar radiation (I_G) is the sum of the beam and the diffuse solar radiation on a surface, or simply it is the most common measurements of total solar radiation on a horizontal surface, often referred to as global solar radiation on the surface. The solar energy reaching on the earth's surface is reduced while crossing the atmosphere because of absorption, reflection, and scattering by liquid and solid aerosols, etc., especially in the case where a cloud cover is present. The monthly average daily global radiation on a horizontal surface may be estimated from sunshine records by the Angstrom correlation, as (**Tiwari, 2018**):

$\frac{I_G}{I_O} = a_1 + b_1(\frac{n_s}{N_s})$ 3.11

where: n_s is the daily bright sunshine hours as shown in the Fig.3.2 and N_s is the maximum possible daily bright sunshine hours and a and b are regression constants, the values are determined by Angstrom correlation as follows:

a_1 = -0.110 + 0.235cos ϕ + 0.323($\frac{n_s}{N_s}$) 3.12

b_1 = 1.449 – 0.533 cos ϕ – 0.694 ($\frac{n_s}{N_s}$) 3.13

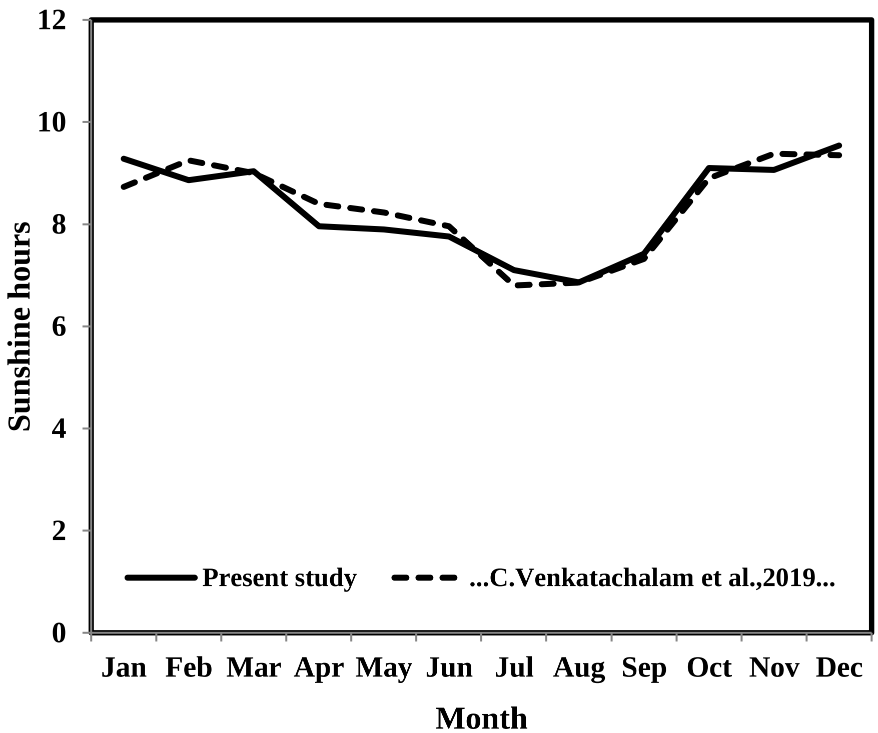

Fig.3.2 Bright sunshine hours for the representative days of each month in Adama (**Ethiopia National Meteorology Agency**)

Therefore, from Fig.3.2 we obtained a maximum bright sunshine hour in December and a minimum bright sunshine hour in July whose values are 9.54 and 7.1 hours respectively in the present location. Similarly, it also a good agreement after validated with **(Venkatachalam *et al.*, 2019)** published work.

3.4.3 Calculation of the beam and diffuse daily solar irradiation on a horizontal surface

The monthly average daily beam, I_B and diffuse radiation, I_D (kWh/m^2/day) on a horizontal surface, can be determined from the monthly average daily global radiation on a horizontal surface and the number of bright sunshine hours (**Duffie and Beckman, 2013**):

$$\frac{I_D}{I_G} = 0.931 - 0.814\ \left(\frac{n_S}{N_S}\right) \qquad 3.14$$

The average daily beam solar radiation hitting on a horizontal surface at ground level, I_B, is can be found by simple deduction:

$$I_B = I_G - I_D \qquad 3.15$$

The monthly average global, diffuse and beam radiation on a horizontal surface in Adama for an average climatic condition of five years is given in Fig 3.3.

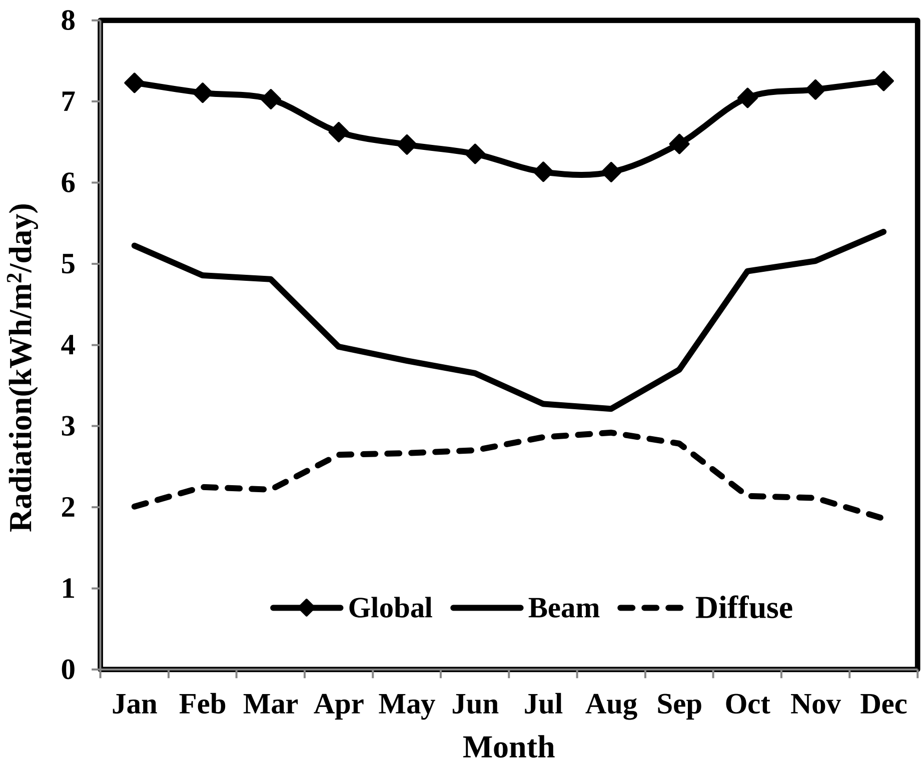

Fig.3.3 Monthly for daily average global, diffuse and beam radiation on a horizontal surface

3.4.4 Calculation of monthly average hourly solar incidence on a horizontal surface

The monthly average hourly beam (I_B^*) and diffused (I_D^*) solar irradiances (kW/m^2) on a horizontal surface as a function of the time of the day can be calculated from a relationship with the above equation of the monthly average daily global radiation on a horizontal surface by using the expression proposed by Collares-Pereira correlation (**Duffie and Beckman, 2013**). In this study, a one-second resolution of solar radiation is taken for transient analysis in the subsequent sections. During day time, I_B^* and I_D^* are given by:

$$I_D^* = \frac{\pi}{24*3600}[a + b\cos\omega] * \frac{\cos\omega - \cos\omega_{\mathbf{sr}}}{\sin\omega_{\mathbf{sr}} - \frac{\pi\omega_{\mathbf{sr}}}{180}\cos\omega_{\mathbf{sr}}} * I_D \qquad 3.16$$

$$I_B^* = \frac{\pi}{24*3600}[a + b\cos\omega] * \frac{\cos\omega - \cos\omega_{\mathbf{sr}}}{\sin\omega_{\mathbf{sr}} - \frac{\pi\omega_{\mathbf{sr}}}{180}\cos\omega_{\mathbf{sr}}} * I_B \qquad 3.17$$

where: $a = 0.409 + 0.502\sin(\omega_{\mathbf{sr}} - 60)$ 3.18

$b = 0.661 - 0.477\sin(\omega_{\mathbf{sr}} - 60)$ 3.19

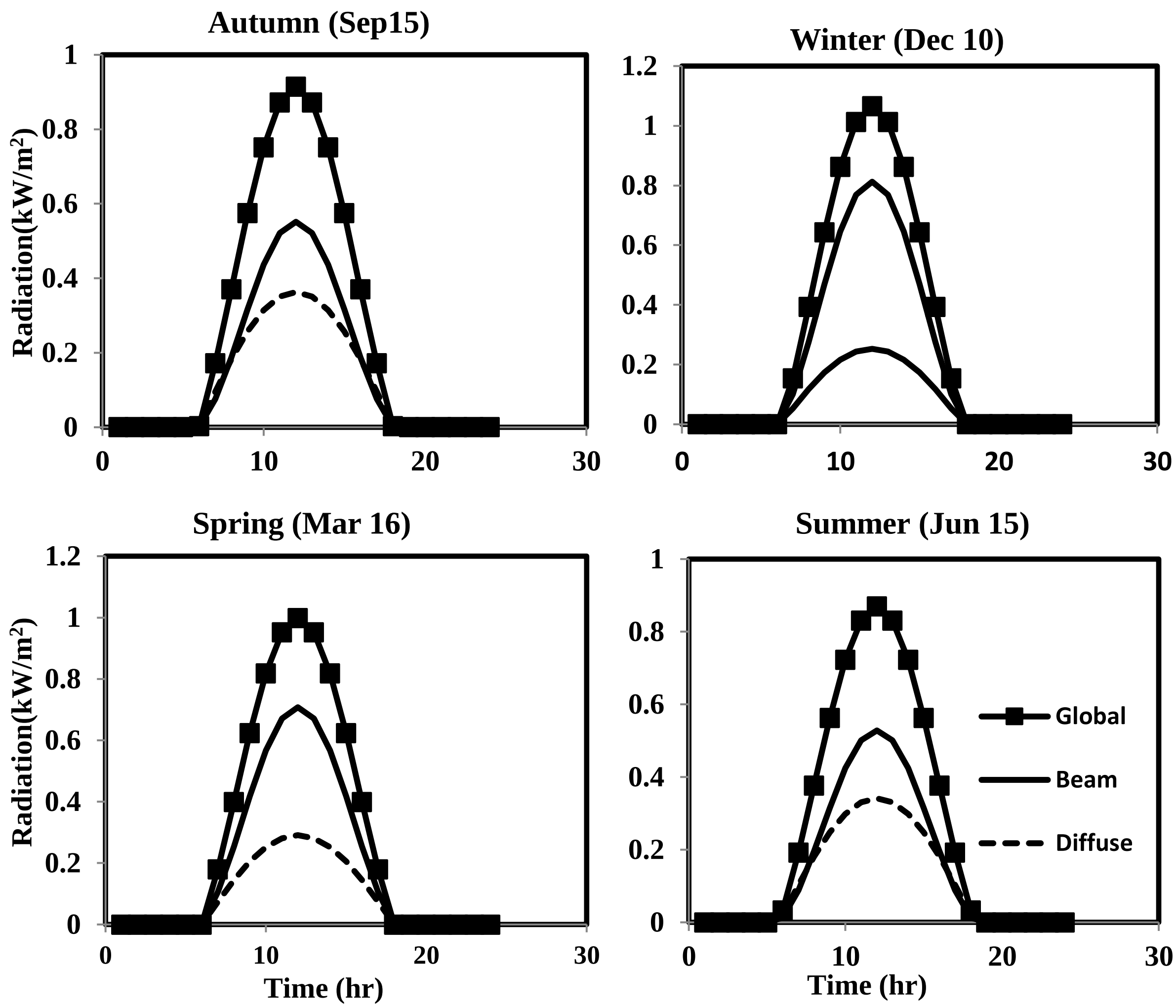

Fig.3.4 Hourly global, beam and diffused radiation on a horizontal surface for the representative day of each season of the first month

The monthly average hourly global solar radiation is the sum of the average hourly beam and the diffuse solar radiation on a surface, (I_G^*) and it can be found by simple summation and the radiation for the representative day of each season of the first month is as shown in Fig 3.4.

$$I_G^* = I_D^* + I_B^* \tag{3.20}$$

3.4.5 Estimation of hourly variation of ambient temperature

Estimation of hourly variation of ambient temperature can be approximated from the daily mean maximum and the daily mean minimum temperature because it is difficult to get data for hourly variation of ambient temperature in this location. A sinusoidal variation of the ambient temperature throughout the day and the maximum temperature at 15:00 h sun time is assumed as shown in Fig 3.5. The hourly variation of temperature, $T(h)$ at any time t is given by **(Reicosky *et al.*, 1989**):

$$T(h) = \frac{T_{max} + T_{min}}{2} + \frac{T_{max} - T_{min}}{2} \sin \frac{(\pi h - 9\pi)}{12} \quad 3.21$$

where: T_{max} is mean daily maximum temperature at 15:00 h sun time and T_{min} is mean daily minimum temperature and 'h' is time in hours.

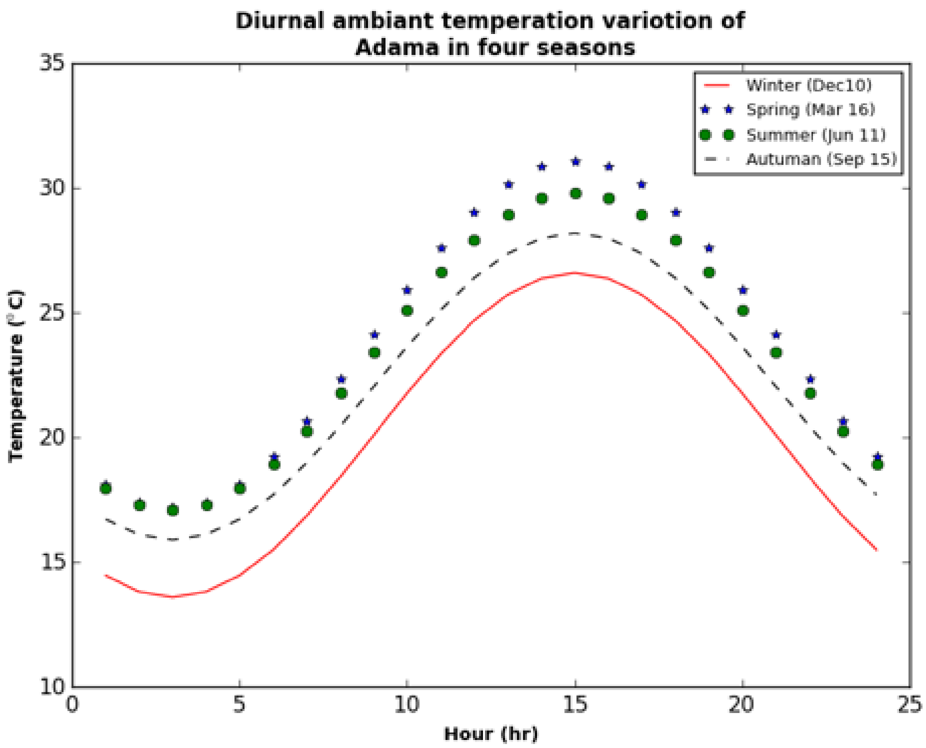

Fig.3.5 Diurnal ambient temperature variation of Adama for the representative day of each season of the first month

In the present investigation, it can take the ambient temperature is 25 ℃ as illustrated in Fig.3.5. This value is bounded within the range, during estimation of hourly variation of ambient temperature for the representative day of each season of the first month at the present location as shown in the above figure.

3.4.6 Useful energy gained by HTF in the solar collector

There is a rough estimation has been done in this section to find out the mass flow rate of the HTF by applying the energy balance in the solar collector. The TES system is worked by integrated two types of solar collectors as theoretically described in the preceding chapter which is; flat plate solar collector integrated for low-temperature TES system and parabolic trough for high-temperature TES system. The value of different parameters of the two collectors is taken from specifications that have listed out by different manufacturers. In steady-state, the performance of a solar collector is described by applying an energy balance that indicates the distribution of incident solar energy into useful energy gain, thermal losses, and optical losses. The solar radiation absorbed by a tilted collector per unit area of the absorber (S) is equal to the difference between the incident solar radiation, which is determined by the relationship **(Duffie and Beckman, 2013)**.

$$S = \tau \alpha I_T \qquad 3.22$$

where: τ, α, and I_T are the transmissivity of the glass cover, the absorptivity of the absorber, and the incident solar radiation on the collector respectively.

The incident solar irradiant energy on the solar collector surface, which is inclined at an angle of (β_a) to the horizontal surface is defined in terms of a global, diffuse, beam, and reflected radiation as shown in Fig.3.6. Total solar radiation incident on a surface can be evaluated by taking arbitrary orientation from the previous result of a beam, diffuse, and global radiation on a horizontal surface **(Duffie and Beckman, 2013)**.

$$I_T = I_B R_B + I_D \left(\frac{1+\cos\beta}{2}\right) + I_G \rho_G \left(\frac{1-\cos\beta}{2}\right) \qquad 3.23$$

$$\beta_a = \phi + 15° \qquad 3.24$$

where: ρ_G is the ground reflectivity factor whose value is 0.2 for ordinary ground and R_B (beam radiation factor) is the ratio of beam solar radiation on the inclined surface to that on a horizontal surface, which is given by:

$$R_B = \frac{\cos\theta_i}{\cos\theta_z} \qquad 3.25$$

As shown in Fig.3.6 the average hourly solar irradiance on a tilted collector surface is varies from 873 W/m^2 in August to 961 W/m^2 on March.

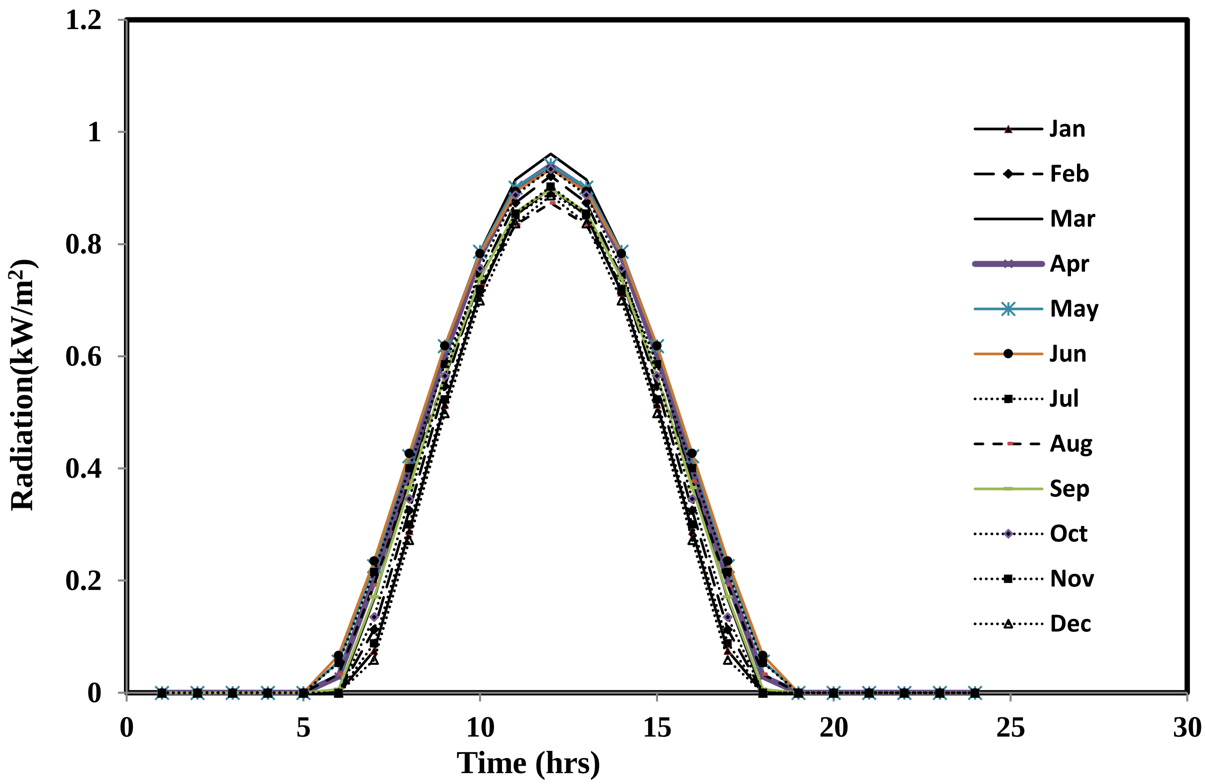

Fig.3.6 Monthly average hourly incidence of solar radiation on a tilted collector surface

For the present investigation the average hourly solar irradiance on a tilted collector surface is on the first months of the summer season which is June 15 detected from 8AM up to 5PM of the day as shown in Fig.3.7. Assume three sunshine hours starting from 10AM up to 13PM can achieve the required amount of temperature enable to charge the thermal energy storage material, so to determine the useful energy from collector outlet. So, the average hourly solar irradiance on a tilted collector 730 W/m^2 at 10AM is taken for low temperature TES system. The amount of solar radiation received by the collector (Q_i), the useful energy output (Q_u) from the collector with a collector area (A_c) express in terms of the inlet (T_i) and outlet (T_o) temperature of the HTF is given by Eq. (3.27) and Eq. (3.28). A measure of collector performance known as thermal efficiency (η) of the collector is also determined by Eq. (3.29) (**Duffie and Beckman 2013**).

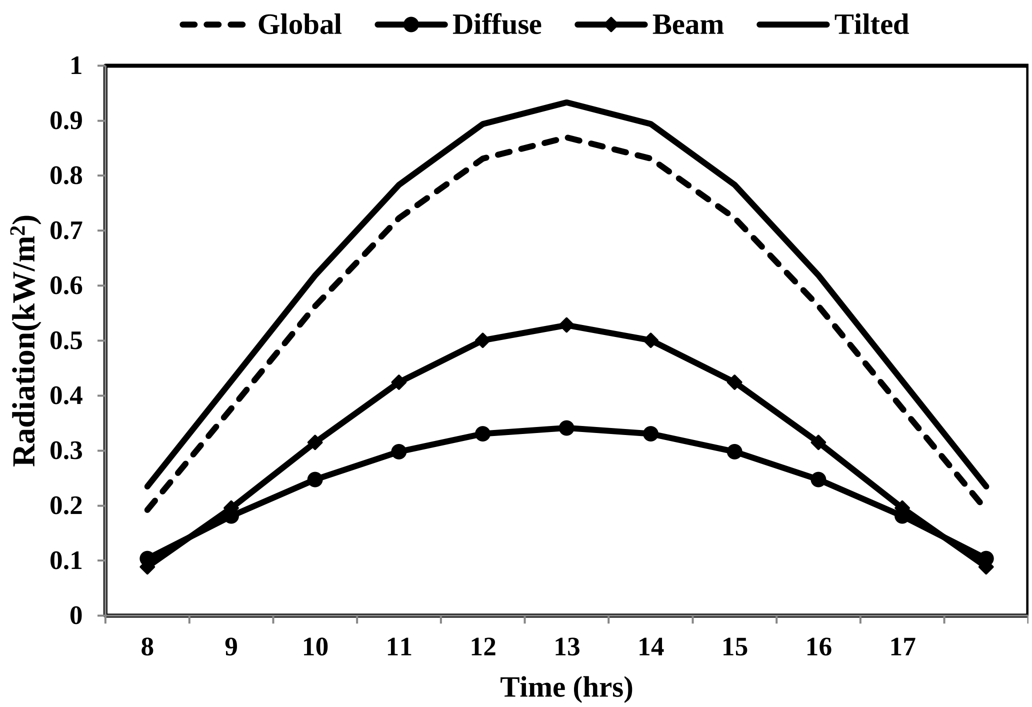

Fig.3.7 Estimated hourly variation of solar radiation of Adama on June 15

$$\dot{Q}_\iota = S * A_c \qquad 3.26$$

$$\dot{Q}_u = \dot{m}C_P(T_o - T_i) \qquad 3.27$$

$$\eta_{FPC} = \frac{useful\ energy\ output\ (\dot{Q}_u)}{the\ absorbed\ solar\ energy\ (\dot{Q}_\iota)} = \frac{\dot{m}C_P(T_o - T_i)}{S * A_c} \qquad 3.28$$

Flat plate collector systems can be operated with different flow rates, at the same collector output, whenever the flow rate is higher, a lower temperature will be obtained and higher efficiency in the collector circuit. On the other hand, a lower flow rate results in a higher temperature output but lower efficiency. According to **(Gunjo *et al.*, 2017),** the total heat loss from the commercial flat plate solar collector is (33-50 %), that means the efficiency of FPC have been obtained from 50 to 67 %, so for the present study select the minimum heat loss or the maximum efficiency i.e., (η = 67%) for flat plate solar collectors. The mass flow rate of the system can be estimated from the efficiency of the collector and the required outlet temperature of HTF using Eq. (3.28). The collector outlet temperature that has taken for low-temperature TES model varies from 70 to 80 ℃ and the required outlet temperature from the collector to heated the low temperature TES is 75 ℃ and the average ambient temperature of Adama city are 25℃. Then, the mass flow rate of HTF in the system form total estimated average solar radiation collected within the given aperture area is found to be 0.0041kg/sec.

Similarly, the efficiency (η_{PTC}) of parabolic trough collectors can be expressed as follows:

$$\eta_{PTC} = \frac{\dot{Q_u}}{I_B^* * A_{ap}} = \frac{\dot{m} C_P (T_O - T_i)}{I_B^* * A_{ap}} \quad 3.30$$

According to **(Kalogirou, 1996)** the parabolic trough collector is applicable in many solar power plants with operate at temperatures up to 400 ℃ and synthetic oil is used as a heat transfer fluid. The optical efficiency of PTC is within the range of 53-71% and similar to the preceding selection criteria for the present collector takes the maximum efficiency of PTC (71%) **(Huang *et al.*, 2012)**. The additional specification of parabolic trough collector that have used in the present study is given in Table B1 in the ANNEX B. Similar to the flat plate collector, to determine the useful energy from parabolic trough collector outlet, the average hourly solar incidence that have taken is the average hourly beam radiation on June 15 at noon, which is 528 W/m^2. Finally, substituting the values in Eq. (3.30), the mass flow rate of the HTF working on the PTC is 0.01 kg/s.

The other thing is the temperature of the HTF from the collector outlet is 5-20 K exceeds than the melting or fully charging temperature of storage material **(Wang *et al.*, 2013)** and **(El Qarnia, 2009)**. So, the collector outlet temperature that has taken for low-temperature TES model varies from 70 to 80 ℃ and also for high-temperature TES model it varies from 380 to 390 ℃ temperatures range. Those values are used as a prerequisite to finding out the mass flow rate of the HTF and it can be calculated from Eq.3.29 and Eq. (3.30). Then the obtained results that can be found in both collectors (FPC and PTC) are 0.0041 kg/s and 0.01 kg/s respectively. The detail specification of the solar collectors that have selected for the present investigation is given in APPENDEX-A and APPENDEX- B

CHAPTER FOUR

PERFORMANCE ANALYSIS OF TES SYSTEM FOR LOW-TEMPERATURE APPLICATION

The aim of this chapter is to presents the performance analysis of the thermal energy storage (TES) system for low-temperature applications (used in domestic water heating purposes). It contains system description, sizing the physical model of the thermal energy storage system, and the developed mathematical modeling of the TES system. The theoretical assumption, governing equation, initial and boundary condition, mesh generation, and numerical simulation are also included to study the thermal performance parameters in this chapter.

4.1 System description

One of the proposed systems in the present study has to build a low-temperature thermal energy storage system integrated for domestic solar water heating purposes as illustrated in Fig 4.1. The system has three main components; a solar collector element (flat plate collector), shell-tube type thermal energy storage bed, and water storage tank with well-insulated. However, the main objective of the present investigation is concerned with the performance analysis of the thermal energy storage (TES) component and studied numerically in-depth. The working principle is shown in Fig.4.1 and Fig. 4.2, which is during the charging cycle the cold heat transfer fluid (HTF) is pumped into the solar collector to be heated up and then goes through the thermal energy storage (TES) material to store the heated energy. As the HTF flows through the TES material, heat is transferred from the HTF to the TES material and the process is continued until the TES material attains its inlet temperature of the HTF.

During the discharging cycle, the hot HTF flows from the storage material into the water storage tank to use for domestic heating purposes, while the cold HTF is pumped back into the TES material through the bottom. This process also controlled by a regulator or control valves to open and closed the piping system. The HTF coming from the solar collector is used to supply heated water for domestic applications, so the aim of building thermal energy storage for this application is to store the heat energy collected from the flat plate collector during the sunshine hour and released during the absence of solar radiation. The selection of TES material is based on the temperature range of the present application and tested both sensible and latent heat storage material with the same model and the same size, then compare which one can perform to fulfill the energy demand. The TES material for low-temperature application (domestic water heating purpose) that was select from the literature is based on the thermo-physical properties, cost-effectiveness, easily availability, and flexibility, and also it can be easily compatible with a different application. Which is a technical grade paraffin wax and water (**Ukrainczyk *et al.*, 2010**), **(Sharma *et al.*, 2004)** and **(Alva *et al.*, 2017)** are selected as latent and sensible heat TES material respectively in the developed TES model. The thermo-physical properties of selected storage materials are given in Table 4.1.

Table 4.1 Thermo-physical properties of low-temperature TES material

TES material	Melting Point (K)	Latent heat of fusion (kJ/kg)	Density (kg/m^3)		Specific heat capacity (kJ/kgK)		Thermal conductivity (W/mK)	
			Solid Phase	Liquid Phase	Solid Phase	Liquid Phase	Solid Phase	Liquid Phase
Paraffin	327	238	912	769	1.8	2.4	0.21	0.15
Water	273-373	-----	------	1000	-----	4.18	------	0.58

4.2 Sizing of sensible TES system water used as a storage material

The water storage tank can be sized according to the daily heating load requirements. The schematic diagram of the system under study of water storage tank, which is shown in Fig. 4.2, consisted of an insulated cylindrical TES tank containing water as a storage material and a flat plate collector. The water thermal energy storage that builds for low-temperature applications is responsible to fulfill the energy demand of 66 L/day hot water at 50℃. The hot water needed for one person was 11 liters per day, then in one family average 6 persons are live, then the total hot water needed in that family was 66 L/day at 50 ℃ **(Nallusamy *et al.*, 2006)** and **(Ledesma, 2010)** take as a reference for the present investigation to achieve objectives. The loads ($\dot{Q}_L$) to be met by water heating systems as shown in Fig. 4.1 are calculated by **(Duffie and Beckman, 2013)**:

$$\dot{Q}_L = (\dot{m}C_p)_f(T_s - T_a) \quad 4.1$$

The rate of energy of a water storage unit ($\dot{Q}_s$) can be found out by applying the first law of thermodynamics over the control volume gives as the energy balance of the storage tank.

Energy of the system = input energy - output energy 4.2

$$\dot{Q}_s = \dot{Q}_u - \dot{Q}_L \quad 4.3$$

where: $\dot{Q}_u$is the rate of useful energy gain from the collector, $\dot{Q}_L$ is the rate of heat removal by load and T_a is the ambient temperature.

The energy storage capacity of a water storage unit at a three charging hour time (t) with factor of safety taken as 1.5 is also given by:

$$Q_s = 1.5 * t * \dot{Q}_s \quad 4.4$$

Then, the volume of the storage tank is calculated from Eq. (4.) as follows:

$$Q_s = \rho_s V_S C_{ps} * (T_s - T_a) \quad 4.5$$

The solar water storage tanks usually used in domestic systems are within the range of aspect ratios H/D = 1.5 to 3.5. Assume, the geometry of the reservoir tanks are a right cylinder with height to diameter ratio of 2. So, the height of storage tank is given $H = 2 * D_i$.

The diameter and height of water storage tank is calculated from volume of the storage tank is given as:

$$V_S = \frac{\pi D_i^2}{4} * H \quad 4.6$$

Then, the diameter of the storage tank is given by:

$$D_i = \sqrt[3]{\frac{2 * V_S}{\pi}} \quad 4.7$$

Finally, after substituting the values Q_S= 6940.89kJ, V_S= 0.066 m^3, the diameter of the tank (D_i) and height of the tank (H) is obtained 0.347 m and 0.695 m respectively.

4.3 Energy analysis for water used as a storage material

A typical storage system using water storage tank, with water is also used as a HTF (un-stratified type) which is circulated through collector to gain heat energy and flow through the load to remove energy.

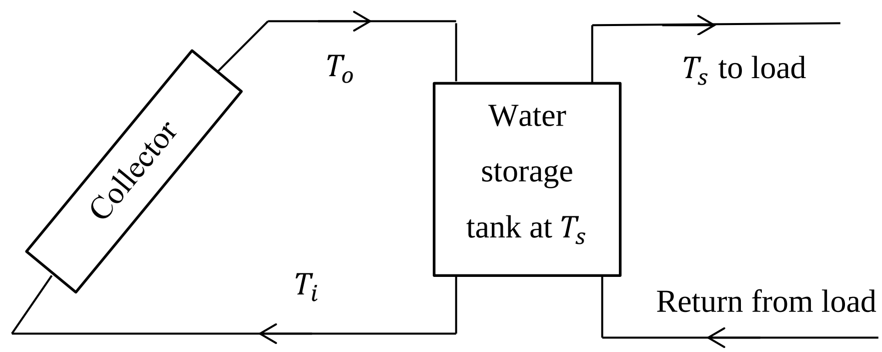

Fig.4.1 A typical water thermal energy storage system **(Duffie and Beckman, 2013)**

The energy balance performed in this un-stratified type water storage system is the help of the above schematic diagram as shown in Fig.4.2 and flow rates into and out of the tanks, to collector and load, can also be determined. Energy delivery to the load could be across a shell and tube type heat exchanger. An initial thermal analysis was performed to determine the transient energy analysis of the solar water heater and aid in decisions regarding design modifications. So, the assumptions used in the governing equations are includes:

i. **Theoretical assumptions with initial and boundary conditions**

- ✓ Inlet temperature of the system is an ambient temperature (T_a) then the cold supply of water temperature at ambient is 25°C for Adama weather climate.
- ✓ The inlet water temperature to the collector would be the same as the mean storage tank water temperature.
- ✓ The temperature of the water entering the tank would be the same as the outlet water temperature of the collector.

ii. **Governing Equation**

The thermal energy analysis assumes a lumped capacitance model for fluid in the tank. Then the energy balance on the system yields the net energy stored in the water is equal to the net solar irradiation (insolation) minus the heat loss from the tank the flow of water out of the storage tank to load and that is refilled at the same rate by cooler water supplied to the storage tank. Then, to determine the transient energy analysis and also to solve for the temperature distribution of the water storage tank without stratified is given as **(Duffie and Beckman, 2013)**:

$$(mC_p)_s \frac{dT_s}{dt} = \dot{Q}_u - \dot{Q}_L - (UA)_s(T_s - T_a) \qquad 4.8$$

To determine the long-term performance of the storage unit Eq. (4.8) is to be integrated over time using Euler integration approach because, long-term analytical solutions are not possible due to the complex time dependence of some of the terms.

$$T_{s,new} = T_{s,new} + \frac{\Delta t}{(mC_p)_s}[\dot{Q}_u - \dot{Q}_L - (UA)_s(T_s - T_a)] \qquad 4.9$$

Similarly, the transient energy analysis in a finite difference scheme with set of N first-order, ordinary differential equations resulting from each node's energy balance is assembled, and energy balance written about the i^{th} tank node is given by:

$$\frac{dT_s}{dt} = \frac{T_s^{t+\Delta t} - T_s^t}{\Delta t} \qquad 4.10$$

$$T_s^{t+\Delta t} = \frac{\Delta \tau}{(mC_p)_s}[(\dot{m}C_p)_f(T_{f,i}^t - T_s^t) - (\dot{m}C_p)_f(T_{s,i}^t - T_a^t) - (UA)_s(T_s^t - T_a^t)] + T_s^t \qquad 4.11$$

Eq. (4.9) and Eq. (4.11) can be used for the estimation of hourly storage water temperature for a known hourly heat addition and withdrawal. The furthermost time period for this estimation is an hour because the solar radiation data are available on an hourly basis. For a known time variation of $\dot{Q}_u$ and, $\dot{Q}_L$, the new storage water temperature $T_s^{t+\Delta t}$ or $T_{s,new}$, can be determined as a function of time.

4.4 Sizing of paraffin TES systems

The paraffin heat storage is a shell and tube heat exchanger. The HTF passes through the tubes and the shell is filled with paraffin wax. Heat is transferred from the hot water to the paraffin wax through the tubes during the charging process and the process is reversed during the discharging time. The heat was stored during the day time when the solar radiation was available to heat the water in the solar collector and this stored heat will then be supplied to the water storage tank as shown in Fig.4.2. The paraffin thermal energy storage system was designed for storing the heat needed in the water heating process. Assuming the storage will store the heat for 3 off-sunshine hours per day, the quantity of heat needed to be stored in the paraffin heat thermal energy storage system can be estimated by considering a safety factor of 1.5 for the change in temperature $\Delta T = T_d - T_a$ **(Niyas *et al.*, 2017)**.

$$Q_s = \dot{m}_f C_{pf} t(1.5\Delta T) \tag{4.12}$$

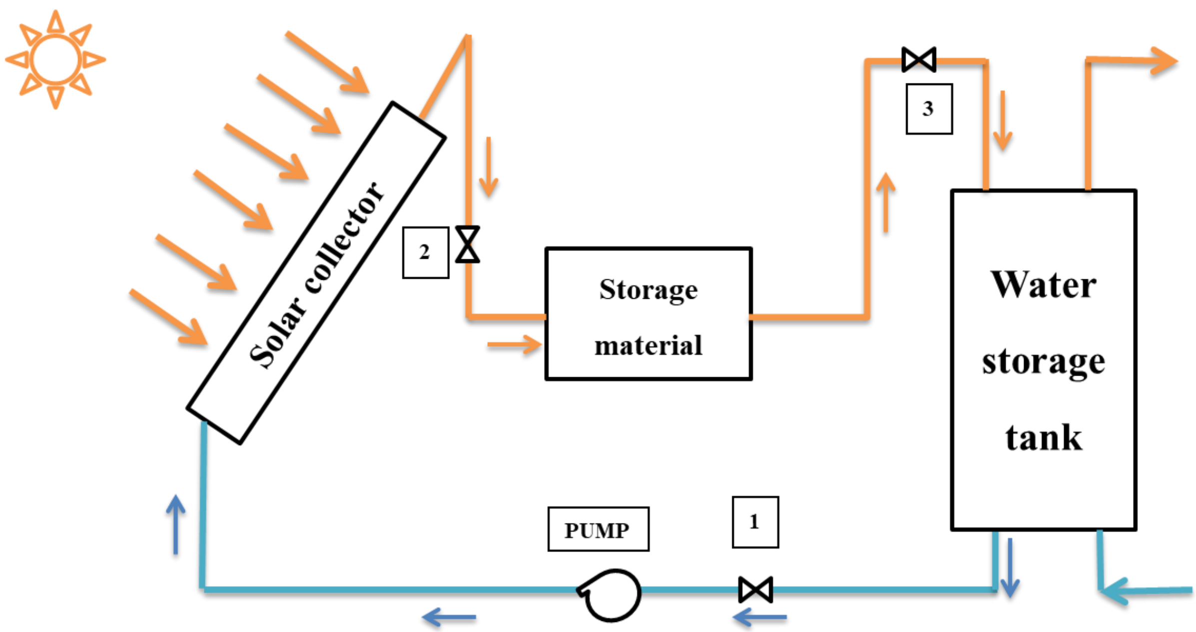

Fig.4.2 Low-temperature TES systems for domestic water heating purpose

The storage capacity of a paraffin storage material heated from T_{m1} to T_{m2}, if it undergoes a phase transition at T_m is the sum of the sensible heat change of the solid (the lower temperature phase) from T_{m1} to T_m, the latent heat at T_m, and the sensible heat of the liquid (the melt, or higher temperature phase) from T_m to T_{m2}:

$$Q_s = m_s[C_{p,s}(T_m - T_{m1}) + L_f + C_{p,l}(T_{m2} - T_m)] \tag{4.13}$$

where: m_s and L_F are the mass and latent heat of fusion of paraffin wax in kg and kJ/kg.

The volume of the paraffin wax can be calculated from:

$$V_S = \frac{m_s}{\rho_p} \tag{4.14}$$

The volume of the tank is the sum of the volume of the PCM and the volume of the tubes.

$$V_T = V_S + V_t \qquad 4.15$$

The volume of the tubes is obtained based on the design of the shell and tube latent heat thermal energy storage system procedure proposed by **(Shamsundar *et al.*, 1992)** which is given in the ANNEX C:

$$V_t = \pi n_t {R_o}^2 L \qquad 4.16$$

where: n_t is number of tubes and $R_o$outer radius of the tube which is obtained n_t=5, R_o=9mm in the ANNEX C. The length of the storage bed is obtained according to authors the ratio of length to diameter was taken 5 up to 9, consequently in the present case length to diameter ratio is taken to be 5 ($\frac{L}{D_o} = 5$) to improve the convective heat transfer in axial direction compared to radial direction (**Velraj *et al.*, 1997**) and (**Sharma *et al.*, 2005**)

$$V_T = \frac{\pi}{4} D^2 L \qquad 4.17$$

Finally, substituting the values of $\dot{m}_f$ =0.0041 kg/s, C_{pf}= 4.18 kJ/kg. K, T_d = 50℃, T_a = 25 ℃ and t = 3 h into Eqn. (4.12) gives Q_s = 6940.89 kJ and also substituting the values of Q_s = 6940.89 kJ and L_F =238 kJ/kg into Eqn. (4.13) gives m_s =27.69 kg. From equation (4.14), (4.15) and (4.16), V_s = 0.032 m^3, V_t=0.0012 m^3 and V_T=0.033 m^3 and from Eqn. (4.17), D = 0.2 m and L = 1 m.

4.5 Energy analysis for paraffin wax used as a storage material

The developed a model applicable to paraffin heat storage in containers, where the length in flow direction is L, the cross-sectional area of the material is A, and the wetted perimeter is P as shown in Fig.4.3 The heat transfer fluid passes through the storage unit in the x direction at the rate $\dot{m}_f$˙ and with inlet temperature (T_{fi}). A developed model for paraffin TES can be based on three assumptions: (a) Neglect the axial conduction in the fluid during flow process; (b) Neglect the Biot number which is low enough that temperature gradients normal to the flow; and (c) Neglect heat losses from the bed. Then the energy balance on the HTF is given as **(Morrison, 1978)**:

$$\frac{\partial T_f}{\partial t} + \frac{\dot{m}_f}{\rho_f A_f}\frac{\partial T_f}{\partial x} = \frac{UP}{\rho_f A_f C_{pf}}(T - T_f) \quad 4.18$$

where: ρ_f, A_f, and C_{pf} are the density, flow area, and specific heat of the heat transfer fluid.

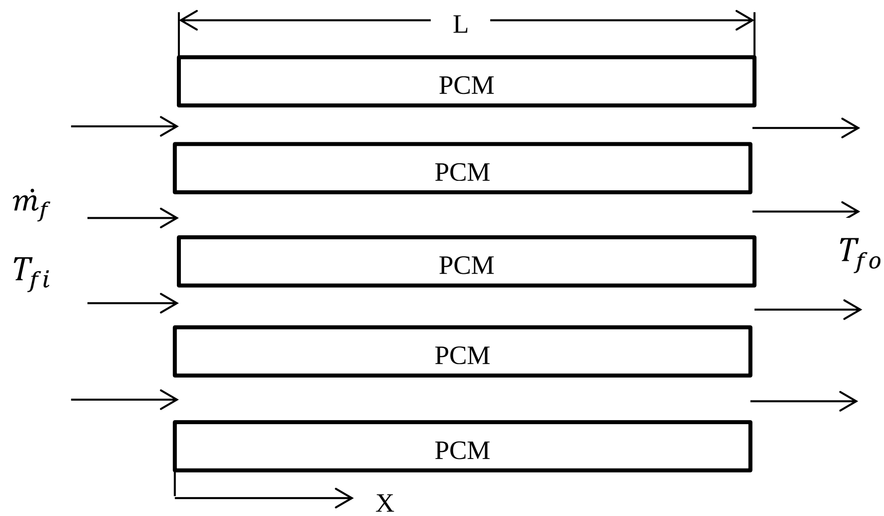

Fig.4.3 Schematic of paraffin heat storage unit model **(Morrison, 1978)**

The energy balance on the paraffin storage material is given as **(Morrison, 1978)**:

$$\frac{\partial u}{\partial t} = \frac{k_p}{\rho_p}\frac{\partial^2 T}{\partial x^2} + \frac{UP}{\rho_p A}(T_f - T) \quad 4.19$$

where: u, k_p, ρ_p and T are the specific internal energy, thermal conductivity, density and temperature of paraffin wax storage material; U and $T_f$are overall heat transfer coefficient between the fluid and phase change material and the circulating fluid temperature with a rate of time (t). The specific internal energy is related to temperature T, liquid fraction (λ), and the specific heats of the liquid and solid phases C_{ps} and C_{pl} by **(Morrison, 1978)**:

$$u = \begin{cases} C_{ps}(T - T_{ref}) & if\ T < T_m \\ C_{ps}(T_m - T_{ref}) + \lambda L_F & if\ T = T_m \\ C_{ps}(T_m - T_{ref}) + \lambda + C_{pl}(T - T_m) & if\ T > T_m \end{cases} \quad 4.20$$

where: T_m-is the melting temperature of paraffin wax and T_{ref} is the reference temperature at which the internal energy is taken as zero.

The boundary conditions for the above equations are:

$$\text{at x} = 0, \frac{\partial T}{\partial x} = 0, \text{at x} = \text{L} \ \ \frac{\partial T}{\partial x} = 0 \quad 4.21$$

$$T_f(0, t) = f(t) \quad 4.22$$

Eq. (4.22), tells the inlet fluid temperature is as a function of time, $f(t)$ to be determined by simultaneously solving the governing equations of the different system components. It has been shown that axial conduction during flow is negligible, and if the fluid capacitance is small, Equations 4.18 and 4.19 becomes **(Morrison, 1978)**:

$$\frac{\partial T_f}{\partial x} = \frac{UP}{(\dot{m}C_p)_f}(T - T_f) \quad 4.23$$

$$\frac{\partial u}{\partial t} = \frac{UP}{\rho_p A}(T_f - T) \quad 4.24$$

These two equations can be rewritten in terms of *NTU* as:

$$\frac{\partial T_f}{\partial (x/L)} = NTU(T - T_f) \quad 4.25$$

$$\frac{\partial u}{\partial \theta} = NTU(T_f - T) \quad 4.26$$

where: $\theta = {t(\dot{m}C_p)_f}/{\rho_p AL}$ and $NTU = {UPL}/{(\dot{m}C_p)_f}$ 4.27

4.6 3-D simulation of TES system by COMSOL Multiphysics

The procedure that has taken in COMSOL Multiphysics 4.3a simulation software in the developed all TES model is as shown in Fig.4.4.

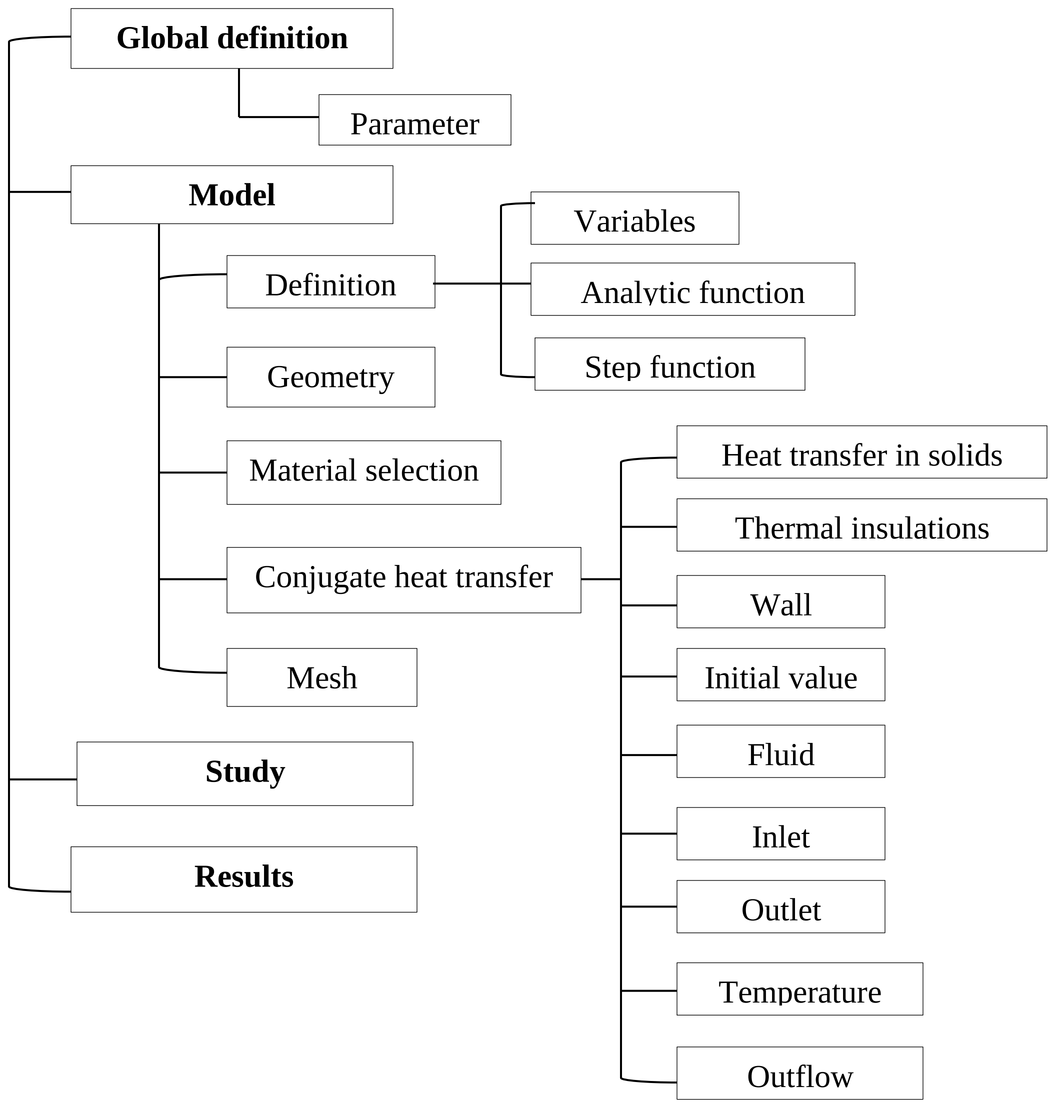

Fig.4.4 Flow chart integrated with COMSOL Multiphysics 4.3a simulation software

4.6.1 Physical modeling of thermal energy storage

The shell and tube type TES geometric configuration is used in the present study because shell and tube type geometry have minimal heat loss from the system, relatively smaller volume and higher efficiency **(Mao, 2016)**. One-fourth of thermal energy storage bed has been selected for the present study to minimize the computational time and cost. In this geometric configuration the storage material fills in the annular shell space around the tube and the HTF flows through the tube. Thermal energy storage is modeled and analyzed by using COMSOL Multi-physics 4.3a simulation software during the investigation. The 3D isometric and sectional view of shell-tube type thermal energy storage bed is illustrated respectively as shown in Fig. 4.5.

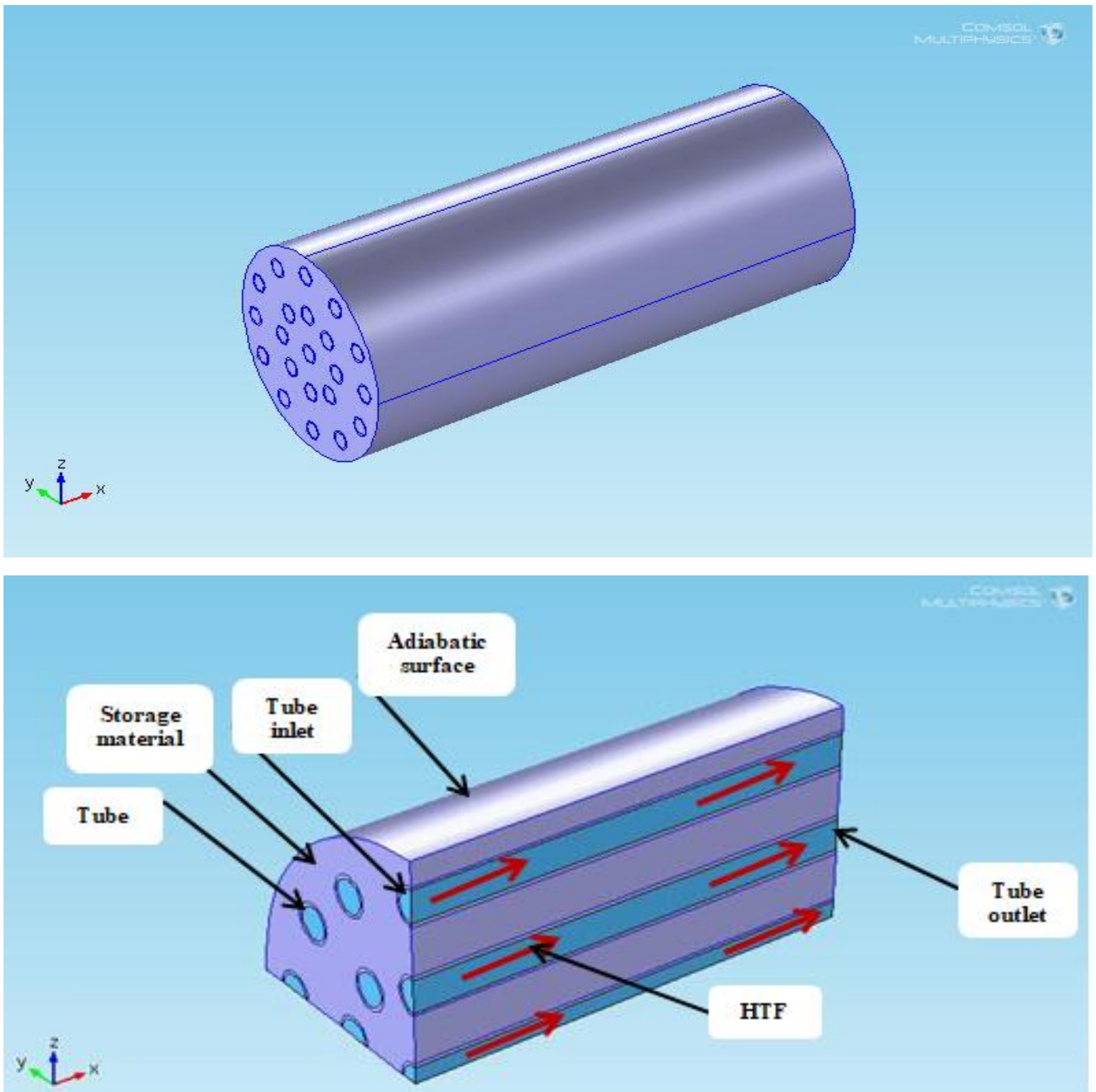

Fig.4.5 3-D Isometric and sectional view of TES bed

4.6.2 Mathematical modeling of TES systems

This section presents the theoretical assumption, governing equation, initial, and boundary condition of the TES system. A 3D transient numerical model is developed to study the performance characteristics of the shell-tube TES bed using COMSOL Multi-physics software.

When in the case of the LHS material both liquid and solid phases are present and they are separated by a moving interface between them, so there have been several numerical methods developed to solve such phenomenon but the most attractive and common ones are the enthalpy methods. This method simplifies such phase change problems since the governing equations are the same for the two phases which means the method does not require explicit treatment of conditions on phase change boundary (**Zivkovic & Fujii, 2001**).

i. Theoretical assumptions

To simplify the developed thermal energy storage model theoretical assumptions were made without affecting the end outcomes. Those assumptions are:

- ✓ The tank and all pipes in the thermal energy storage system were fully insulated
- ✓ The thermal energy storage material homogeneous and isotropic
- ✓ Neglect the viscous dissipation of the HTF and laminar HTF flow regime
- ✓ Uniform initial temperature of the storage material (T_{ini}= 298 K)
- ✓ Melting and solidification can occur only within the melting temperature range
- ✓ The thickness of the tube wall is negligible, thus the HTF is directly in contact with the storage material and neglected the contact resistance of the HTF tubes.
- ✓ The radiant heat transfer in the storage is neglected
- ✓ The effect of volume change associated with phase change is neglected

ii. Governing equation

The conservation of mass, momentum, and energy have been used in this work to study the performance of the TES system, and also three physical processes; such as fluid flow, heat transfer by conduction and convection, and the phase transition of the storage material (LHS case) have been simulated.

Continuity equation: the law of conservation of mass is applied to the given model by considering a fluid passing through an infinitesimally small element that leads to the continuity equation given in Eq. (4.28):

$$\nabla\vec{v} = 0 \qquad 4.28$$

Similarly, it is expressed as:

$$\frac{\partial u}{\partial x} + \frac{\partial v}{\partial y} + \frac{\partial w}{\partial z} = 0 \qquad 4.29$$

Momentum equation: Newton 2nd law of motion is applied to the given LHTES model by a fluid passing through an infinitesimally small element that leads to the momentum equation given in Eq. (4.30) **(Jad, 2018)**:

$$\rho \frac{\partial \vec{v}}{\partial t} + \rho(\vec{v}.\nabla)\vec{v} = -\nabla P + \mu\nabla^2\vec{v} + \vec{F} + \vec{S} \qquad 4.30$$

where: $\vec{F}$ is the buoyancy effect term and $\vec{S}$ is the momentum source term known as Darcy's law source term and it is given by:

$$\vec{F} = \rho g \beta (\mathrm{T} - T_m) \qquad 4.31$$

$$\vec{S} = \frac{(1-\lambda)^2}{(\lambda^3+\epsilon)} * A_{mush} * \vec{v} \qquad 4.32$$

The buoyance effect ($\vec{F}$) term is included in the general momentum equation to simplify the complexity of the Navier-stokes equation. Similarly, the momentum source term included the governing momentum equation to nullify the velocity field in the solid region of the phase change storage material. Finally, after substituting Eq. (4.31) and (4.32) into Eq. (4.30), the momentum equation used to simulate latent heat storage is given by:

$$\rho \frac{\partial \vec{v}}{\partial t} + \rho(\vec{v}.\nabla)\vec{v} = -\nabla P + \mu\nabla^2\vec{v} + \rho g \beta (\mathrm{T} - T_m) + \frac{(1-\lambda)^2}{(\lambda^3+\epsilon)} * A_{mush} * \vec{v} \qquad 4.33$$

where: β is thermal expansion of the phase change storage material. A_{mush} is mushy zone constant which is defined as how steeply the velocity is reduced to zero when the material solidifies, this input parameter has an impact on the result because usually, it has a very large number, ranging between 10^3 to 10^8. **Colella *et al.*, (2012)**, suggested the value of this constant taken as a small value to reduce the fluctuation of the result in liquid volume fraction due to these for the present case taken as 10^3. The liquid fraction (λ) is given in Eq. (4.37) and ϵ is a small number typically around 10^{-3} to avoid the division by zero.

Energy equation: the energy equation is applicable in the HTF, the storage bed and between the HTF and storage bed, then applied 1st law of thermodynamics yields the energy equation given in in the following expression.

$$k\nabla^2 T = \rho H \ \frac{DT}{Dt} \tag{4.34}$$

Similarly, the energy equation expressed as:

$$k\left[\frac{\partial^2 T}{\partial x^2} + \frac{\partial^2 T}{\partial y^2} + \frac{\partial^2 T}{\partial z^2}\right] = \rho * H * \left[\frac{\partial T}{\partial t} + u\frac{\partial T}{\partial x} + v\frac{\partial T}{\partial y} + w\frac{\partial T}{\partial z}\right] \tag{4.35}$$

By using the enthalpy method (H(T)) it is easy to handle the latent heat storage material with its range and it introduces as follows **(Tehrani *et al.*, 2016)**:

$$H(T) = \begin{cases} C_{p,s}T & T < T_{m1} \\ C_{p,l}T + \frac{L_F*(T-T_{m1})}{\Delta T_m} & T_{m1} \leq T \leq T_{m2} \\ C_{p,l}T + L_F & T > T_{m2} \end{cases} \tag{4.36}$$

where: $\Delta T_m = T_{m2} - T_{m1}$, L_F is the latent heat of fusion and, T_{m1} and T_{m2} are the solidus and liquidus temperatures respectively.

iii. Initial and boundary condition

As mention in the assumption, the temperature of the boundary (HTF, storage material, and HTF tubes) is initially constant and the velocity of the HTF is set to zero initially (no flow condition). The control volume is fixed (i.e. both the TES material and HTF tubes are stationary) and the HTF is flow domain. The outer surface of the storage bed is adiabatically insulated and at t > 0 a constant inlet temperature given into inlet HTF tubes with constant fluid velocity. The same governing equations are used during charging and discharging processes. However, during the discharging process when the heat transfer rate is changed, and the storage unit starts discharged. It should also be noted that in the LHS material phase transition does not occur isothermally, but it occurs over a certain range of temperatures, which is called the phase transition range **(Rathod & Banerjee, 2014)**. As a result, the phase transition of paraffin wax storage material that has used in the present study is 324-330 K as shown in Table 4.1

4.6.3 Solution of the 3-D governing formulation

The three-dimensional governing formulation involved in the given TES model is solved by using a special type of FEM based solver COMSOL Multiphysics 4.3a software. PARDISO solver is used during the study. To handle the time-stepping a backward difference formula is taken with the minimum time steps 0.01 s and the maximum time step is not set (to set automatically maximize the time stepping). The solution of the developed numerical model diverges based on the convergence criterion (between 10^{-2} and,10^{-3}) and for the present study set to be,10^{-3} this is due to the non-linear nature of the problem.

4.6.4 Mesh generation

Mesh generation is a second step next to geometry formation to solve the developed thermal model described by the above governing equation. A free tetrahedral and triangular unstructured mesh is generated as shown in Fig.4.6 with the help of a special meshing feature of COMSOL Multiphysics 4.3a software. The free tetrahedral mesh is important for discretize smaller geometries like HTF tubes with a sufficient number of element similarly, the domains are meshed by a free tetrahedral element which is best to mesh curved geometry with little distortion of mesh **(Prasad & Muthukumar, 2013)**. All domains; HTF domain and storage material domain have meshed with different mesh quality parameters and also domain decomposition techniques are used in those domains. The generated mesh has been used to get a numerical solution of the developed model that means the numerical solution of the TES model depends on the number of mesh size elements.

Fig.4.6 A 3D meshed model of the thermal energy storage bed

4.7 Performance parameters of TES systems

This section contains the overall performance parameters of TES systems such as:

- ✓ Charging and discharging time,
- ✓ A liquid fraction in case of latent heat TES model and
- ✓ Energy stored/released

4.7.1 Charging and discharging time

Charging/discharging time is one of the basic performance parameters in TES systems and it is defined as concerning the temperature rise and temperature decrease of the storage material respectively. When in the case of sensible storage material, the storage bed is said to be fully charged at the volume average temperature of the storage reaches the inlet HTF temperature and also fully discharged when the volume average temperature of sensible storage reaches its initial condition. Similarly, in the case of latent heat storage, the storage system is fully charged when the storage material is completely melted; similarly, the storage system is fully discharged when the storage material is completely solidified.

4.7.2 Liquid fraction for latent heat TES model

The liquid fraction is a fraction that happens for the case of latent heat thermal energy storage model, the storage material exists in two-phase forms. It is a non-dimensional parameter that quantifies the percentage of the liquid phase in the mushy region operating between the highest temperature at which, the material is completely in the solid-state and the lowest temperature at which, the material is completely in the liquid state. Liquid fraction (λ) of the PCM can be calculated based on the given equation **(Seddegh *et al.*, 2017)**:

$$\lambda = \begin{cases} 0 & T < T_{m1}\ (Solid), \\ \frac{T-T_{m1}}{T_{m2}-T_{m1}} & T_{m1} < T < T_{m2}\ (Mushy\ zone), \\ 1 & T > T_{m2}\ (Liquid). \end{cases} \tag{4.37}$$

4.7.3 Energy stored/released of the storage material

This also other main performance parameters used to study the TES system that has developed in the present investigation. The total heat stored ($Q_{T,C}$) is a combination of both energies stored in the form of sensible heat ($Q_{S,C}$) and latent heat ($Q_{L,C}$) form in the LHTES model. While, in the case of sensible heat thermal energy storage system, the energy stored/released (Q_{TS}) is only in the form of sensible heat and it can be calculated by Eq. (19). The total heat stored during the charging process can be obtained from the (**Stutz *et al.*, 2017**) relationship as follows.

$$Q_{S,C} = \int_{T_{ini}}^{T_m} m.c_{ps}\,dT + \int_{T_m}^{T} m.c_{pl}\,dT = m.c_{ps}(T_m - T_{ini}) + m.c_{pl}(T - T_m) \tag{4.38}$$

$$Q_{L,C} = m.L_F\lambda \tag{4.39}$$

$$Q_{T,C} = m.c_{ps}(T_m - T_{ini}) + m.L_F\lambda + m.c_{pl}(T - T_m) \tag{4.40}$$

The total heat released ($Q_{T,D}$) from the latent heat thermal energy storage system during the discharging period can be obtained from the (**Stutz *et al.*, 2017**) relationship.

$$Q_{S,D} = \int_{T}^{T_m} m.c_{pl}\,dT + \int_{T_m}^{T_{ini}} m.c_{ps}\,dT = m.c_{pl}(T_m - T) + m.c_{ps}(T_{ini} - T_m) \tag{4.41}$$

$$Q_{L,D} = m.L_F(1 - \lambda) \tag{4.42}$$

$$Q_{T,D} = m.c_{pl}(T_m - T) + m.L_F(1 - \lambda) + m.c_{ps}(T_{ini} - T_m) \tag{4.43}$$

To demonstrate which one is preferable storage material to store the required amount of heat energy integrated for low-temperature application is simply to compare the amount of stored energy. Which means if sensible (water) storage material is taken to be a heat storage material within the same storage volume size of paraffin wax, the stored energy is:

$$Q_{TS} = \rho_s * V_s * C_{p,s} * \Delta T \tag{4.44}$$

Q_{TS} = 1000 * 0.033 * 4.18 * 30 = 3.45 MJ

Therefore, the value indicates that the stored energy by using sensible storage material used as a TES bed is 3.45 MJ. However, in the previous paraffin used as a TES material, it could achieve to store 7 MJ amount of heat energy with the same storage volume size.

CHAPTER FIVE

PERFORMANCE ANALYSIS OF TES SYSTEM FOR HIGH-TEMPERATURE APPLICATION

The aim of this chapter is to presents the performance analysis of the thermal energy storage system that integrated for high-temperature applications (i.e., integrated for a concentrated solar power plant to generate steam). It contains system description, sizing of the storage model, and mathematical modeling of the developed TES model such as; theoretical assumption, governing equation, initial and boundary condition and enhancement technique also included in this chapter.

5.1. System description

The proposed system presented in this section has to build a high-temperature thermal energy storage system used for steam generation in the CSP plant as shown in Fig.5.1. It has two parts in this system; the solar cycle such as a solar collector element (parabolic trough collector), shell and tube type thermal energy storage and heat exchanger to accomplish harnessing of solar irradiation and convert into heat energy by a solar collector. The collected heat energy is stored into the TES system and finally, the outlet of this stored energy is used to generate saturated steam in the heat exchanger (generator). The other part is a power block cycle that accomplishes power production using steam generated previously in the solar cycle.

However, the present investigation, concerned mainly on the former one, which is studying the performance analysis of the TES system integrated with concentrated solar power (CSP) plants to generate saturated steam during the intermittent solar irradiation. The process as illustrated in Fig.5.1 is the parabolic solar collector collects radiant energy and transferred to the HTF that circulates in the solar cycle by converting into heat energy. Then the HTF flows into the TES material, the heat stored in TES material which is transferred from the HTF, and finally, the HTF generates steam in the heat exchanger then the HTF again back to the solar collector. The generated steam circulates in the power block cycle to produce power in the turbine. This process also controlled by the control valves to open and closed the piping system. Likewise of the preceding chapter, the aim of building thermal energy storage for the present application is to store the heat energy collected from the parabolic trough collector during the sunshine hour and released the stored energy during the absence of solar radiation. So, this system tested both sensible and latent heat storage material with the same model and the same volume size, then compare which one can perform to fulfill the energy demand in a steam power plant.

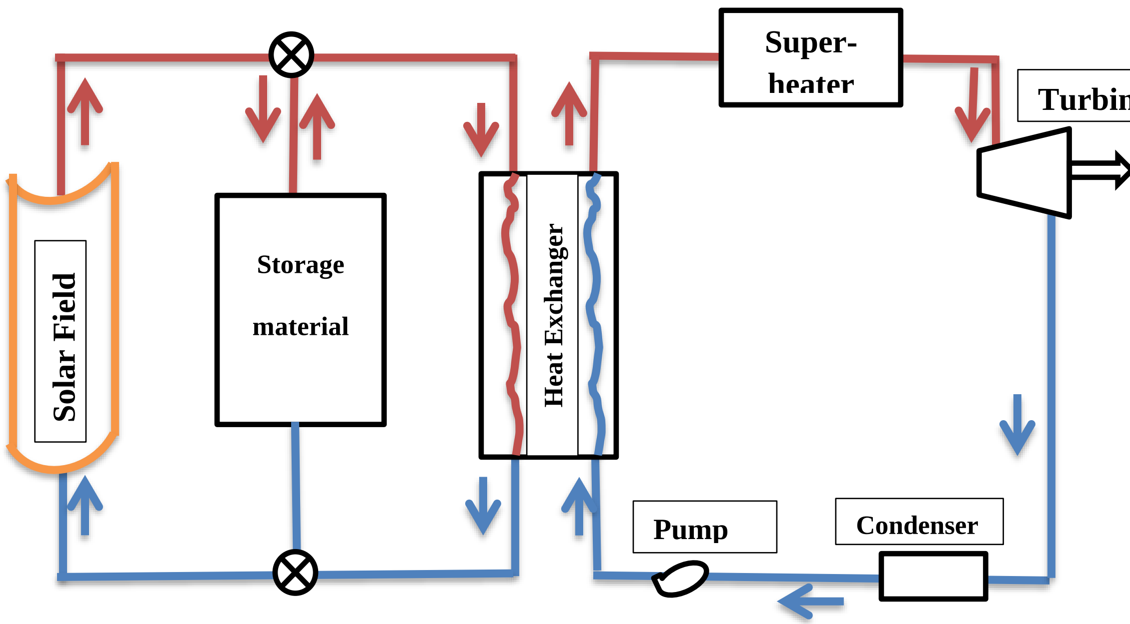

Fig.5.1 High-temperature TES systems for steam generation purpose in CSP plants

The thermal energy storage material used for the high-temperature application is selected from the literature. Which are concrete used as a sensible TES material (**Tian & Zhao, 2013**) and nitrate salt (KNO_3) **(Shabgard *et al.*, 2010**) is used as a latent heat thermal energy storage material based on the temperature range. Mainly due to the cost-effectiveness and easily availability those materials are selected for the present study. The HTF in both cases is selected thermal oil due to the applicability for high-temperature range. The thermo-physical properties of concrete storage and HTF are given in Table 5.1.

5.2 Sizing of concrete TES model for high-temperature application

The sizing of concrete and nitrate salt thermal energy storage for the high-temperature application also depending on considered environmental impacts, cost-effectiveness, and technical properties similar to the preceding chapter. Because high thermal energy storage capacity and excellent heat transfer rate can significantly reduce the system volume and the storage cost. Likewise, the selection criteria for sizing of shell and tube type thermal energy storage model such as; diameter of the shell, length, and a number of charging tubes in the storage used for high- temperature applications is the same concept from the previous TES model shown in Fig 4.2.

Table 5.1 Thermo-physical properties of concrete storage and HTF (**Tian & Zhao, 2013**)

Property	Concrete	HTF(Therminol VP-1)
Density (kg/m^3)	2200	815
Thermal conductivity (W/mK)	2	0.11
Specific heat capacity (kJ/kgK)	1.5	2.32
Temperature range (℃)	300 – 380	300 – 380

The physical model of concrete and nitrate salt TES is taken with similar to the figure presented as shown in Fig.4.5. Assuming the concrete storage will store the heat for one and half hours per day, the quantity of heat needed to be stored in the concrete thermal energy storage system can be estimated by Eq. (5.1) with considering a safety factor of 1.5 for the change in temperature of the storage material ΔT **(Niyas *et al.*, 2017)**. Fixing the temperature change which is 80 ℃ due to the working temperature range of the storage material as shown the thermo-physical properties in Table 5.1 and also fix the diameter of HTF tube and its thickness is 0.015m, 0.002 m respectively. Then, the capacity of the concrete thermal energy storage is calculated by:

$$Q_s = \dot{m}_f C_{pf} t(1.5\Delta T) \quad 5.1$$

Similarly, the capacity of the storage material is also expressed by Eq. 5.2, and also the volume of the concrete storage bed (V_S) can be calculated using the following relation:

$$Q_s = \rho_s V_s C_{ps} \Delta T \quad 5.2$$

The volume of the cylinder is the sum of the volume of the concrete bed and the volume of the HTF tubes.

$$V_T = V_S + V_t \quad 5.3$$

The volume of the HTF tubes is obtained based on the design of the shell and tube thermal energy storage system as follow:

$$V_t = \pi n_t {R_o}^2 L \tag{5.5}$$

Similarly, the volume of the concrete storage cylinder is expressed as:

$$V_T = \frac{\pi}{4} {D_o}^2 L \tag{5.6}$$

The length of the storage bed is obtained according to authors the ratio of length to diameter was taken 5 up to 9, consequently in the present case length to diameter ratio is taken to be 5 ($\frac{L}{D_o} = 5$) to improve the convective heat transfer in axial direction compared to radial direction (**Velraj *et al.*, 1997**) and (**Sharma *et al.*, 2005**).

where: D_o is the outer diameter of the storage cylinder, n_t is number of tubes and $R_o$outer radius of the tube which is obtained n_t=13, R_o= 10 mm with the same procedure taken in the ANNEX C.

Substitute the value in Eq. (5.1), the capacity of the concrete thermal energy storage is obtained 15MJ, the value D_o and length of the storage bed is 0.27 m and 1.35 m respectively and there is a need of 0.061 m^3 total volume of storage cylinder used to store heat energy of 15 MJ for high-temperature TES system.

5.3 Energy analysis for concrete used as a storage material

A concrete storage unit as the one considered here is composed of a tube register embedded within concrete for allowing fluid flow through it. The HTF tube parallel one to the other; have axes. For the definition of the physical model, the same conditions have been assumed for each parallel channel, so that the storage module is considered to be composed by sub-units, named elements, put in parallel **(Jian *et al.*, 2015)**. One element is made by a concrete drilled cylinder with radius (r_o), in contact with a tube with internal radius (r_i). By having this in mind, the problem of analyzing the storage system moves from the study of the module to that of the single channel for which the initial section is the one of the incoming HTF during charge, whereas the final section is the outgoing one during the same phase. Even if the storage material outside the cylindrical elements is neglected, such a simplification is necessary for implementing an efficient model (**Salomoni *et al.*, 2014**).

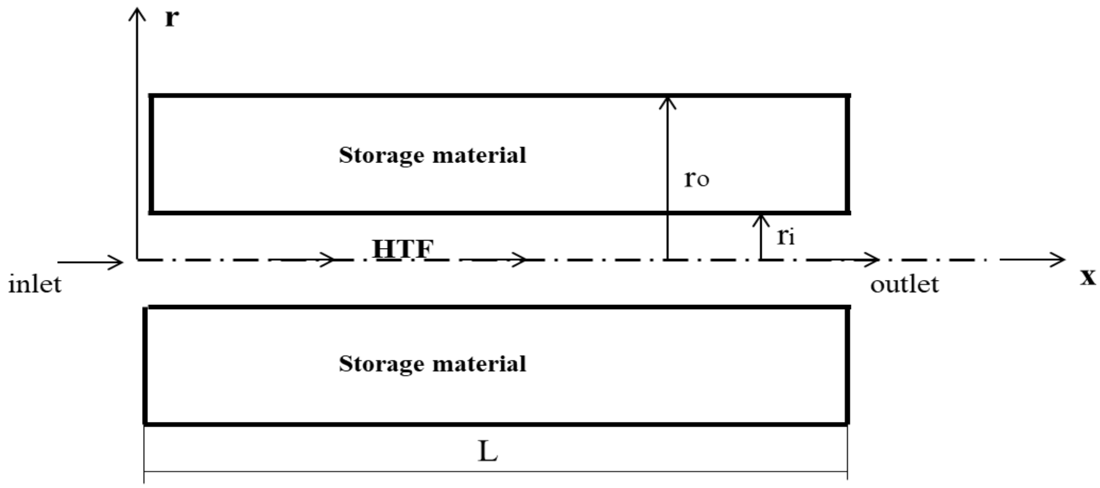

Fig.5.2 Sectional view of cylindrical bed TES model for one unit **(Jian *et al.*, 2015)**

i. Theoretical assumptions of the concrete storage model

To simplify the developed concrete thermal energy storage model the following theoretical assumptions were made without affecting the end outcomes. Thus assumptions are: (a) The geometry is axis-symmetric, (b) the HTF is assumed to be in direct contact with the concrete storage material, due to the small thickness of the tube, (c) The outer surface of the storage is perfectly insulated, (d) The storage material is homogeneous and isotropic, (e) Storage material and HTF contained initially at a constant temperature on the whole domain, that is conditions of first heating (T_{ini} = 573K), (c) The implemented algorithm for analyzing the discharging phase assumes as initial temperature fields, both for HTF and concrete, those calculated at the end of the charging phase.

The energy balance for solid thermal energy storage material (concrete) uses the same control volume (fixed). In addition to the above theoretical assumptions, the lumped capacitance method with some modifications applies to the thermal conduction of solid media in the radial direction; thus, $\frac{\partial \mathrm{Ts}}{\partial \mathrm{r}} = 0$. The two-dimensional transient models for the solid storage unit can be simplified to a one-dimensional model. So, the governing energy equation after simplification of the model with the theoretical assumption is given by (**Jian *et al.*, 2015**):

ii. Governing equations

Assuming that the mass flow rate of the HTF ($\dot{m}_f$), in the tubes is constant, so, the energy balance for the fluid in the differential control volume, dx in the concrete storage is given by:

$$\rho_f A_f dx \frac{\partial T_f}{\partial t} = hPdx(T_S - T_f) + (\dot{m}C_p)_f (T_{f,x} - T_{f,x+\Delta x}) \quad 5.7$$

where: h represents the convective heat transfer coefficient in the tube, the heat transfer surface perimeter ($P = 2\pi r_i$) and the wetted area in the HTF tube ($A_f = \frac{\pi d_i^2}{4}$). The average fluid velocity in the concrete heat storage unit is also given by:

$$\bar{u} = \frac{\dot{m}_f}{\rho_f A_f} \quad 5.8$$

Substituting Eq. (5.8) into Eq. (5.7) the HTF energy balance is becomes:

$$\frac{\partial T_f}{\partial t} + \bar{u}\frac{\partial T_f}{\partial x} = \frac{hP}{\rho_f A_f C_{pf}}(T_S - T_f) \quad 5.9$$

Similarly, the energy balance for the concrete storage material uses the same control volume, can be given by (**Salomoni *et al.*, 2014**):

$$hPdx(T_s - T_f) = -(\rho C_p)_s A_s \frac{\partial T_s}{\partial t} \quad 5.10$$

where: A_s is the cross-sectional of solid material can be calculated $\pi(r_o^2 - r_i^2)$. After rearranging Eq.5.4 is written as:

$$\frac{\partial T_s}{\partial t} = -\frac{hPdx}{(\rho C_p)_s A_s}(T_s - T_f) \quad 5.11$$

After a forward finite difference formulation for temporal variation and backward finite difference formulation for spatial variation is described by:

<u>For HTF:</u>

$$\frac{\mathrm{T}_{f,i}^{t+\Delta t} - \mathrm{T}_{f,i}^{t}}{\Delta t} + \bar{u}\frac{\mathrm{T}_{f,i}^{t} - \mathrm{T}_{f,i-1}^{t}}{\Delta x} = \frac{hP}{\rho_f A_f C_{pf}}(\mathrm{T}_{s,i}^{t} - \mathrm{T}_{f,i}^{t}) \quad 5.12$$

<u>For concrete storage:</u>

$$\frac{(T_{s,i}^{t+\Delta t} - T_{s,i}^{t})}{\Delta t} = -\frac{hP}{(\rho C_p)_s A_s}(T_{s,i}^{t} - T_{f,i}^{t}) \quad 5.13$$

Some rearrangement for simplification:

$$T_{s,i}^{t+\Delta t} = (1-\lambda)T_{s,i}^{t} + \lambda T_{f,i}^{t} \quad 5.14$$

where: $\lambda = \Delta t \frac{hP}{(\rho C_p)_s A_s}$ 5.15

iii. Initial and boundary condition

The heat transfer fluid and the concrete element are assumed to be at the same initial temperature**.** The HTF from the solar field is fed into the storage system as a boundary condition. However, for parametric study, a constant heat transfer fluid temperature is taken.

5.4 Energy analysis for nitrate salt (KNO_3) used as a storage material

The present study also developed a 2-D mathematical model of the nitrate salt TES system to study the energy analysis for the HTF and the storage material, the sizing procedure also the same, the storage consists of an inner tube (r_i) to transfer the HTF and an outer tube (r_o) located the storage material as a shell to exchange heat from HTF as shown in Fig.5.2.

Table 5.2 Thermo-physical properties of nitrate salt (KNO_3) and Therminol VP-1 (HTF) **(Shabgard *et al.*, 2010**)

Property	Nitrate salt (KNO_3)	HTF(Therminol VP-1)
Density (kg/m^3)	2109 (solid)	815
Thermal conductivity (W/mK)	0.5 (liquid), 0.42 (solid)	0.11
Specific heat capacity (kJ/kgK)	0.95	2.32
Melting temperature (℃)	335	370-400
Latent heat of fusion (kJ/kg)	266	-------

i. Governing equation

Similar to concrete storage material, to simplify the developed nitrate salt thermal energy storage model the following theoretical assumptions were made without affecting the end outcomes. Thus assumptions are: (a) The HTF is assumed to be in direct contact with the PCM storage material, due to the small thickness of the tube, (b) The outer surface of the storage is perfectly insulated, (c) The thermal energy storage material is homogeneous and isotropic, (d)

Storage material and HTF contained initially at a constant temperature on the whole domain, that is conditions of first heating (T_{ini} = 573K). Then, The 2-dimensional energy balance equation for both the HTF and the nitrite storage material is expressed as follows (**Adine & Qarnia, 2009**):

HTF:

$$(\rho C_P)_f \pi r_i^2 \frac{\partial T_f}{\partial t} = -\left(\frac{\dot{m}}{N} C_P\right)_f \frac{dT_f}{dx} + h2\pi r_i\left(T_{r=r_i} - T_f\right) \quad 5.16$$

where: N is the number of HTF tubes embedding on the TES bed.

Nitrate storage material:

$$\left(\rho C_p\right)_s \frac{\partial T}{\partial t} = div(k_s\ grad\ T) \quad 5.17$$

Similarly, the energy equation of the storage bed in differential form is given by:

$$\frac{\partial}{\partial x}\left(\alpha \frac{\partial H}{\partial x}\right) + \frac{1}{r}\frac{\partial}{\partial r}\left(\alpha r \frac{\partial H}{\partial r}\right) = \frac{\partial H}{\partial t}\ dV \quad 5.18$$

where: α is thermal diffusivity (m^2/s), H is enthalpy as a function of temperature it expressed by Eq. (5.19) and r is a radial coordinate (m), it is easy to handle the latent heat storage material with its range and it introduces as follows **(Tehrani *et al.*, 2016)**:

$$H(T) = \begin{cases} C_{p,s}T & T < T_{m1} \\ C_{p,l}T + \frac{L_F * (T - T_{m1})}{\Delta T_m} & T_{m1} \le T \le T_{m2} \\ C_{p,l}T + L_F & T > T_{m2} \end{cases} \quad 5.19$$

ii. Initial and boundary condition

For the 2D numerical formulation, the following initial and boundary conditions are used.

$$t = 0: \vec{v} = 0; T_f = T = T_{ini} \quad 5.20\ (a)$$

$$t > 0: T(x = 0, r) = T_{inlet} \quad 5.20\ (b)$$

$$\frac{\partial T}{\partial x}(x = 0, r) = 0, \quad \frac{\partial T}{\partial x}(x = L, r) = 0 \quad 5.20\ (c)$$

$$k_s \frac{\partial T}{\partial r}(x, r = r_i) = h\left(T_{r=r_i} - T_f\right) \quad 5.20\ (d)$$

$$\frac{\partial T}{\partial r}(x, r = r_o) = 0 \qquad 5.20\ (e)$$

The governing equation between the two processes (charging and discharging) is the same. However, during the discharging process when the heat transfer rate is changed and the storage unit starts discharged.

iii. Numerical solution

The first order backward finite difference method is formulated for the developed 2D mathematical model to discretization in the axial-direction (x) and the (x, r) plane respectively as follows.

<u>HTF:</u>

$$T_{f,i} = \frac{aT_{r=r_i} + \frac{b}{\Delta x}T_{f,i-1} + \frac{1}{\Delta t}T_{f,i}^{n-1}}{a + \frac{b}{\Delta x} + \frac{1}{\Delta t}} \qquad 5.21$$

where: a and b is given by the following expression;

$$a = \frac{2h}{(\rho C_p)_f r_i} \quad , b = \frac{\dot{m}_f}{N\rho_f \pi r_i^2} \qquad 5.22$$

The convective heat transfer coefficient (h) depends on the fact that the flow is laminar or turbulent, and it expressed in terms of Reynolds number and Nusselt number as follows (**Esen & Ayhan, 1996**):

$$Re_f = \frac{2\dot{m}_f}{\pi N \mu_f r_i} \qquad 5.23$$

$$h = \frac{Nu_f * 2r_i}{k_f} \qquad 5.24$$

For laminar flow, the Nusselt number is: $Nu_f = 3.66$

The Gnielinski correlation is applied for the turbulent flow as follows:

$$Nu_f = \frac{\frac{f}{8}(Re_f - 1000)Pr}{1 + 12.7(f/8)^{0.5}(Pr^{2/3} - 1)}, \qquad 3000 \le Re_f \le 5 * 10^6 \qquad 5.25$$

where: f- is Darcy friction factor given by ;

$(0.79 \ln Re_f - 1.64)^{-2}$ 5.26

Nitrate salt storage material:

The heat transfer equation in the storage material is found by applying the conservation of energy principle on a fixed control volume element (i, j) as shown in Fig.5.2, which the inner radius is $r_{,j-1}$ and the outer radius is $r_{,j}$ as follows (**Esen & Ayhan, 1996**):

$$k_s A_i \frac{\partial T}{\partial x_i} - k_s A_{i-1} \frac{\partial T}{\partial x_{i-1}} + k_s A_j \frac{\partial T}{\partial r_j} - k_s A_{j-1} \frac{\partial T}{\partial r_{j-1}} = \rho V_{i,j} \frac{\partial H}{\partial t} \quad 5.26$$

where:

$$\frac{\partial T}{\partial x_i} = \frac{T_{i+1,j}^n - T_{i,j}^n}{\Delta x} \quad , \quad \frac{\partial T}{\partial x_{i-1}} = \frac{T_{i,j}^n - T_{i-1,j}^n}{\Delta x} \quad 5.27$$

$$\frac{\partial T}{\partial r_j} = \frac{T_{i,j+1}^n - T_{i,j}^n}{\Delta r} \quad , \quad \frac{\partial T}{\partial r_{j-1}} = \frac{T_{i,j}^n - T_{i,j-1}^n}{\Delta r} \quad 5.28$$

$$\frac{\partial H}{\partial t_{i,j}} = \frac{H_{i,j}^n - H_{i,j}^{n-1}}{\Delta t} \quad 5.29$$

Substituting the discretized spatial and temporal equations into, the following equation:

$$k_s \pi\left(r_j^2 - r_{j-1}^2\right) \frac{T_{i+1,j}^n - T_{i,j}^n}{\Delta x} - k_s \pi\left(r_j^2 - r_{j-1}^2\right) \frac{T_{i,j}^n - T_{i-1,j}^n}{\Delta x} + k_s 2\pi r_j dx \frac{T_{i,j+1}^n - T_{i,j}^n}{\Delta r} -$$
$$k_s 2\pi r_{j-1} dx \frac{T_{i,j}^n - T_{i,j-1}^n}{\Delta r} = \rho\pi\left(r_j^2 - r_{j-1}^2\right) dx \frac{H_{i,j}^n - H_{i,j}^{n-1}}{\Delta t} \quad 5.30$$

The algebraic equation should be solved with the boundary condition which was mentioned previously and also solved using the Tri-Diagonal Matrix Algorithm in the following computational procedure, which is given in Fig.5.3.

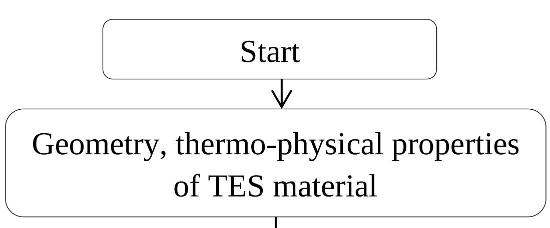

Fig.5.3 Flow chart

5.5 3-D simulation of concrete and nitrate salt TES model

Similar procedure that has taken low-temperature TES model as shown in Fig.4.4 is applied in the present two model by COMSOL Multiphysics 4.3a simulation software. This section also presents the theoretical assumption, governing equation, initial and boundary conditions, and also a 3D numerical model formulation is applied for high-temperature TES systems like that of the presiding chapter. The conservation of mass, momentum, and energy have been used in this work to study the performance of the TES system, and also three physical processes; such as fluid flow, heat transfer by conduction and convection, and the phase transition of the storage material have been simulated with a 3D model **(Jad, 2018)**.

Fluid flow: the law of conservation of mass is applied to the developed concrete and nitrate salt based TES model by considering a fluid passing through an infinitesimally small element that leads to the continuity equation given in Eq. (4.28):

Momentum equation: Newton 2nd law of motion is applied to in the given concrete TES model by a fluid passing through an infinitesimally small element that leads to the momentum equation given in Eq. (5.31) **(Jad, 2018)**, similarly the momentum equation taken for nitrate salt latent heat storage is expressed using Eq. (4.33):

$$\frac{\partial \vec{v}}{\partial t} + \rho(\vec{v}.\nabla)\vec{v} = -\nabla P + \mu\nabla^2\vec{v} \qquad 5.31$$

Energy equation: the energy equation is applicable in the HTF, the storage bed, and between the HTF and storage bed, which is convection on the HTF side and conduction on the sensible storage material given in Eq. (5.4) and (5.5).

$$\rho_f * C_{p,f} * \frac{DT}{Dt} = \nabla.(k_f \nabla T_f) \qquad 5.32$$

$$\rho_s * C_{p,s} * \frac{\partial T}{\partial t} = \nabla.(k_s \nabla T_s) \qquad 5.33$$

Eq. (4.35) and Eq. (4.36) is applicable for the energy equation in the nitrate salt storage bed, and between the HTF and storage bed.

5.5.1 Energy stored/released of in the high-temperature TES model

The quantity of heat, Q, stored/released in an elemental volume of the TES for high-temperature application both sensible and latent heat storage material is calculated by Eq. (4.44), (4.40) and Eq. (4.43) respectively. The thermal energy storage material used for a high-temperature application that selected from the literature is concrete as a sensible storage material and nitrate salt (KNO_3) are also selected as a latent heat storage material based on the thermo-physical properties, cost-effectiveness and easily availability (**Tian & Zhao, 2013**) and (**Shabgard *et al.*, 2010**). The thermo-physical properties of those storage materials are presented in Table 5.1 and Table 5.2.

Finally, to demonstrate which one is a preferred storage material used for high-temperature application with the same volume size, simply compare the amount of stored energy is given below. If the storage material is a latent heat (KNO_3) then the stored/released energy is given by Eq. (4.40) and Eq. (4.43) similar to Eq. (5.34):

$$Q_{T,C} = \rho_s * V_s * C_{ps} * (T_{inlet} - T_{ini}) + \rho_s * V_s * L_F * \lambda \qquad 5.34$$

$$Q_{T,C} = 2109 * 0.057 * 0.95 * (80) + 2109 * 0.057 * 266 = 41.1MJ$$

CHAPTER SIX

RESULTS AND DISCUSSIONS

6.1 Introduction

This chapter presents results obtained from the developed TES model such as; optimization of the number of HTF tubes, the effect of geometric configuration, storage orientation (horizontal and vertical), grid independence test, temperature variation on TES bed. The performance parameters such as; charging/discharging time, amount of energy stored/released, and heat transfer enhancement is discussed in detail with an illustrated figure. Validation of the model with both experimental and numerical previous published work is also done in this chapter.

6.2 Optimization of the number of HTF tubes in the TES bed

The result of charging and discharging time is to be influenced by the number of HTF, so in this section, it is performed optimization of the number of HTF tubes. Different authors implemented various techniques to enhance the heat transfer rate as explained in the preceding chapter such as; pouring highly conductive material, extended surface, and using-multiple PCM. However, in the present study implemented using embedded multi-HTF tubes, to increase the overall heat transfer surface area of the TES system and also improves the thermal conductivity of the storage material especially for PCM.

Consequently, to decide the number of HTF tubes embedded in the developed TES model, optimization technique has been done by developing a 2D numerical model. The number of charging/discharging tubes taken for the present investigation is 13, 17, 21, 25, and 29 in both the TES model as shown in Fig.6.1. As illustrated in Table 6.1 and 6.2 the optimization is done based on charging time for low-temperature TES model and discharging time for high-temperature TES model due to computational time considered into account. When in the case of paraffin wax TES model there is a marginal reduction in the charging time (5.6%) with 25 tubes when compared to 21 tubes, but when 17 HTF tubes compared to 13 and 25 compared to 29 tubes there is massive % reduction in time. Similarly, in the case of the concrete TES model, there is a marginal reduction in the discharging time (7.7%) with 28 tubes when compared to 25 HTF tubes, but when 21 HTF tubes compared to 17 and 25 compared to 21 tubes there is massive % reduction in time.

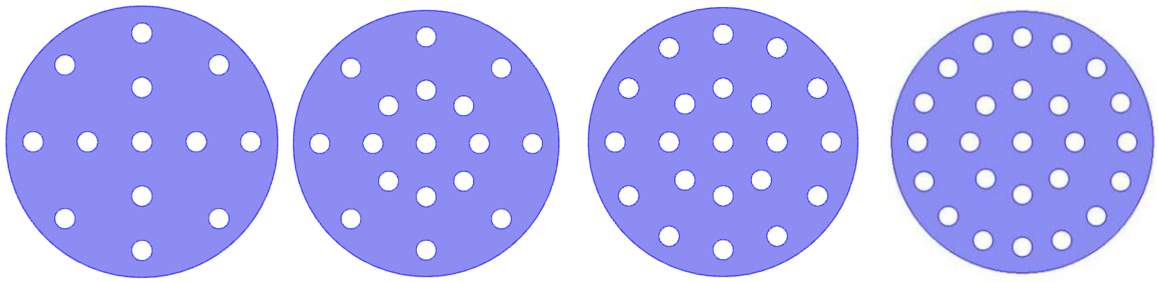

Fig.6.1 Number of HTF tubes taken for optimization

Table 6.1 Optimization of the number of HTF tubes for low-temperature TES bed

No of HTF tubes	Charging time (sec)	% reduction in time
13	13,000	
17	11,600	10.8
21	10,800	6.9
25	10,200	5.6
29	9,800	4.0

Table 6.2 Optimization of the number of HTF tubes for high-temperature TES bed

No of HTF tubes	Discharging time (sec)	% reduction in time
17	8800	
21	7800	11.3
25	7200	7.7
29	6800	5.5

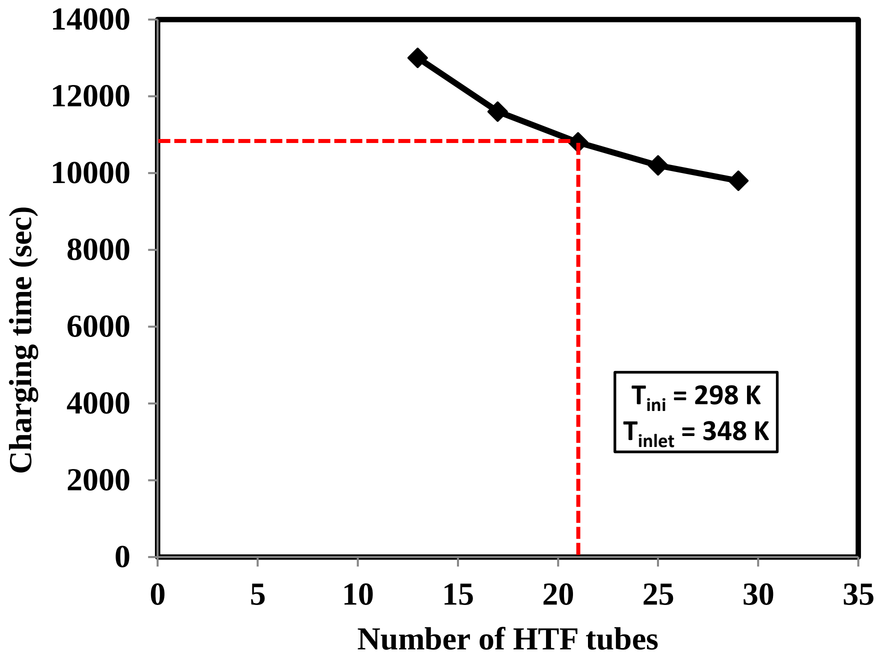

(a)

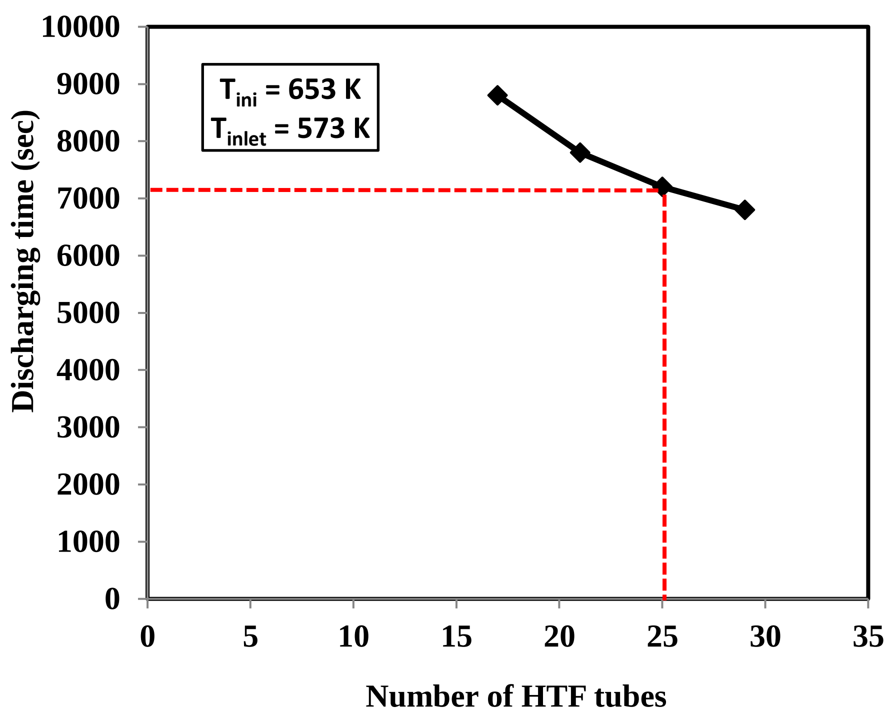

(b)

Fig.6.2 Optimization of number of HTF for (a) paraffin wax (b) concrete storage model

In both cases when further increasing the HTF tubes above 21 and 25 tubes the % reduction in time is not vary significantly as shown in Fig.6.2, but it leads to additional cost and also reduces the effective storage volume. As a result, in the present study select 21 and 25 HTF tubes for low and high–temperature TES models respectively.

6.3 Grid independence test

Grid independence test is performed to check which the numerical result of a developed mathematical model is weather depending or not on the number of mesh element size because the variation of mesh element size has a major controller in the numerical results of all nodes. So, in the present study simulation with different mesh sizes is generating for both TES models during the charging/discharging processes respectively. Comparisons are made for results obtained from different mesh densities for both the TES model to make sure that the results are mesh independent. The range of the densities is varied from 125,165 to 369,561 elements for low-temperature TES bed and varied from 99,034 to 326,602 elements for concrete TES model with three different mesh profiles at the predefined temperatures as shown in Fig. 6.3.

The three grid profiles are coarse (125,165 elements), normal (221,624 elements) and fine (369,561 elements) for paraffin storage bed and coarse (99,034 elements), normal (199,528 elements) and fine (326,602 elements) for concrete storage model. For all the cases of the grid-independent test, the developed two models are initially at 298/573 during the charging process and 348/653 during the discharging process. The results obtained from the mesh element sizes of 221,624 and 369,561 in the first model and 199,528 and 326,602 in the second model are matched closely as shown in the Fig.6.3. That means the % reduction in element size between 369,561 and 221,624 is 40% however, between 221,624 and 125,165 is 43.5% in the first model and similar method used in the second model. It is also noted that increasing the mesh elements leads to an increase in the computational time above 10 hr. The developed TES models are converged with mesh elements less than 369,561 and 326,602. Therefore, to save the computational time, mesh size of 221,624 for the paraffin TES model and 199,528 for concrete TES model has been chosen in the present two models for further analysis.

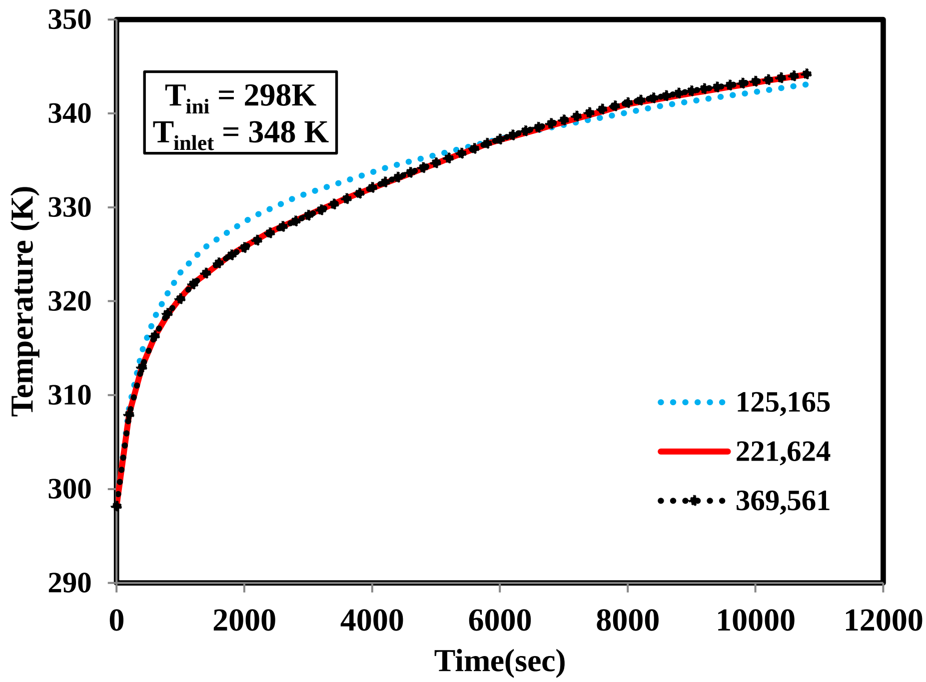

(a)

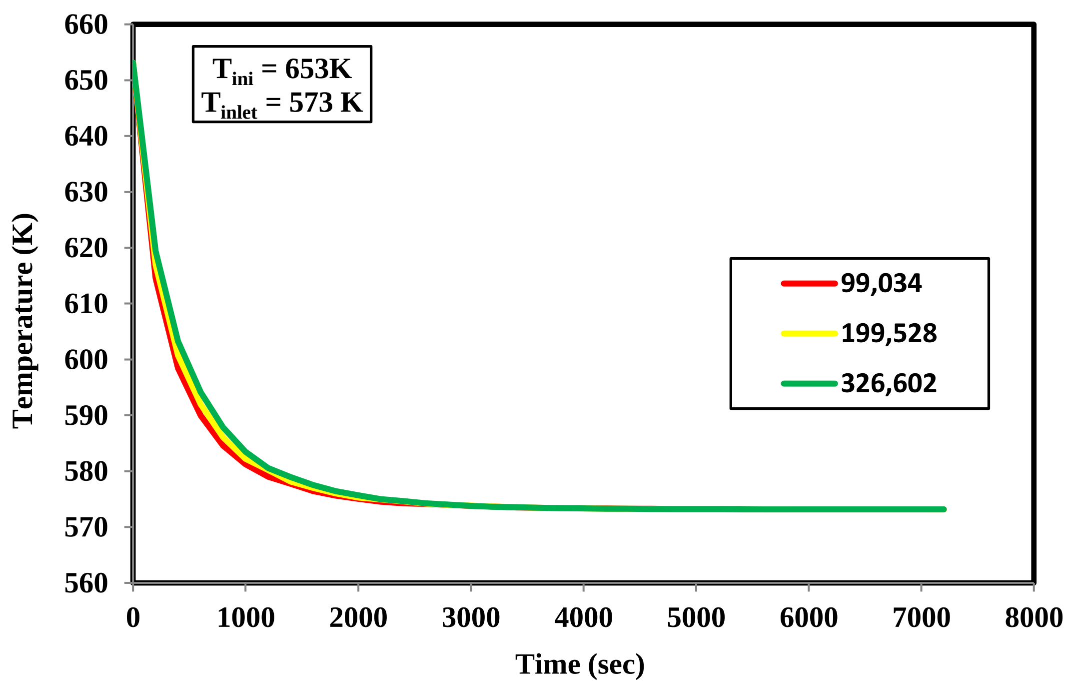

(b)

Fig.6.3 Grid independent test for both TES model during the charging/discharging processes

6.4 Effect of TES bed configuration, orientation and tube arrangement

Cylinder orientation, storage bed geometrical configuration and tube arrangement have an impact on the charging/discharging rate of the TES system for both temperature ranges.

6.4.1 Geometrical configurations

This section examines the effect of different geometrical configurations of TES bed with maintained constant storage volume and heat transfer area, such as; rectangular (square) and cylindrical configurations of TES bed as shown in the Fig.6.4. The geometric configuration effect is tasted based on a concrete based TES model, mainly due to low computational time takes than the paraffin wax TES model by using developed a 2D numerical model.

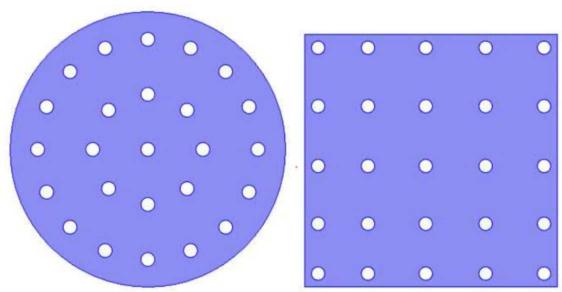

Fig.6.4 Cross-sectional view of cylindrical and rectangular (square) geometries

The effect is tested based on charging time as shown in the Fig.6.5, which is the charging time of cylindrical configuration is 5400 sec. However, in the rectangular configuration, it takes 6800 sec, which is more time required for fully charging the rectangular shape bed relatively compared to cylindrical configurations. Similarly, the % reduction in charging time is 20.58 % between them. The reason behind this is the outer surface of the cylindrical bed is smooth and curved but in the case of rectangular geometry there is a sharp corner and edges in the lateral face, this leads to a limitation of symmetric heat transfer. Similarly, there is an increase of charging time as increasing the number of corners and edges in the outer periphery of a rectangular bed, so due to this fact, a cylindrical configuration is chosen for the present study.

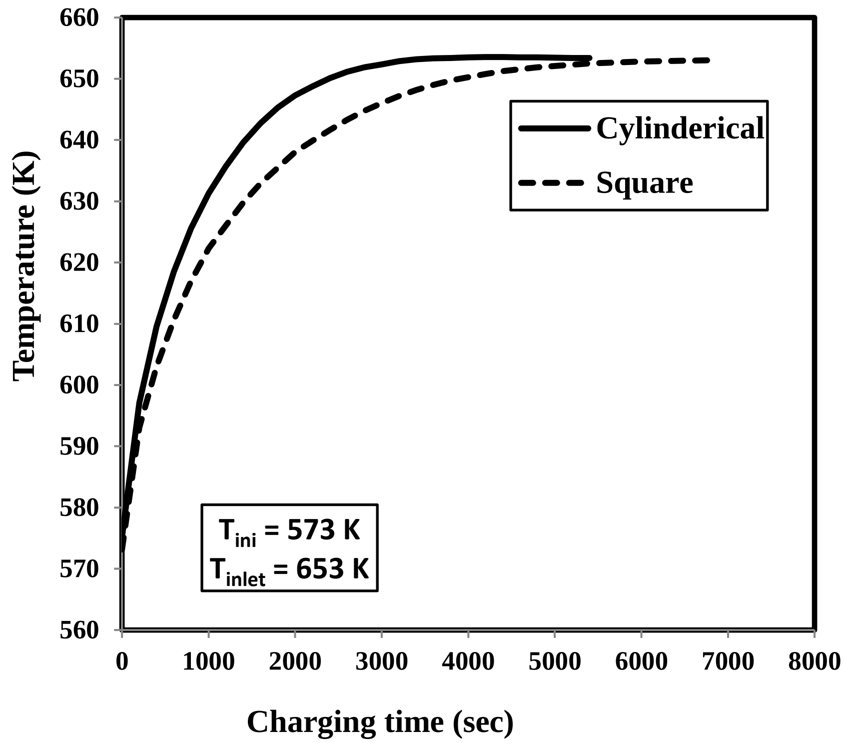

Fig.6.5 Comparison of the charging time between cylindrical and square geometries

6.4.2 Storage bed orientation

A 3D shell-tube TES model which is LHTES and SHTES model are considered to study the effect of cylinder orientation on charging time. As illustrated in Fig.6.6 (a) and (b) comparison between the two different orientations is made during the charging process. As depicted in Fig.6.6a, selected the shortest time take to complete the charging process in the LHTES model. That means the charging time for horizontal orientation is takes 10800 sec but it takes 11800 sec in the case of vertical orientation. The horizontal orientation is approximately 8.5% faster than the vertical orientation. The main reason for the discrepancy of this orientation on the charging time is the effect of buoyancy upon the recirculation of melted LHTES material that creates a strong convective heat transfer rate. But in the case of vertical orientation, the liquid storage material is highly sediments at the bottom due to the effect of gravity. A similar result was reported by **(Gunjo *et al.*, 2018)** on the effect of cylinder orientation. However, in the case of concrete TES bed, there is no effect between the two orientations as shown in Fig.6.6b. Due to this fact, the horizontal orientation is better than vertical orientation and it is also selected for the present investigation.

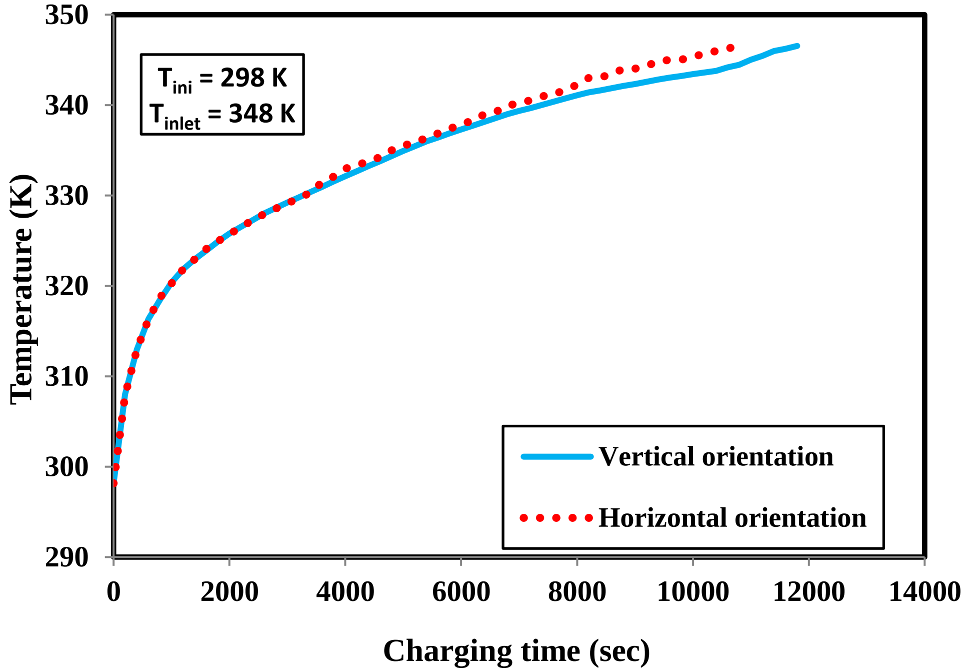

(a)

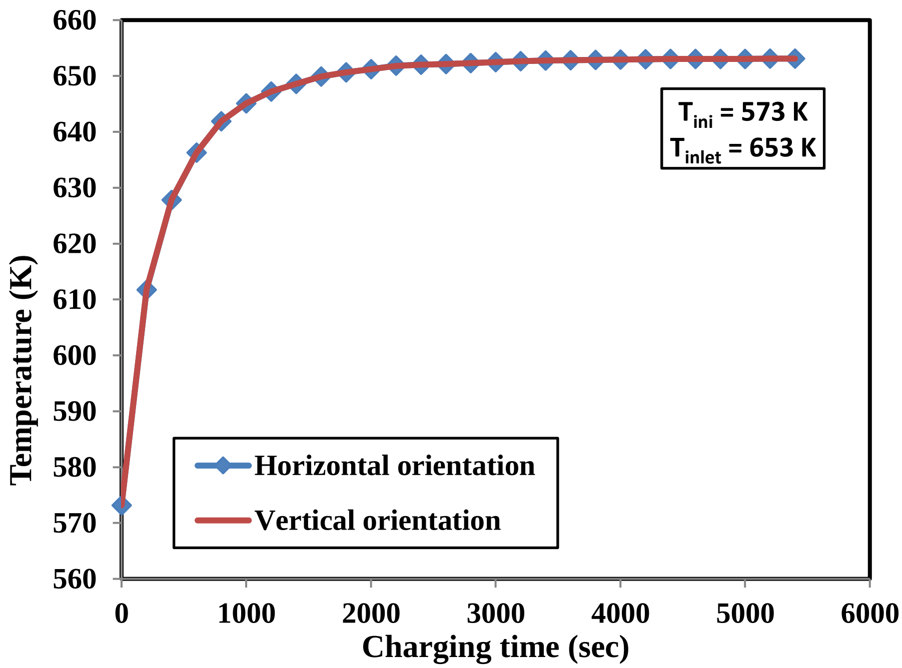

(b)

Fig.6.6 Effect of cylinder orientation on charging time

6.4.3 Tube arrangement

Fig.6.7 (a)-(c) illustrated the effect of tube arrangement in the developed paraffin TES model after optimization of number of HTF tubes during charging process.

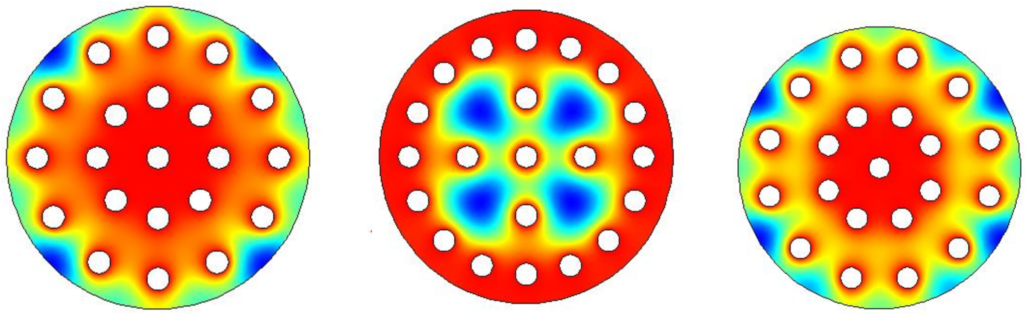

(a) (b) (c)

Fig.6.7 The effect of tube arrangement

The temperature of the paraffin wax bounded in the shell is 298 K initially and 348 K HTF is flow in the inlet HTF tube during charging process. As shown in Fig.6.7 (a) the melting rate of 9 tubes at the center bounded with 12 tubes at the outer is faster than the other two arrangements, the entire temperature of the paraffin wax reaches the inlet temperature of the HTF. Therefore, 9 tubes at the center bounded with 12 tubes at the outer is achieve the required tube arrangement of the TES model in the present investigation

6.5 Performance parameters

This section presents the main performance parameters such as; charging and discharging time, amount of energy stored/released and a liquid fraction (in case of LHTES bed) for both low and high-temperature TES models (sensible and latent) with an illustrated figure.

6.5.1 Charging time

The charging time is tested in two TES model that has developed in the present study i.e., water with paraffin wax and concrete with nitrate salt as shown in Fig.6.8 (a) and (b) respectively. The storage bed is said to be fully charged when its volume average temperature reaches the HTF temperature. That means the storage bed is said to be fully charged when its volume average temperature reaches to 348 K for paraffin and 653 K for concrete storage material.

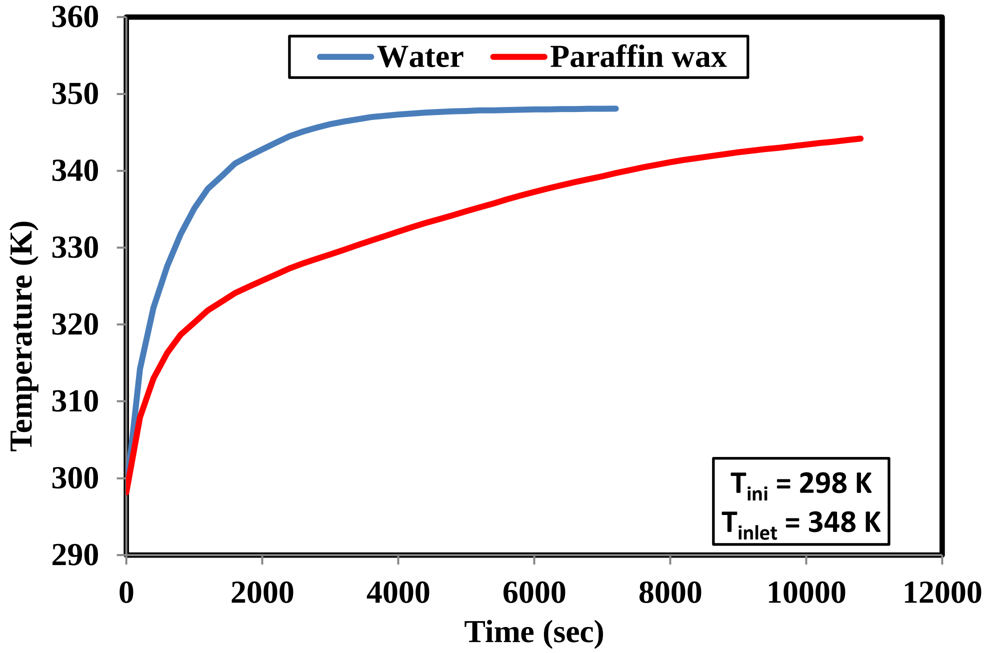

(a)

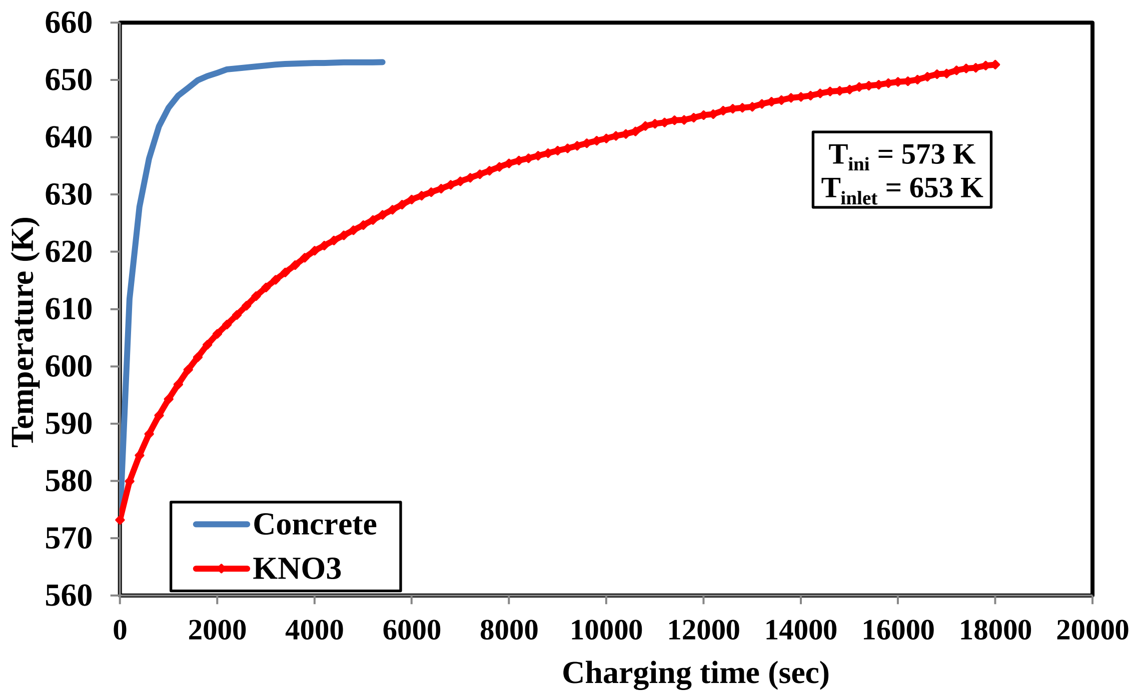

(b)

Fig.6.8 Comparison between charging time of SHTES material and LHTES material

The charging time for SHTES storage material is taken 4600/5400 sec for water and concrete storage model, but it takes 10800/18000 sec for paraffin and KNO_3 salt LHTES model. It is observed in the figure that the time required to fully charging the sensible storage material is relatively less compared to latent heat storage material. This is due to the fact that sensible storage material has less energy density than latent heat storage material with the same storage volume.

6.5.2 Discharging time

Similarly, the discharging time takes to released heat energy from the developed low and high-temperature TES model i.e. water with paraffin wax and concrete with nitrate salt are shown in Fig.6.9 (a) and (b) respectively. The storage bed is said to be fully discharged when its volume average temperature reaches the initial temperature. That means the TES storage bed is said to be fully discharged when its volume average temperature reaches 302 K for paraffin and 573 K for the concrete storage model. The discharging time for SHTES storage material is taken 5400/7200 sec for water and concrete storage model, but it takes 12000/19800 sec for paraffin and KNO_3 salt LHTES model. Similar to the charging time the discharging time as observed in the figure that the time required for fully discharging for sensible storage material is a short time duration compared to LHS material. This is because PCMs have a higher energy density than sensible storage material.

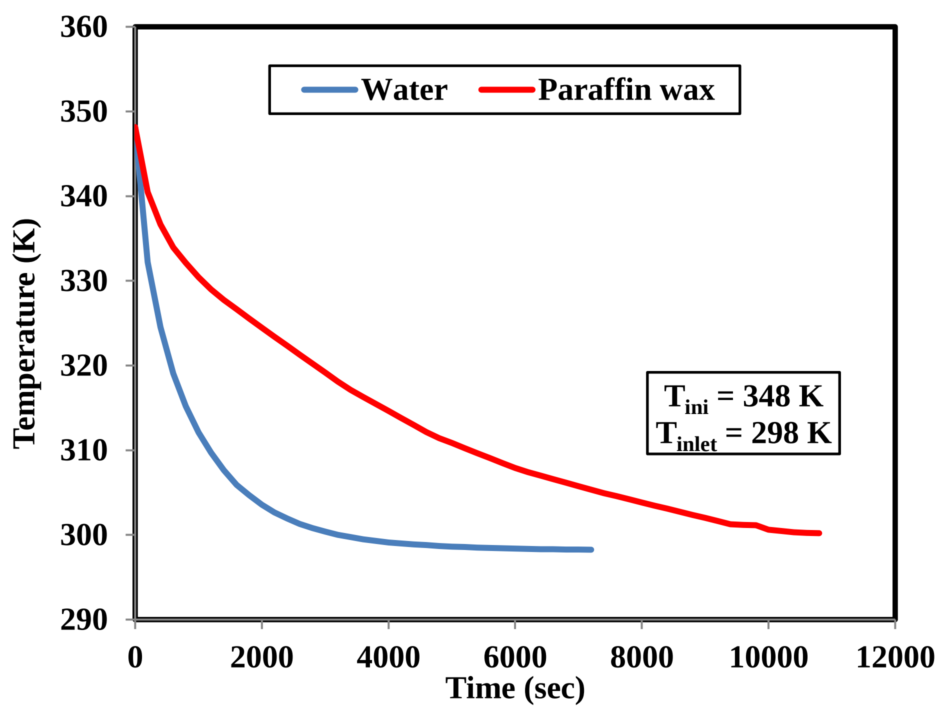

(a)

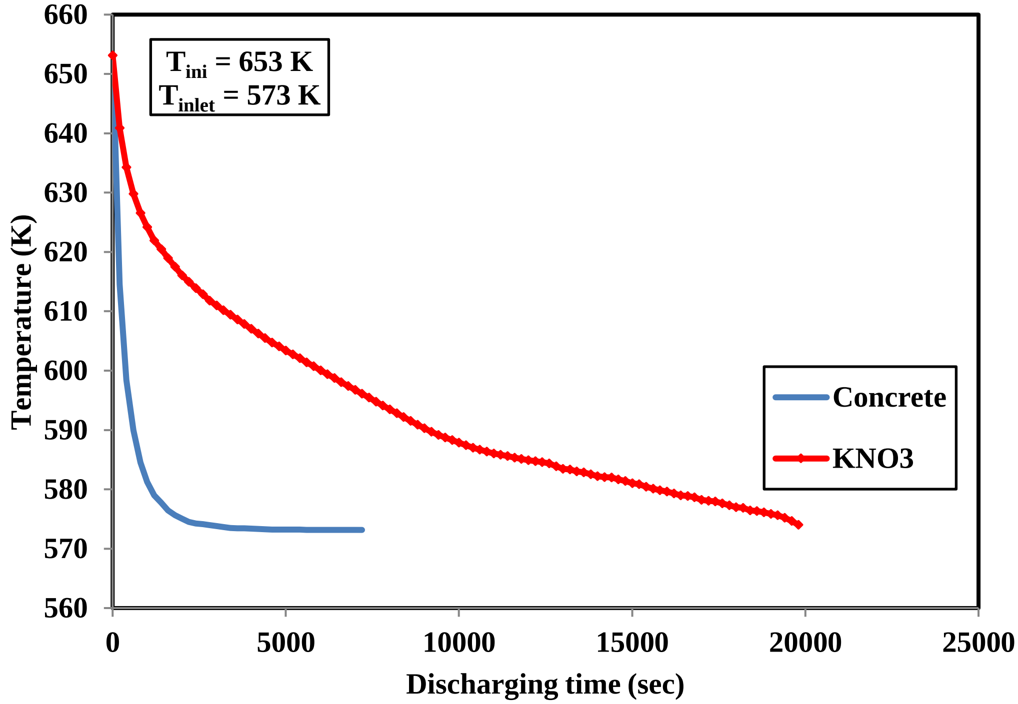

(b)

Fig.6.9 Comparison between discharging time of SHTES material and LHTES material

6.5.3 Liquid fraction

Another performance parameter is the average liquid fraction that has done only in the LHTES model (paraffin wax) to determine the storage is whether fully charged or fully discharged as illustrated in Fig. 6.10 (a) and (b). It can be seen from the figure at the beginning of the charging/discharging processes, the average liquid fraction of the paraffin wax is 0/1, and similarly, the paraffin wax is fully charged/discharged at 10800/12000 sec. At time t = 10800 sec, it can be noted that the storage bed is almost fully charged during the charging process. But during the discharging process at the same time, the storage bed is discharged to a limited extent only and not fully as in the case of charging.

As illustrated in Fig.6.10 the liquid fraction curve indicates the charging process is faster than the discharging process. This is mainly due to the presence of additional heat transfer by natural convection in the charging process. Additionally, the liquid fraction variation is a conduction dominated process during the discharging process. The average liquid fraction variation can be steadily increasing or decreasing at the initial period during both charging and discharging processes, which is mainly due to the higher heat transfer potential availability at the entrance than the exit of the TES model.

6.5.4 Energy stored/released

This section presents the stored/released of heat energy from both low and high-temperature TES beds with an illustrated figure as shown in Fig.6.11 and Fig.6.12 (a) and (b). When in the case of low-temperature TES bed the storage material is used paraffin wax so, initially heat gets stored or released in the form of sensible heat only. Once again the storage bed temperature reaches nearly the phase change temperature (327 K); heat gets stored or released in the form of latent heat and then again above 327 K also stored/released in the form of sensible heat. The amount of sensible, latent, and total energy stored for low-temperature TES bed during the charging process is 2.9, 6.9, and 9.8 MJ respectively at the average temperature of PCM reaches inlet HTF temperature (348 K) within 10,800 sec. The amount of sensible, latent, and total energy stored for low-temperature TES bed during the discharging process is 2.7, 6.9, and 9.6 MJ respectively at the average temperature of PCM reaches 302 K within 12,000 sec. The temperature range at which the PCM stored 2.9 and 2.7 MJ amount of sensible heat are 50 and 46 K during the charging and discharging process respectively.

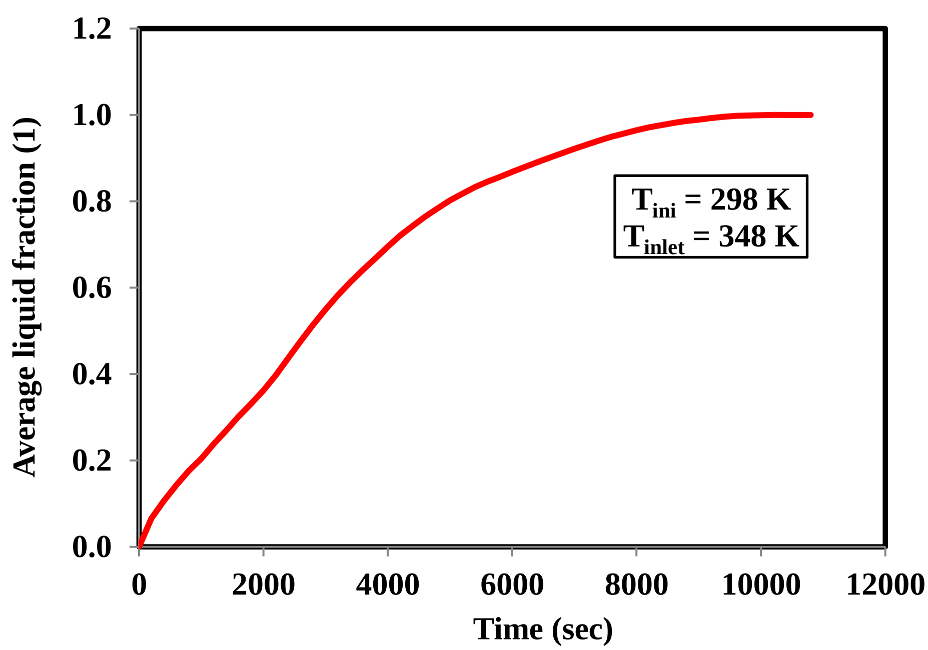

(a)

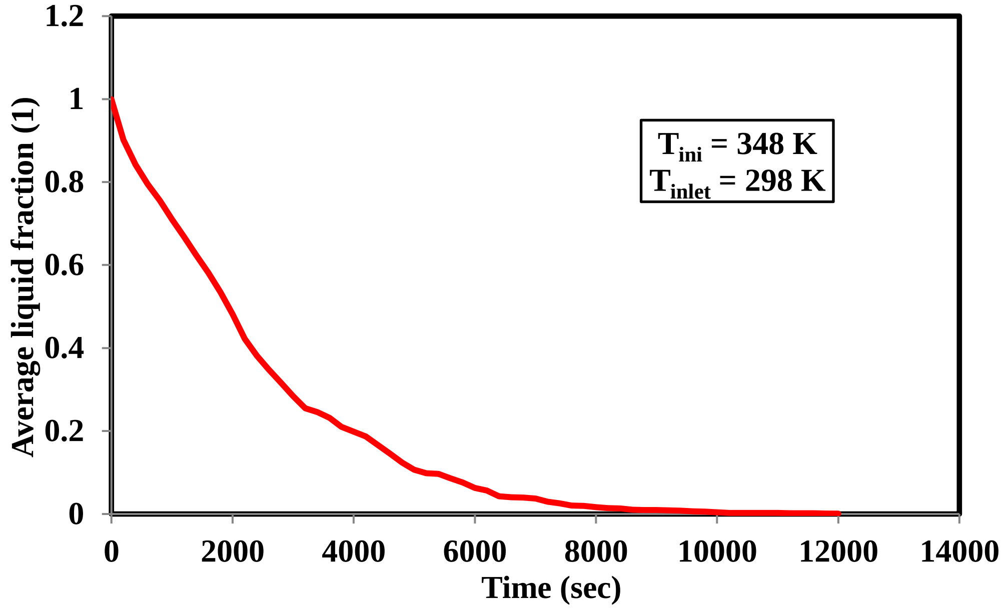

(b)

Fig.6.10 Average liquid fraction curve for low-temperature LHTES model during the charging/discharging process

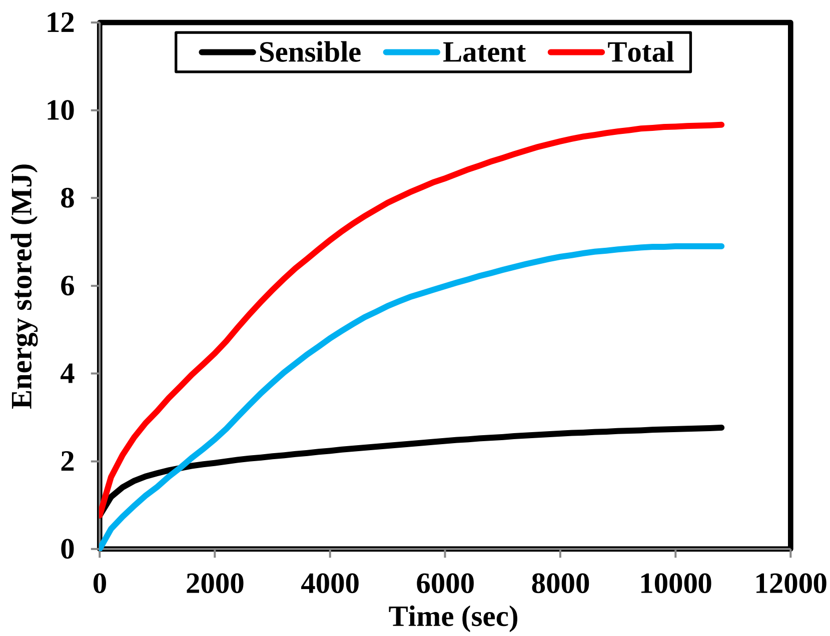

(a)

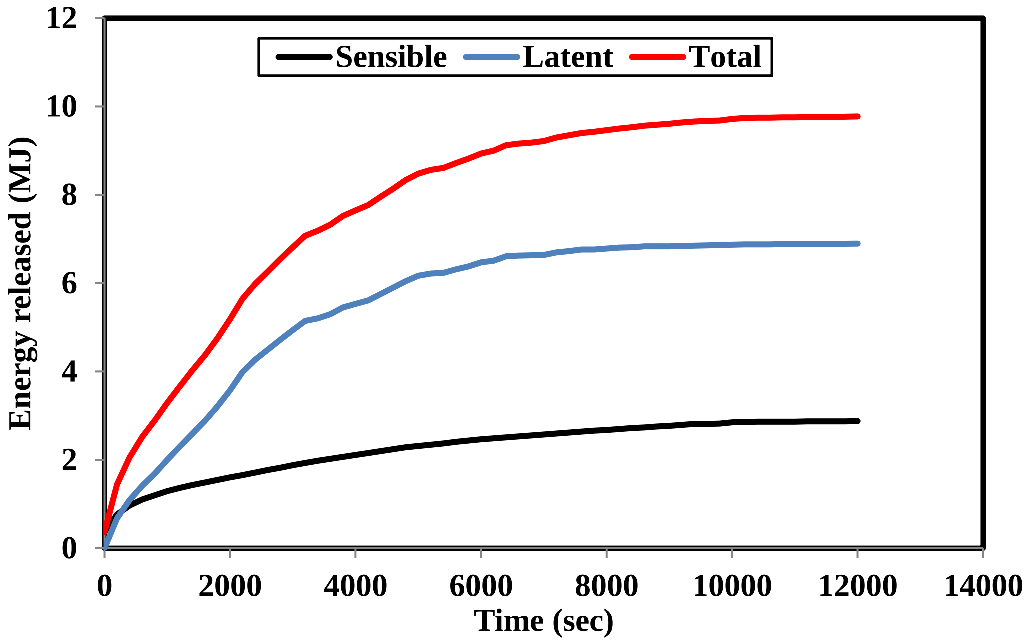

(b)

Fig.6.11 Amount of energy stored/released for low-temperature TES model

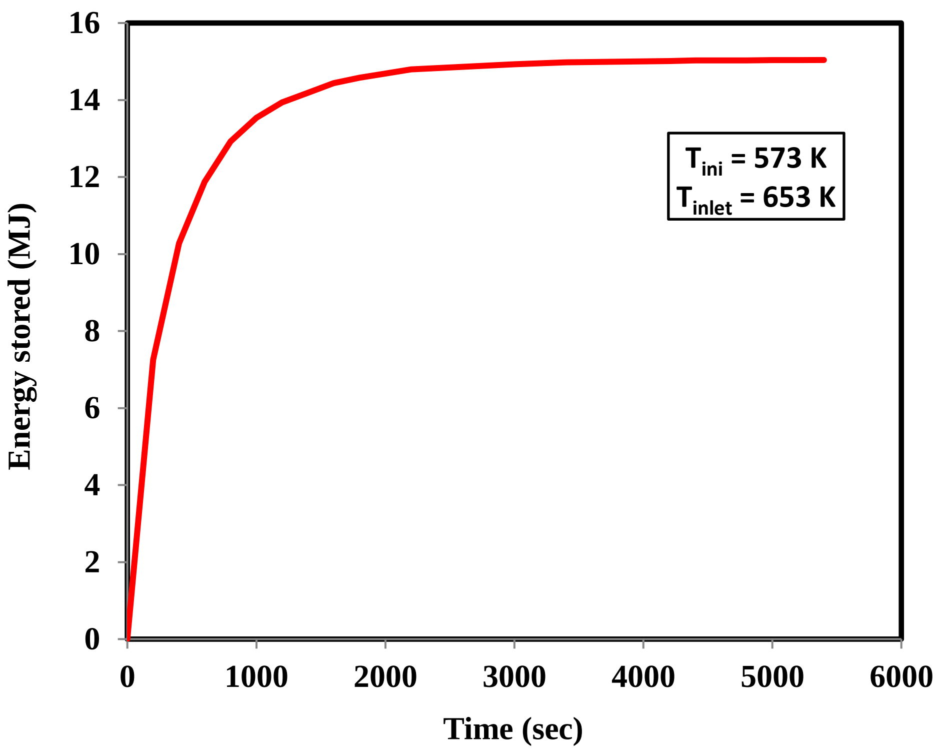

(a)

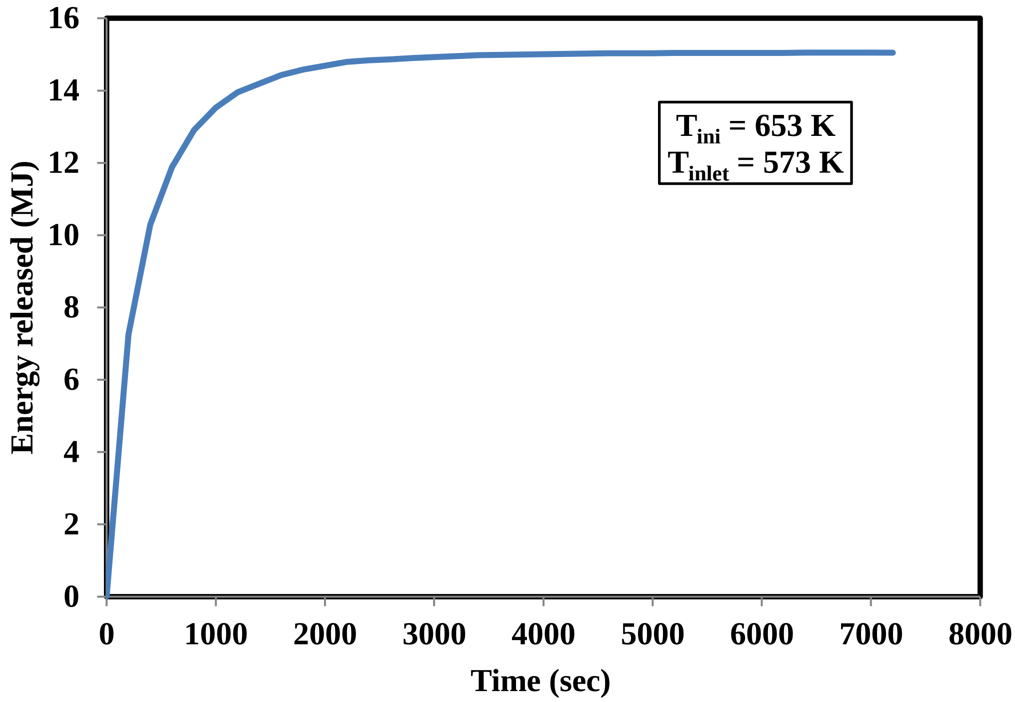

(b)

Fig.6.12 Amount of energy stored/released for high-temperature TES model

However, in the case of high-temperature TES bed, the storage material that has used is concrete, so the stored/released heat energy is in the form of sensible heat only during the charging/discharging processes as shown in Fig.6.12 (a) and (b). The amount of sensible energy stored for high-temperature TES bed during the charging process is 15.06 MJ at 573-653 K average temperature range of concrete within 5,400 sec. Similarly, the amount of sensible energy released from this TES bed is 15 MJ at 573-653 K average temperature range of concrete within 7,200 sec.

6.6 The TES model contour plots

The contour plots of both low and high-temperature thermal energy storage models are as shown in Fig.6.13 (a) - (c). The first plot shows the average liquid fraction contour plot of paraffin wax during the charging/discharging processes with time in Fig.6.13 (a) and (b). At the beginning of the charging/discharging processes (at t = 0 sec), the average liquid fraction is 0 and 1. The paraffin wax completely charged at t = 10800 sec, but not fully discharged at this time duration, it takes 12000 sec to fully discharged. As a result, charging is a faster process than the discharging process mainly due to charging is convection heat transfer dominated process, and discharging is a conduction dominated process. The second contour plot shows the average temperature distribution of high- temperature TES model (concrete) during the charging process. Fig.6.13 c illustrated the temperature distribution inside the concrete at a different time interval which is 0 sec, 1200 sec… 5400 sec. There is no heat transfer between HTF and the concrete storage bed initially or at t = 0 sec. It is noticed from the contour plot that the left end of the storage bed first charged then followed to the right end as a result there is a temperature drop at the end of the storage bed, however, at t = 5400 sec the storage bed fully charged during the charging process.

6.7 Average temperature variation of TES bed

This section discusses the average temperature variation of the thermal energy storage bed in both low and high-temperature ranges during charging and discharging processes, which is the volumetric average temperature of all mesh elements of the numerical model. Initially, the TES bed is at 298/348 and 573/653 K for paraffin and concrete respectively during the charging and discharging processes. When the HTF at 298/348 and 573/653 K are passed through the HTF tubes, the heat transfer takes place between the heat transfer fluid and TES material. During this process, there is a temperature distribution as shown in Fig.6.14. It is observed from the Fig.6.14 (a) – (d) that the average temperature variation curve shows a steady increase or decrease of temperature during charging and discharging at the beginning of the process. This indicates that there is a higher heat transfer potential available at the initial period of the process.

When in the case of low-temperature TES bed, after 2000 sec the slope of the average temperature variation curve started decreasing. The temperature of the storage material reaches approximately 348/302 K during the charging and discharging process in time of 10800/12000 sec, this implies that the process of charging is faster than the discharging process. This is the reason due to the additional convective heat transfer that increases the overall heat transfer rate of the paraffin wax during the charging process.

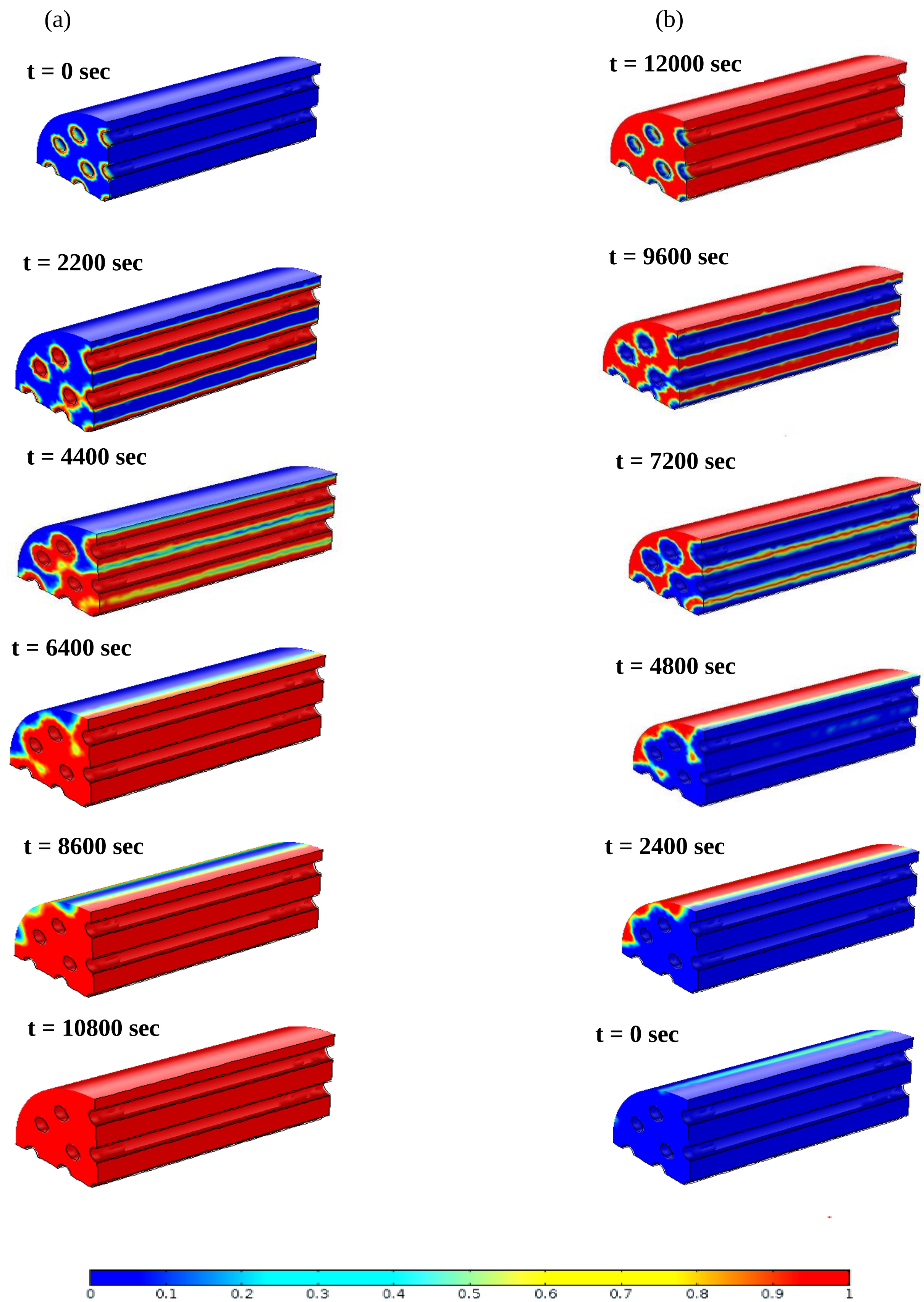
(a)
(b)
t = 0 sec
t = 12000 sec
t = 2200 sec
t = 9600 sec
t = 4400 sec
t = 7200 sec
t = 6400 sec
t = 4800 sec
t = 8600 sec
t = 2400 sec
t = 10800 sec
t = 0 sec
0
0.1
0.2
0.3
0.4
0.5
0.6
0.7
0.8
0.9
1

(c)

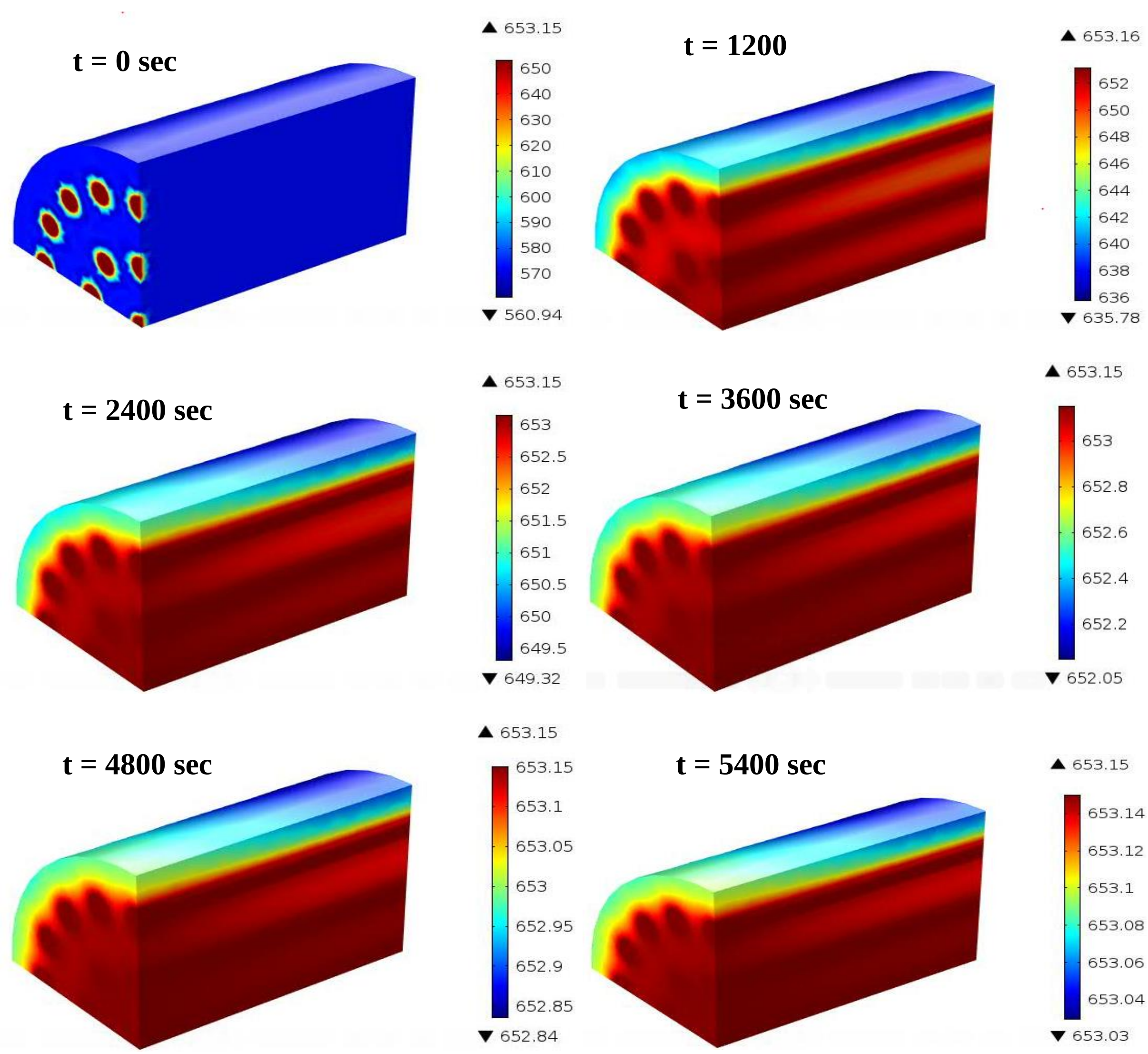

Fig.6.13 Contour plots of low and high-temperature TES model during (a) and (c) are charging and (b) are discharging process.

Similarly in the case of high-temperature TES as shown Fig .6.14 (c) and (d) the rate of temperature rises is up to 600 sec during charging processes, and the average temperature variation curve decreasing up to 800 sec during discharging temperature. This is mainly due to higher heat transfer potential happen during the initial period and then decreasing above this time interval. The rising of the average temperature of the storage bed during this initial period leads to the decreasing of in the HTF temperature gradient.

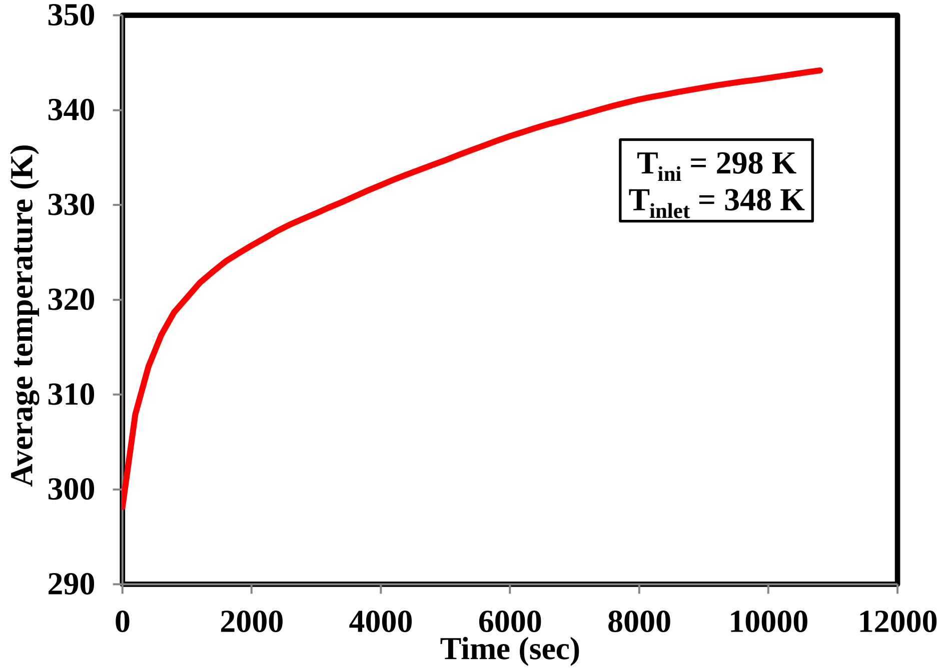
350
340
330
320
310
300
290
Average temperature (K)
0
2000
4000
6000
8000
10000
12000
Time (sec)
T_{ini} = 298 K
T_{inlet} = 348 K

(a)

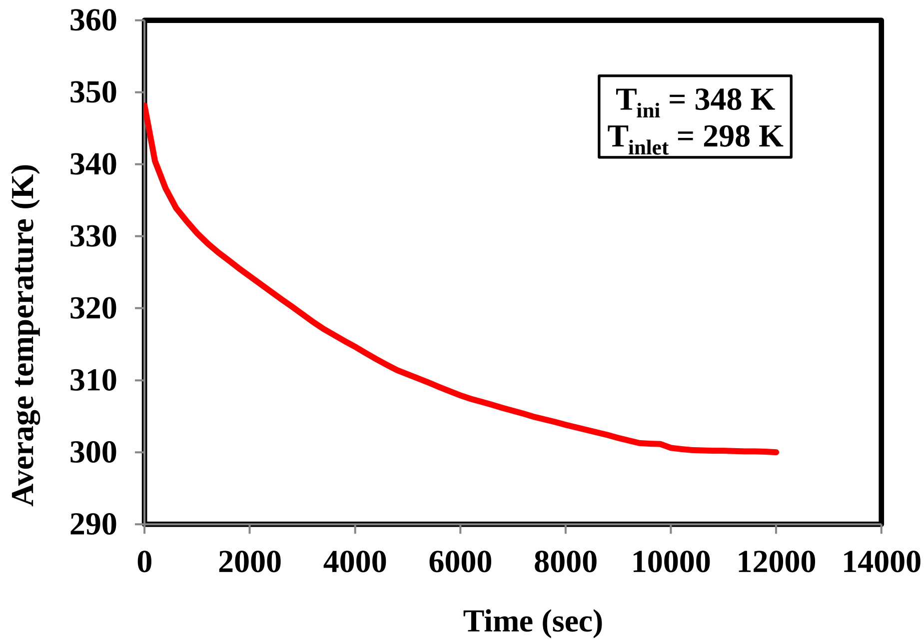
360
350
340
330
320
310
300
290
Average temperature (K)
0
2000
4000
6000
8000
10000
12000
14000
Time (sec)
T_{ini} = 348 K
T_{inlet} = 298 K

(b)

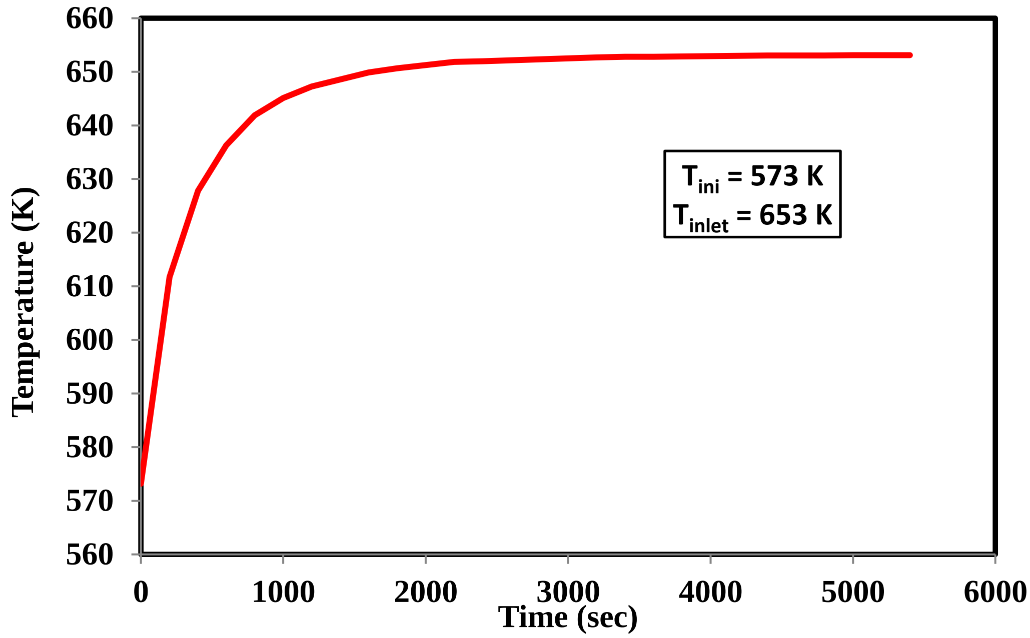

(c)

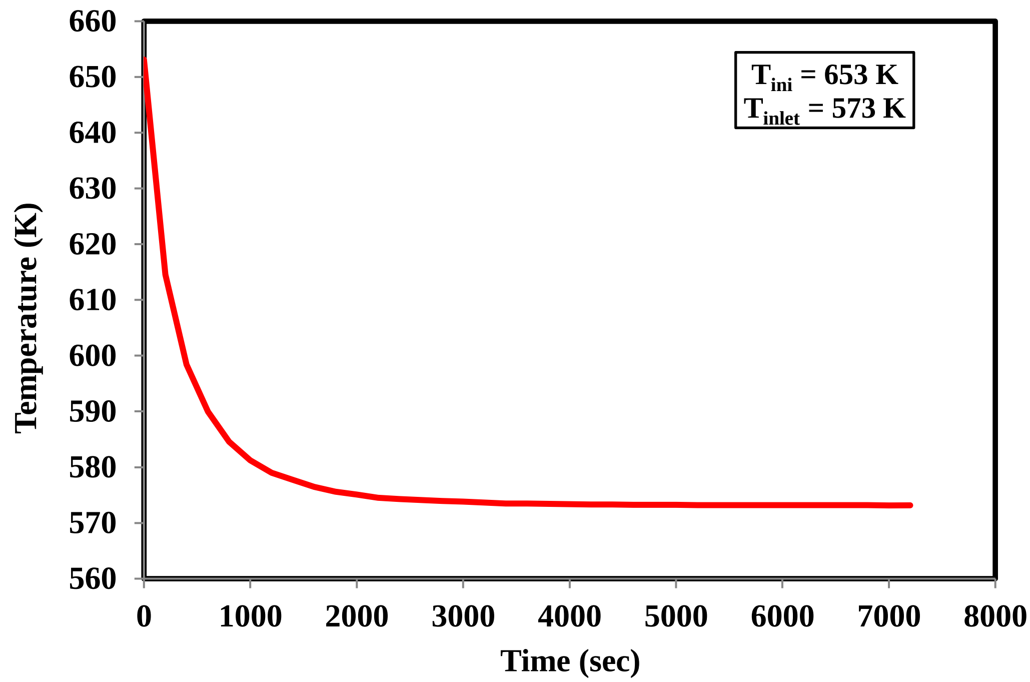

(d)

Fig.6.14 Average temperature variation curve for low and high-temperature TES model during the charging /discharging processes respectively

6.7.1 Temperature variation of outlet HTF

This sub-section presents the outlet HTF temperature variation of both TES models during charging processes as illustrated in Fig.6.15 (a) and (b). This is the outlet HTF temperature variation and the temperature variation difference of inlet and outlet of the TES bed during the charging processes. The outlet HTF temperature variation mainly depends on the thermo-physical property of storage material and the heat transfer potential between the HTF and storage material. There is a steady increase/decrease of the outlet HTF temperature at the beginning of the charging process and after a certain period, reduced the steady increase/decrease of outlet HTF temperature variation as shown in Fig.6.15. This is mainly due to the higher heat transfer potential available between the HTF and storage material at the beginning of the processes and the decline of this heat transfer potential after a certain period. The inlet-outlet HTF temperature variation difference reaches near about zero at 10800/5400 sec for LHTES and SHTES model respectively during the charging process. This indicates that the average temperature of the storage material reaches approximately the inlet temperature of the heat transfer fluid.

6.7.2 Effect of inlet temperature of the HTF

In this section, a numerical simulation was conducted to illustrate the effect of inlet HTF temperature during the charging rate of the paraffin wax. Inlet heat transfer fluid temperature is the main controller in the performance of the TES system. As shown in Fig.6.16 three different inlet temperature (343, 348 and 353 K) are taken for investigation in this section with the constant initial temperature at T_{ini} = 298 K during the charging process. The result gives when an increase in the inlet HTF, decreases the charging time this is due to the addition of extra heat transfer potential between the HTF and the paraffin wax. Consequently, the varying inlet HTF temperature has a great impact on charging time reduction.

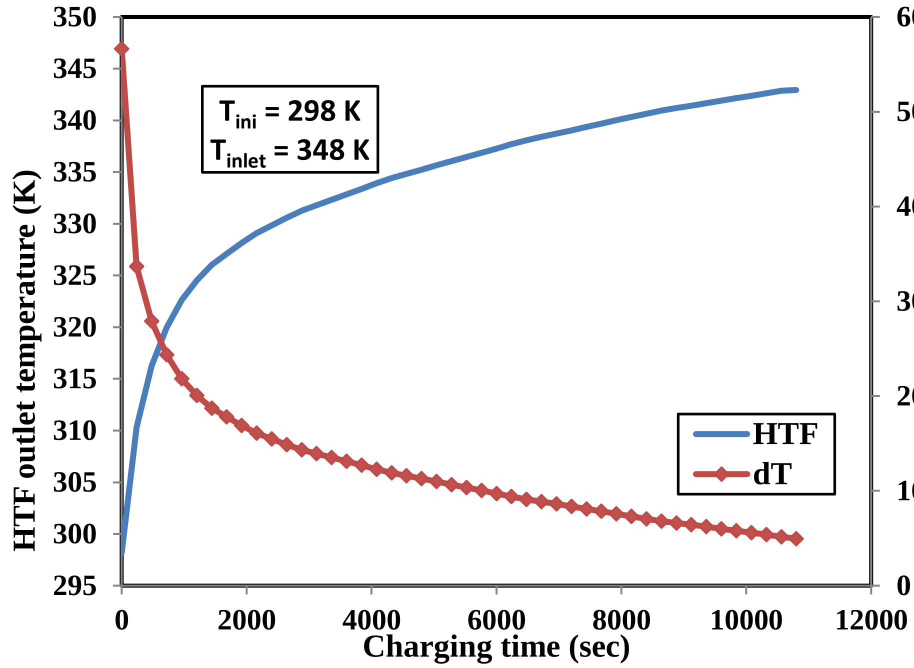

(a)

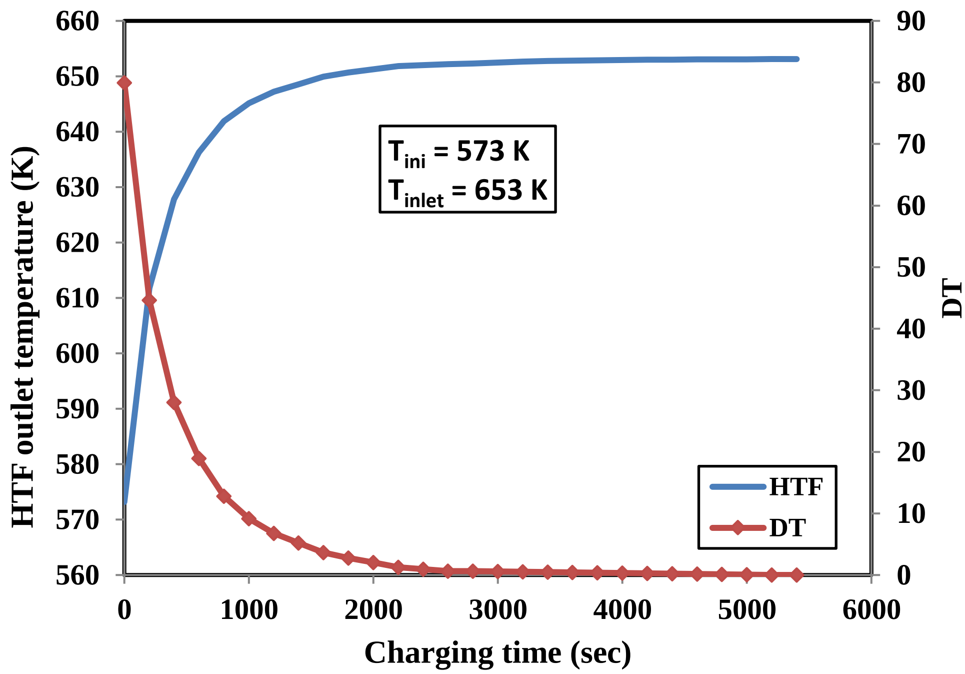

(b)

Fig.6.15 Outlet HTF temperature variation of (a) paraffin wax TES model and (b) concrete TES model during the charging process

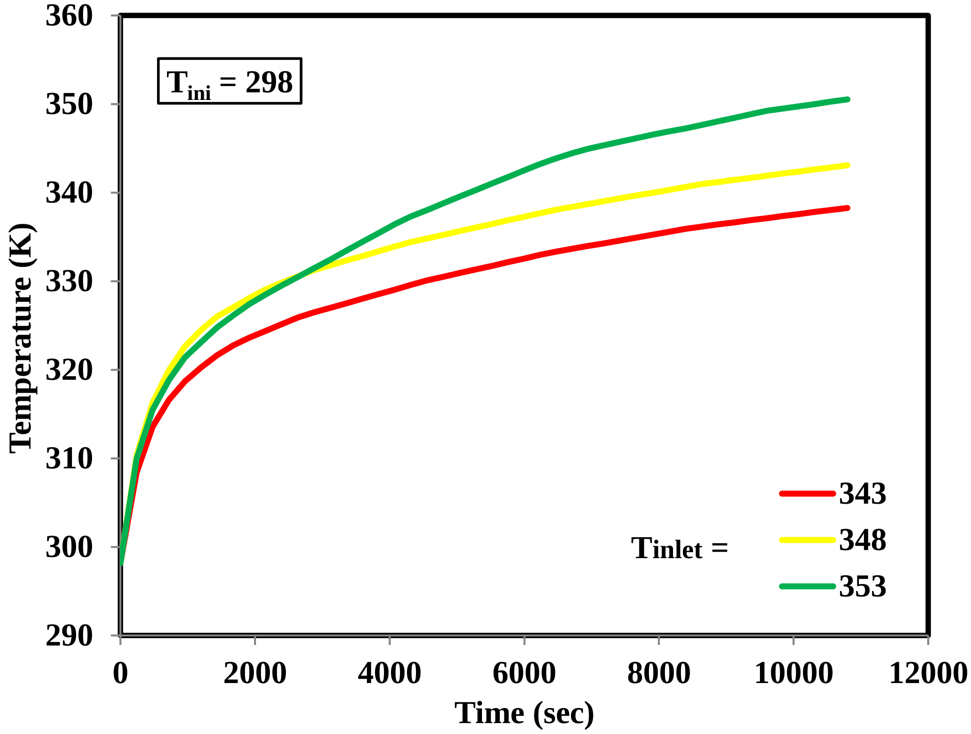

Fig.6.16 The effect of inlet HTF temperature on paraffin wax during the charging process

6.8 Heat transfer enhancement technique

This section presents the comparison study between single shell-tube (double pipe) type TES model and embedding of multi-HTF tubes between the storage materials for the paraffin wax model to enhance the heat transfer rate. Similarly, in the case of concrete storage model inserting copper tube between the HTF and concrete storage bed is another enhancement technique applied in this paper. From the obtained result the single shell-tube storage model is not attainable the required temperature as illustrated in Fig.6.17a. At charging time takes (t = 10800 sec) the average temperature is attained at 327 K but in the case of multi-HTF tubes storage model attain the average temperature of 348 K with similar charging time. That means the time needed to complete charging for a single shell-tube TES model is considerably large as compared to the multi-HTF tube model.

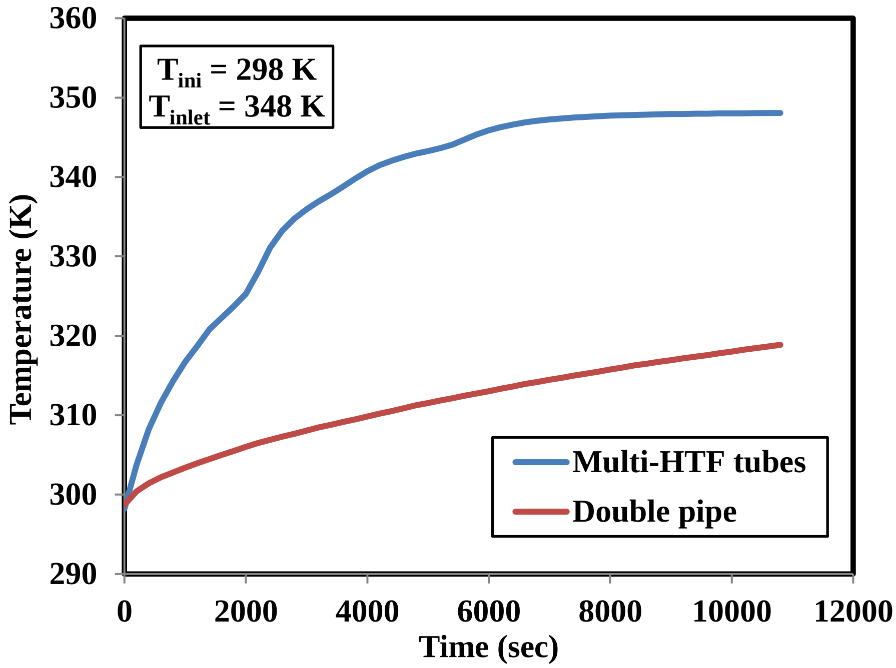

(a)

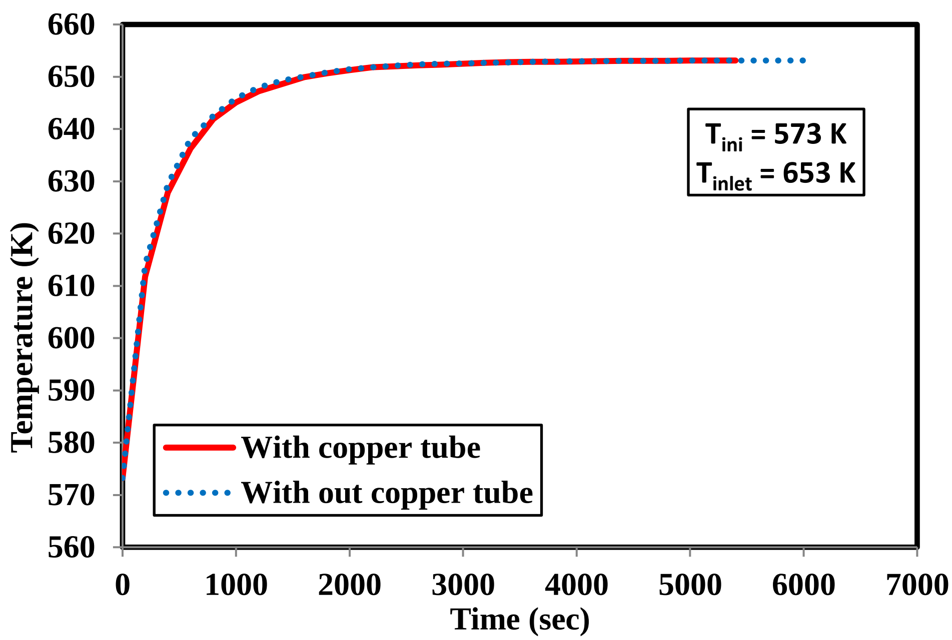

(b)

Fig.6.17 Heat transfer enhancement technique (a) for LHTES model and (b) for SHTES model

This is mainly due to centrally located inner HTF tubes in the double pipe model but an increasing number of HTF tubes inserting between the storage materials is decreasing the complete charging time because the bottom region of the shell is influenced by the extra effective heat transfer surface. The second enhancement technique that applies in a concrete storage model is the comparison between embedding of the copper tube between the concrete, and the HTF and without this tube. As shown in the Fig.6.17b, the time to fully charged concrete with copper tube storage model it takes 5400 sec, but it requires 6200 sec to completely charge the concrete storage model without inserting the copper tube. As a result mainly due to copper metal increase the heat transfer rate of the storage, the embedding of a copper tube between the HTF and concrete is reducing the charging time by 13%.

6.9 Validation of the present TES model

The developed numerical TES model integrated for both low and high-temperature applications is validated with similar work that was done experimentally and numerically by different authors to prove the reliability. The low-temperature TES model is validated with both experimental and numerical data reported by **(Gunjo *et al.*, 2018)**, which is the same storage material (paraffin wax) was used as a storage material. The comparison is held based on charging time as illustrated in Fig.6.18a; the figure indicates that the two numerical investigation result curves have similar shape. However, there is a little variation between the two curves due to the difference in size of the geometry and some thermo-physical properties of the TES model.

The second TES model (concrete) is validated with experimentally reported by **(Tamme *et al.*, 2003)** and also numerically reported by **(Singh & Sørensen, 2017)**. Charging time is the parameter used for validation and also the same concept or the same boundary conditions, the thermo-physical property of the concrete TES model are selected during validation. However, the charging time of the two studies is short as compared to the present study, mainly due to different initial and inlet HTF temperature values are taken in the validation as shown in Fig.6.18b. That means the inlet HTF temperature for the two studies was taken 663 K, but in this study, it is 653 K. Finally, it is understood from the validation result is obtained a good agreement between the present TES model developed numerically and other experimental and numerical developed works reported by different authors.

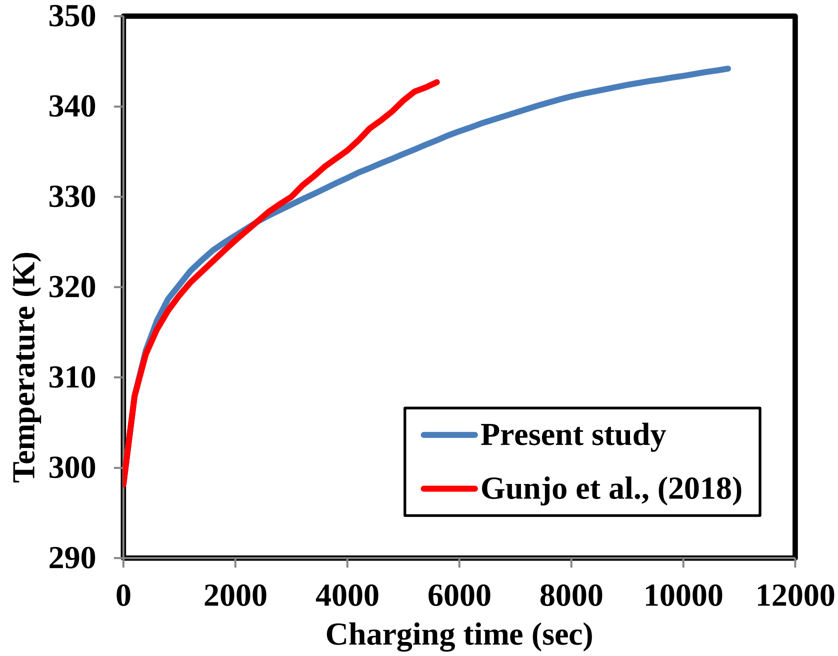

(a)

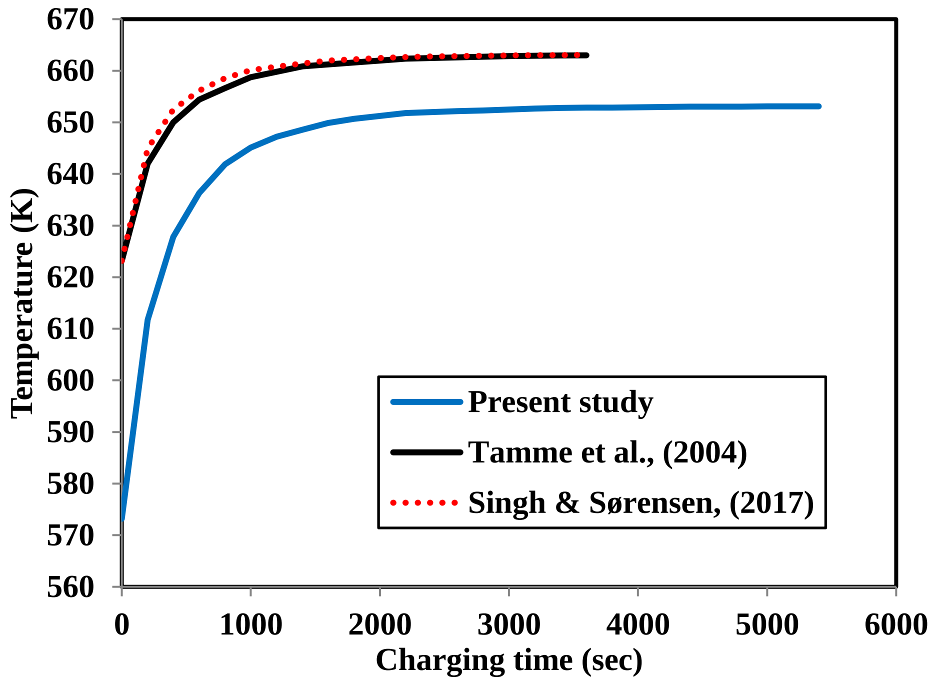

(b)

Fig.6.18 Model validation (a) for the LHTES model and (b) for SHTES model during the charging process

6.10 Summary

A numerical investigation is carried out by developing a 3-D TES model for both low and high-temperature TES systems to study the characteristics of the TES system during the charging and discharging process. Optimization of the number of HTF tubes is done by developing a 2-D model, the effect of geometric configuration and cylinder orientations are also carried out during the study. Additionally, performance parameters like charging and discharging time, liquid fraction, and energy stored/released rate was estimated. The results of the present numerical study are briefly summarized as follows:

- ✓ During the number of HTF tube optimization, 21 and 25 HTF tubes are selected for low and high-temperature TES models respectively.
- ✓ Cylindrical geometry with horizontal orientation is selected for the present study.
- ✓ The charging/discharging time takes 10800/12000 sec for paraffin wax and 5400/7200 sec for the concrete TES model for charging/discharging the TES bed completely.
- ✓ The charging/discharging time of sensible storage material is very less compared to LHTES material and also it stored/released a small amount of heat energy.
- ✓ The developed model is grid-independent.
- ✓ The total amount of energy stored/released was 9.8/9.6 MJ from the paraffin wax TES model and 15.06/15 MJ from the concrete TES model and finally achieved the required amount of heat energy.
- ✓ The developed thermal energy storage models are validated with previous patented experimental and numerical work reported by different authors.
- ✓ The study also applies the heat transfer enhancement technique.

Generally, the simulation result of the present developed TES model is useful in the design and development of TES system integrated for both low and high-temperature application with sensible and latent heat storage material

CHAPTER SEVEN

CONCLUSIONS AND RECOMMENDATIONS

The major conclusions drawn from the developed numerical TES model integrated for low and high-temperature solar thermal applications are presented in this chapter. A summary of the key outcomes arrived from the developed TES model are listed. Some of the recommendations for future work to study further are also presented in this chapter.

7.1 Conclusions

Build thermal energy storage (TES) system in any solar thermal energy application is a robust technology to tackle intermittent and fluctuating nature of solar radiation. In the present study, the performance analysis of the TES system for low and high-temperature applications is investigated. A 3D numerical TES model had been developed for low and high-temperature ranges by optimizing the number of HTF tubes initially. The sizing of the developed TES model was based on the amount of stored energy for the required application.

The developed 3D numerical model simultaneously solved the behavior of both heat transfer fluid flow and heat transfer of sensible (concrete) and latent (paraffin wax) storage material, which is known as based on conjugate heat transfer problem. COMSOL Multiphysics 4.3a commercial software had been used to solve the governing equation of the developed TES model. The results of a developed numerical model are validated with previous numerical and experimental patented work and finally, it was obtained a good agreement between them. The performance parameters such as; charging/discharging time, liquid fraction, and energy stored/released were evaluated in both developed models. Heat transfer enhancement technique which is embedding of multi-HTF tubes between HTF and paraffin wax and inserting copper tube between concrete storage bed was implemented to decrease the charging time. The overall conclusions summarized from the numerical investigations are as follows:

- ✓ It can be achieved by stored 7 MJ heat energy used for low-temperature application (domestic water heating purpose) by using paraffin wax and 15 MJ heat energy for high-temperature application (steam generated purpose in CSP plants) by using concrete as a storage material.

- ✓ Optimize to be 21 and 25 HTF tubes for paraffin and concrete TES model respectively after an implemented number of HTF tube optimization techniques.
- ✓ The charging/discharging time takes for the low-temperature TES model is 10800/12000 sec respectively, similarly, it takes also 5400/7200 sec for the concrete TES model.
- ✓ Discharging is a slower process than the charging process, this is mainly due to discharging is conduction dominated process but charging is a convective dominated process.
- ✓ The inlet HTF is highly impacted on both the charging and discharging time.
- ✓ Embedding of highly conductive metal (copper) with a multi-HTF tube in the storage bed is the best choice to enhance heat transfer rate with decrease charging time, i.e., apply in concrete storage model is decreases charging time by 13%.

7.2 Recommendations for future works

The present study was carried out the performance evaluation of the TES system at various performance parameters. However, this study area offers several opportunities to broaden other investigations, some of such future works are given below.

- ➢ This study was presented the performance analysis of the TES system for only low and high-temperature applications. Numerical investigations could be carried out for the intermediate temperature range.
- ➢ The laminar flow regime is considered in the present numerical study with a significantly low HTF flow rate. However, if the study is extended to a turbulent flow regime in the future it may be several advantages achieved to enhance the heat transfer rate.

Additionally, the TES system is a robust technology to efficiently utilize the harvested solar energy during the absence of solar radiation in any kind of solar thermal application. Therefore, different companies, governmental, and NGOs should build this technology during the promotion and development of solar renewable energy.

REFERENCES

Adinberg, R., Zvegilsky, D., & Epstein, M. (2010). Heat transfer efficient thermal energy storage for steam generation. *Energy Conversion and Management*, *51*(1), 9–15. https://doi.org/10.1016/j.enconman.2009.08.006

Adine, H. A., & Qarnia, H. El. (2009). Numerical analysis of the thermal behaviour of a shell-and-tube heat storage unit using phase change materials. *Applied Mathematical Modelling*, *33*(4), 2132–2144. https://doi.org/10.1016/j.apm.2008.05.016

Agyenim, F., Eames, P., & Smyth, M. (2009). A comparison of heat transfer enhancement in a medium temperature thermal energy storage heat exchanger using fins. *Solar Energy*, *83*(9), 1509–1520. https://doi.org/10.1016/j.solener.2009.04.007

Agyenim, F., Eames, P., & Smyth, M. (2010). Heat transfer enhancement in medium temperature thermal energy storage system using a multitube heat transfer array. *Renewable Energy*, *35*(1), 198–207. https://doi.org/10.1016/j.renene.2009.03.010

Al-Maghalseh, M. (2014). Compact solar thermal energy storage systems using phase change materials. 322.

Alguacil, M., Prieto, C., Rodriguez, A., & Lohr, J. (2014). Direct steam generation in parabolic trough collectors. *Energy Procedia*, *49*, 21–29. https://doi.org/10.1016/j.egypro.2014.03.003

Alonso, M. C., Vera-agullo, J., Guerreiro, L., Flor-laguna, V., Sanchez, M., & Collares-pereira, M. (2016). Cement and concrete research calcium aluminate based cement for concrete to be used as thermal energy storage in solar thermal electricity plants. *Cement and Concrete Research*, *82*, 74–86. https://doi.org/10.1016/j.cemconres.2015.12.013

Alva, G., Lin, Y., & Fang, G. (2018). An overview of thermal energy storage systems. *Energy*, *144*, 341–378. https://doi.org/10.1016/j.energy.2017.12.037

Alva, G., Liu, L., Huang, X., & Fang, G. (2017). Thermal energy storage materials and systems for solar energy applications. *Renewable and Sustainable Energy Reviews*, *68*(August 2016), 693–706. https://doi.org/10.1016/j.rser.2016.10.021

Asefa, N. S. (2019). Numerical investigation of solar vapor absorption refrigeration system integrated with phase change material for industrial application. *Masters Thesis of Mechanical Engineeering;*

Ataer, (2006). (2006). Storage of thermal energy. *Developed under the Auspices of the UNESCO, Eolss Publishers, Oxford ,UK, [http://www.eolss.net]*.

Bauer, T., Pfleger, N., Breidenbach, N., Eck, M., Laing, D., & Kaesche, S. (2013). Material aspects of solar salt for sensible heat storage. *Applied Energy*, *111*, 1114–1119. https://doi.org/10.1016/j.apenergy.2013.04.072

Behar, O., Khellaf, A., & Mohammedi, K. (2015). A novel parabolic trough solar collector model - Validation with experimental data and comparison to Engineering Equation Solver (EES). *Energy Conversion and Management*, *106*, 268–281. https://doi.org/10.1016/j.enconman.2015.09.045

Bekele, A. (2007). Large scale application of solar water heating system in ethiopia. *Masters Thesis of Mechanical Engineeering;*.

Bellan, S., Gonzalez-Aguilar, J., Romero, M., Rahman, M. M., Goswami, D. Y., & Stefanakos, E. K. (2015). Numerical Investigation of PCM-based Thermal Energy Storage System. *Energy Procedia*, *69*, 758–768. https://doi.org/10.1016/j.egypro.2015.03.086

Bouadila, S., Lazaar, M., Skouri, S., Kooli, S., & Farhat, A. (2014). Energy and exergy analysis of a new solar air heater with latent storage energy. *International Journal of Hydrogen Energy*, *39*(27), 15266–15274. https://doi.org/10.1016/j.ijhydene.2014.04.074

Bugaje, I. M. (1997). Enhancing the thermal response of latent heat storage systems. *International Journal of Energy Research*, *21*(9), 759–766. https://doi.org/10.1002/(SICI)1099-114X(199707)21:9<759::AID-ER254>3.0.CO;2-7

Cárdenas, B., & León, N. (2013). High temperature latent heat thermal energy storage: Phase change materials, design considerations and performance enhancement techniques. *Renewable and Sustainable Energy Reviews*, *27*, 724–737.

https://doi.org/10.1016/j.rser.2013.07.028

Chavan, S., Panwar, V., & Rathod, R. (2015). *Review on Thermal Energy Storage Techniques*. *3*(4), 944–948.

Colella, F., Sciacovelli, A., & Verda, V. (2012). Numerical analysis of a medium scale latent energy storage unit for district heating systems. *Energy*, *45*(1), 397–406. https://doi.org/10.1016/j.energy.2012.03.043

Da Cunha., Jose Pereira., P. E. (2016). Thermal energy storage for low and medium temperature applications using phase change materials - A review. *Applied Energy*, *177*, 227–238. https://doi.org/10.1016/j.apenergy.2016.05.097

Diarce, G., Gandarias, I., Campos-Celador, García-Romero, A., & Griesser, U. J. (2015). Eutectic mixtures of sugar alcohols for thermal energy storage in the 50-90°C temperature range. *Solar Energy Materials and Solar Cells*, *134*, 215–226. https://doi.org/10.1016/j.solmat.2014.11.050

Dinçer, İ., & Zamfirescu, C. (2012). Sustainable energy systems and applications. *Sustainable Energy Systems and Applications*, 1–816. https://doi.org/10.1007/978-0-387-95861-3

Dolado, P., Gil, A., Medrano, M., Martorell, I., La, A., & Cabeza, L. F. (2010). State of the art on high temperature thermal energy storage for power generation . *Part 1 — Concepts , materials and modellization*. *14*, 31–55. https://doi.org/10.1016/j.rser.2009.07.035

Duffie and Beckman, (2013). (2013). Solar engineering of thermal processes-*John Wiley & Sons Ltd (2013).pdf*.

Dutta, R., Atta, A., & Dutta, T. K. (2008). Experimental and numerical study of heat transfer in horizontal concentric annulus containing phase change material. *Canadian Journal of Chemical Engineering*, *86*(4), 700–710. https://doi.org/10.1002/cjce.20075

El Qarnia, H. (2009). Numerical analysis of a coupled solar collector latent heat storage unit using various phase change materials for heating the water. *Energy Conversion and Management*, *50*(2), 247–254. https://doi.org/10.1016/j.enconman.2008.09.038

Esen, M., & Ayhan, T. (1996). Development of a model compatible with solar assisted cylindrical energy storage tank and variation of stored energy with time for different phase change materials. *Energy Conversion and Management*, *37*(12), 1775–1785. https://doi.org/10.1016/0196-8904(96)00035-0

Farid, M. M., Khudhair, A. M., Razack, S. A. K., & Al-Hallaj, S. (2004). A review on phase change energy storage: Materials and applications. *Energy Conversion and Management*, *45*(9–10), 1597–1615. https://doi.org/10.1016/j.enconman.2003.09.015

Fernández-García, A., Zarza, E., Valenzuela, L., & Pérez, M. (2010). Parabolic-trough solar collectors and their applications. *Renewable and Sustainable Energy Reviews*, *14*(7), 1695–1721. https://doi.org/10.1016/j.rser.2010.03.012

Gokon, N., Nakano, D., Inuta, S., & Kodama, T. (2008). High-temperature carbonate/MgO composite materials as thermal storage media for double-walled solar reformer tubes. *Solar Energy*, *82*(12), 1145–1153. https://doi.org/10.1016/j.solener.2008.05.011

González-roubaud, E., Pérez-osorio, D., & Prieto, C. (2017). Review of commercial thermal energy storage in concentrated solar power plants : Steam vs . molten salts. *Renewable and Sustainable Energy Reviews*, *80*(March 2016), 133–148. https://doi.org/10.1016/j.rser.2017.05.084

Gunjo, D. G., Jena, S. R., Mahanta, P., & Robi, P. S. (2018). Melting enhancement of a latent heat storage with dispersed Cu, CuO and Al2O3 nanoparticles for solar thermal application. *Renewable Energy*, *121*, 652–665. https://doi.org/10.1016/j.renene.2018.01.013

Gunjo, D. G., Mahanta, P., & Robi, P. S. (2017). CFD and experimental investigation of flat plate solar water heating system under steady state condition. *Renewable Energy*, *106*, 24–36. https://doi.org/10.1016/j.renene.2016.12.041

Hachicha, A. A., Rodríguez, I., Capdevila, R., & Oliva, A. (2013). Heat transfer analysis and numerical simulation of a parabolic trough solar collector. *Applied Energy*, *111*, 581–592. https://doi.org/10.1016/j.apenergy.2013.04.067

Haillot, D., Bauer, T., Kröner, U., & Tamme, R. (2011). Thermal analysis of phase change materials in the temperature range 120-150 °c. *Thermochimica Acta*, *513*(1–2), 49–59. https://doi.org/10.1016/j.tca.2010.11.011

Hall, D. O., Rosillo-Calle, F., & de Groot, P. (1992). Biomass energy. Lessons from case studies in developing countries. *Energy Policy*, *20*(1), 62–73. https://doi.org/10.1016/0301-4215(92)90148-U

Hasnain, S. M. (1998a). Review on sustainable thermal energy storage technologies, part I: Heat storage materials and techniques. *Energy Conversion and Management*, *39*(11), 1127–1138.

Hasnain, S. M. (1998b). Review on sustainable thermal energy storage technologies, part II: Cool thermal storage. *Energy Conversion and Management*, *39*(11), 1139–1153. https://doi.org/10.1016/S0196-8904(98)00024-7

Heller, A. (2000). 15 years of r & d in central solar heating in Denmark. *69*(6), 437–447.

Huang, W., Hu, P., & Chen, Z. (2012). Performance simulation of a parabolic trough solar collector. *Solar Energy*, *86*(2), 746–755. https://doi.org/10.1016/j.solener.2011.11.018

IBRAHIM DINCER, S. D. A. X. L. (1997). Performance analyses of sensible heat storage systems for thermal applications. *International Journal of Energy Research*, *21*(12), 1157–1171. https://doi.org/10.1002/(SICI)1099-114X(19971010)21:12<1157::AID-ER317>3.0.CO;2-N

Jad, U. M. (2018). Numerical analysis on thermal energy storage tank filled with phase change material. *2581*, 303–307.

Janjai, S., Esper, A., & Mühlbauer, W. (2000). Modelling the performance of a large area plastic solar collector. *Renewable Energy*, *21*(3), 363–376. https://doi.org/10.1016/S0960-1481(00)00087-2

Jegadheeswaran, S., & Pohekar, S. D. (2009). Performance enhancement in latent heat thermal storage system : *A review*. *13*, 2225–2244. https://doi.org/10.1016/j.rser.2009.06.024

Jian, Y., Falcoz, Q., Neveu, P., Bai, F., Wang, Y., & Wang, Z. (2015). Design and optimization of solid thermal energy storage modules for solar thermal power plant applications. *Applied Energy*, *139*, 30–42. https://doi.org/10.1016/j.apenergy.2014.11.019

Kalogirou, S. (1996). Parabolic trough collector system for low temperature steam generation : *Design and Performance Characteristics*. *55*(I).

Kaygusuz, K. (2012). Energy for sustainable development: A case of developing countries. *Renewable and Sustainable Energy Reviews*, *16*(2), 1116–1126. https://doi.org/10.1016/j.rser.2011.11.013

Kefa, B. G. (2019). Study on the performance of linear fresnel solar collector with sensible thermal energy storage for industrial process heat generation. *Masters Thesis of Mechanical Engineeering;*

Kenisarin, M. M. (2010). High-temperature phase change materials for thermal energy storage. *Renewable and Sustainable Energy Reviews*, *14*(3), 955–970. https://doi.org/10.1016/j.rser.2009.11.011

Khan, B., & Singh, P. (2017). The current and future states of Ethiopia's energy sector and potential for green energy: A comprehensive study. *International Journal of Engineering Research in Africa*, *33*(November), 115–119. https://doi.org/10.4028/www.scientific.net/JERA.33.115

Ledesma, J. T. (2010). Numerical simulation of the solar thermal energy storage system for domesic hot water supply located in South Spain. *Institute of Heat Engineering*, *Warsaw University of Technology*, *Warsaw*, *Poland corresponding author*; *e-mail: Piotr.Lapka@itc.pw.edu.pl*, 1–15.

Liu, M., Saman, W., & Bruno, F. (2012). Review on storage materials and thermal performance enhancement techniques for high temperature phase change thermal storage systems. *Renewable and Sustainable Energy Reviews*, *16*(4), 2118–2132. https://doi.org/10.1016/j.rser.2012.01.020

Liu, M., Tay, N. H. S., Bell, S., Belusko, M., Jacob, R., Will, G., Saman, W., & Bruno, F. (2016). Review on concentrating solar power plants and new developments in high temperature thermal energy storage technologies. *Renewable and Sustainable Energy Reviews*, *53*, 1411–1432. https://doi.org/10.1016/j.rser.2015.09.026

Lüpfert, E., Geyer, M., Schiel, W., Zarza, E., Osuna, R., & Nava, P. (2000). Eurotrough – a new parabolic trough collector with advanced light weight structure. *Solar Thermal 2000 International Conference*, *March*, 6.

Mahfuz, M. H., Anisur, M. R., Kibria, M. A., Saidur, R., & Metselaar, I. H. S. C. (2014). Performance investigation of thermal energy storage system with phase change material (pcm) for solar water heating application. *International Communications in Heat and Mass Transfer*, *57*, 132–139. https://doi.org/10.1016/j.icheatmasstransfer.2014.07.022

Mao, Q. (2016). Recent developments in geometrical con fi gurations of thermal energy storage for concentrating solar power plant. *Renewable and Sustainable Energy Reviews*, *59*, 320–327. https://doi.org/10.1016/j.rser.2015.12.355

Medrano, M., Gil, A., Martorell, I., Potau, X., & Cabeza, L. F. (2010). State of the art on high-temperature thermal energy storage for power generation. *Part 2 — Case studies*. *14*, 56–72. https://doi.org/10.1016/j.rser.2009.07.036

Mekhilef, S., Saidur, R., & Safari, A. (2011). A review on solar energy use in industries. *Renewable and Sustainable Energy Reviews*, *15*(4), 1777–1790. https://doi.org/10.1016/j.rser.2010.12.018

Mondal, M. A. H., Bryan, E., Ringler, C., Mekonnen, D., & Rosegrant, M. (2018). Ethiopian energy status and demand scenarios: Prospects to improve energy efficiency and mitigate GHG emissions. *Energy*, *149*, 161–172. https://doi.org/10.1016/j.energy.2018.02.067

Morrison, D. J. (1978). *Liquid-based solar heating systems*. *20*.

Mosaffa, A. H., Talati, F., Tabrizi, H. B., & Rosen, M. A. (2012). Analytical modeling of PCM solidification in a shell and tube finned thermal storage for air conditioning systems. *Energy & Buildings*, *49*, 356–361.

https://doi.org/10.1016/j.enbuild.2012.02.053

Nallusamy, N., Sampath, S., & Velraj, R. (2006). Study on performance of a packed bed latent heat thermal energy storage unit integrated with solar water heating system. *7*(8), 1422–1430. https://doi.org/10.1631/jzus.2006.A1422

Niyas, H., Prasad, S., & Muthukumar, P. (2017). Performance investigation of a lab – scale latent heat storage prototype – Numerical results. *Energy Conversion and Management*, *135*, 188–199. https://doi.org/10.1016/j.enconman.2016.12.075

Odeh, S. D., Morrison, G. L., & Behnia, M. (1998). Modelling of parabolic trough direct steam generation solar collectors. *62*(6), 395–406.

Pielichowska, K., & Pielichowski, K. (2014). Progress in materials science. *Journal of progress in materials science*, *65*, 67–123. https://doi.org/10.1016/j.pmatsci.2014.03.005

Pinel, P., Cruickshank, C. A., Beausoleil-Morrison, I., & Wills, A. (2011). A review of available methods for seasonal storage of solar thermal energy in residential applications. *Renewable and Sustainable Energy Reviews*, *15*(7), 3341–3359. https://doi.org/10.1016/j.rser.2011.04.013

Prasad, L., & Muthukumar, P. (2013). Design and optimization of lab-scale sensible heat storage prototype for solar thermal power plant application. *Solar Energy*, *97*, 217–229. https://doi.org/10.1016/j.solener.2013.08.022

Qi, Q., Jiang, Y., & Deng, S. (2008). A simulation study on solar energy seasonal storage by phase change material. 106–109.

Rangababu, J. A., Kiran Kumar, K., & Srinivasa Rao, S. (2015). Numerical Analysis and Validation of Heat Transfer Mechanism of Flat Plate Collectors. *Procedia Engineering*, *127*, 63–70. https://doi.org/10.1016/j.proeng.2015.11.331

Rathod, M. K., & Banerjee, J. (2014). Experimental investigations on latent heat storage unit using paraffin wax as phase change material. *Experimental Heat Transfer*, *27*(1), 40–55. https://doi.org/10.1080/08916152.2012.719065

Reicosky, D. C., Winkelman, L. J., Baker, J. M., & Baker, D. G. (1989). Accuracy of hourly air temperatures calculated from daily minima and maxima. *Agricultural and Forest Meteorology*, *46*(3), 193–209. https://doi.org/10.1016/0168-1923(89)90064-6

Salomoni, V. A., Majorana, C. E., Giannuzzi, G. M., Miliozzi, A., Di Maggio, R., Girardi, F., Mele, D., & Lucentini, M. (2014). Thermal storage of sensible heat using concrete modules in solar power plants. *Solar Energy*, *103*, 303–315. https://doi.org/10.1016/j.solener.2014.02.022

Sarbu, I., & Sebarchievici, C. (2018). A comprehensive review of thermal energy storage. *Sustainability (Switzerland)*, *10*(1). https://doi.org/10.3390/su10010191

Seddegh, S., Wang, X., Joybari, M. M., & Haghighat, F. (2017). Investigation of the effect of geometric and operating parameters on thermal behavior of vertical shell-and-tube latent heat energy storage systems. *Energy*, *137*, 69–82. https://doi.org/10.1016/j.energy.2017.07.014

Shabgard, H., Bergman, T. L., Sharifi, N., & Faghri, A. (2010). High temperature latent heat thermal energy storage using heat pipes. *International Journal of Heat and Mass Transfer*, *53*(15–16), 2979–2988. https://doi.org/10.1016/j.ijheatmasstransfer.2010.03.035

Shamsundar, N. Stein E., Rooz E., Bascaran E., L. T. C. (1992). Design and simulation of latent heat storage units. *Final reports.Texas: National renewable energy labratory.University of Houston*.

Sharma, Kitano, H., & Sagara, K. (2004). Phase change materials for low temperature solar thermal applications. *29*, 31–64.

Sharma, S. D., Sagara, K., & Sharma, S. D. (2005). International journal of green energy latent heat storage materials and systems : *A Review*. *June 2013*, 37–41. https://doi.org/10.1081/GE-200051299

Sharma, Tyagi, V. V., Chen, C. R., & Buddhi, D. (2009). Review on thermal energy storage with phase change materials and applications. *Renewable and Sustainable Energy*

Reviews, *13*(2), 318–345. https://doi.org/10.1016/j.rser.2007.10.005

Singh, S., & Sørensen, K. (2017). Concrete thermal energy storage for steam generation: A numerical investigation. *Proceedings of the 58th Conference on Simulation and Modelling (SIMS 58) Reykjavik, Iceland, September 25th – 27th, 2017*, *138*, 234–240. https://doi.org/10.3384/ecp17138234

Stutz, B., Le, N., Kuznik, F., Johannes, K., Palomo, E., Barrio, D., Bédécarrats, J., Gibout, S., Marty, P., Zalewski, L., Soto, J., Mazet, N., Olives, R., Bezian, J., & Pham, D. (2017). Comptes Rendus Physique Storage of thermal solar energy Stockage thermique de l ’ énergie solaire. *Comptes Rendus Physique*, *18*(7–8), 401–414. https://doi.org/10.1016/j.crhy.2017.09.008

Tagliafico, L. A., Scarpa, F., & De Rosa, M. (2014). Dynamic thermal models and CFD analysis for flat-plate thermal solar collectors - A review. *Renewable and Sustainable Energy Reviews*, *30*, 526–537. https://doi.org/10.1016/j.rser.2013.10.023

Tamme, R., Laing, D., & Steinmann, W. (2003). Advanced thermal energy storage technology for parabolic trough. *March*, 15–18.

Tehrani, S. S. M., Taylor, R. A., Saberi, P., & Diarce, G. (2016). Design and feasibility of high temperature shell and tube latent heat thermal energy storage system for solar thermal power plants. *Renewable Energy*, *96*, 120–136. https://doi.org/10.1016/j.renene.2016.04.036

Tesfay, A. H., Kahsay, M. B., & Nydal, O. J. (2014). Solar powered heat storage for Injera baking in Ethiopia. *Energy Procedia*, *57*, 1603–1612. https://doi.org/10.1016/j.egypro.2014.10.152

Tesfay, M., & Venkatesan, M. (2013). Simulation of thermocline thermal energy storage system using C. *3*(2), 354–364.

Theses, G., Vasquez Padilla, R., & Padilla, V. (2011). Simplified methodology for designing parabolic trough solar power plants. *Scholar Commons Citation*. 1. http://scholarcommons.usf.edu/etdhttp://scholarcommons.usf.edu/etd/3390

Tian, Y., & Zhao, C. Y. (2013). A review of solar collectors and thermal energy storage in solar thermal applications. *Applied Energy*, *104*, 538–553. https://doi.org/10.1016/J.APENERGY.2012.11.051

Tiwari, G. N. (2018). Handbook of solar energy: theory, analysis and applications. https://doi.org/10.1017/S0021859616000721

Trp, A. (2005). An experimental and numerical investigation of heat transfer during technical grade paraffin melting and solidification in a shell-and-tube latent thermal energy storage unit. *79*, 648–660. https://doi.org/10.1016/j.solener.2005.03.006

Velraj, R., Seeniraj, R.V., Hafner, B., Faber, C., Schwarzer, K. (1997). Experimental analysis and numerical modeling of inward solidification on a finned vertical tube for a latent heat storage unit. *November*, 97105006.

Venkatachalam, C., Samuel, G., & Solomon, G. (2019). Data in brief Dataset of solar energy potential assessment for Adama city (Ethiopia). *Data in Brief*, *24*, 103879. https://doi.org/10.1016/j.dib.2019.103879

Vyshak, N. R., & Jilani, G. (2007). Numerical analysis of latent heat thermal energy storage system. *Energy Conversion and Management*, *48*(7), 2161–2168. https://doi.org/10.1016/j.enconman.2006.12.013

Wang. (2006). Experimental research on a kind of novel high temperature phase change storage heater. *Energy Conversion and Management*, *47*(15–16), 2211–2222. https://doi.org/10.1016/j.enconman.2005.12.004

Wang, W. W., Zhang, K., Wang, L. B., & He, Y. L. (2013). Numerical study of the heat charging and discharging characteristics of a shell-and-tube phase change heat storage unit. *Applied Thermal Engineering*, *58*(1–2), 542–553. https://doi.org/10.1016/j.applthermaleng.2013.04.063

Wei, G., Wang, G., Xu, C., Ju, X., Xing, L., Du, X., & Yang, Y. (2018). Selection principles and thermophysical properties of high temperature phase change materials for thermal energy storage: A review. *Renewable and Sustainable Energy Reviews*, *81*(March 2016), 1771–1786. https://doi.org/10.1016/j.rser.2017.05.271

Wu, Z. G., & Zhao, C. Y. (2011). Experimental investigations of porous materials in high temperature thermal energy storage systems. *Solar Energy*, *85*(7), 1371–1380. https://doi.org/10.1016/j.solener.2011.03.021

Xue, H. S. (2016). Experimental investigation of a domestic solar water heater with solar collector coupled phase-change energy storage. *Renewable Energy*, *86*, 257–261. https://doi.org/10.1016/j.renene.2015.08.017

Yayeh, M. (2013). Addis Ababa Institute of Technology Integration of scheffler concentrator and thermal storage device for indoor injera baking. *Masters Thesis*, *April*, 1–91.

Zalba, B., Marın, J. M., Cabeza, L. F., & Mehling, H. (2003). Review on thermal energy storage with phasechange: materials, heat transfer analysis and applications. In *Applied Thermal Engineering 23 (2003)* (Vol. 704). https://doi.org/10.1017/jfm.2012.219

Zivkovic, B., & Fujii, I. (2001). Analysis of isothermal phase change of phase change material within rectangular and cylindrical containers. *Solar Energy*, *70*(1), 51–61. https://doi.org/10.1016/S0038-092X(00)00112-2

APPENDICES

ANNEX A: Specification of flat plate collector

According to SUNRAIN Company the detailed specification of flat plate collector (FPC1200A) model product used in this study are given in Table A1:

Table A1 Specification of flat plate collector

Description	Specification
Collector type	Sheet- and- tube type
Housing	Aluminum - alloy
Surface	Aluminum - alloy
Black plate	Steel plate
Absorber plate	Cu/Al
Glass	Woven ultra-white toughened
Insulation	Glass wool
HTF	Water
Length of the collector (m)	2.005
Width of the collector (m)	1.005
Length of the absorber plate (m)	1.9
Width of the absorber plate (m)	0.92
Overall area (m^2)	2.02
Absorber area (m^2)	1.745
Aperture area (m^2)	1.96
Plate thickness (m)	0.001
Tube center to center distance (m)	0.092
Number of glass	1
Air gap between glass and the plate (m)	0.025
Thickness of the glass (m)	0.003
Diameter of header plate (mm)	Ø 22 x 0.75
Diameter of the riser plate (mm)	Ø 10 x 0.5
Thickness of the insulation material (m)	0.05
Thermal conductivity of the insulation material (W/mK)	0.044

Thermal conductivity of absorber plate (W/mK)	386
Density of the insulation material (kg/m^3)	200
Density of absorber plate (kg/m^3)	8954
Max. Stagnation temperature (℃)	250
Max. Operating pressure (MPa)	1.2
Rated operating pressure (MPa)	0.8
Emittance of absorber plate	0.95
Emittance of glass	0.86
Transmittance of glass (%)	≥ 91
Absorption of the absorber (%)	94

ANNEX-B: Specification of parabolic trough collectors (PTC)

The detailed specification of parabolic trough collectors (PTC) used for steam power plant is given below Table B1**(Kalogirou, 1996)**:

Table B1 Specification of parabolic trough collectors (PTC)

Description	**Specification**
Collector type	PTC
Aperture area (m^2)	7
Collector aperture (m)	1.46
Aperture – to – length ratio	0.64
Glass - to- receiver diameter ratio	2.17
Rim angle (°)	90
Receiver diameter (mm)	22
Geometric concentration ratio	21.2
Peak optical efficiency	0.71

ANNEX C: Design procedure of shell and tube heat storage

The design of the shell and tube heat thermal energy storage system was done based on the procedure proposed by **(Shamsundar *et al.*, 1992)**. The first step in the design process is selecting the storage material with the required melting temperature. The effectiveness is then estimated at the start of the discharging period since the outlet temperature of the storage is higher at this stage than at any other time whereas at the latter instant of time there will be a buildup of solid which impedes heat transfer. For a shell and tube thermal energy storage, effectiveness is defined as the ratio of the actual heat transfer to the heat transfer corresponding to not only infinite area but also infinite conductance in the storage material.

$$\varepsilon = \frac{T_f - T_i}{T_m - T_i} \qquad \text{C.1}$$

where: T_f and T_i are the outlet and inlet temperatures of air, respectively.

The number of transfer units (NTU) was expressed as:

$$\varepsilon_{max} = 1 - \exp\left(-NTU\right) \qquad \text{C.2}$$

Take the minimum and maximum temperatures required for fulfilling energy demand of hot water are 45℃ and 50℃, respectively. Substituting the values of T_{dmax} = 50°C, T_{dmin}=45°C, T_i=25°C and T_m=54°C into Eqn. B.1 gives ε_{max}=0.76, ε_{min}= 0.61 and NTU = 1.43.

Parameter γ and Biot number B_i as a function of the inner and outer radius of the heat exchanger tubes, respectively, was determined as:

$$\gamma = \frac{hR_i}{k_m} \qquad \text{C.3}$$

$$B_i = \frac{hR_o}{k_m} \qquad \text{C.4}$$

where: h is convective heat transfer coefficient, R_o and R_i are outer and inner radius of the heat exchanger tubes, respectively,k_s is thermal conductivity of the storage material.

To estimate parameter (γ), the Nusselt number (Nu) should be first estimated depending upon the type of flow regime in the tube being either laminar or turbulent. If the fluid flow inside the tubes is considered as laminar and fully developed, the recommended assumption for Nu is

1.84. Nusselt number (Nu) is the ratio of convective to conductive heat transfer across the boundary.

$$N_u = \frac{hR_o}{k_a} \qquad \text{C.5}$$

where: k_f is the thermal conductivity of HTF.

Parameter γ can be written as $\gamma = N_u \left(\frac{k_f}{k_s}\right)\left(\frac{R_i}{R_o}\right)$ C.6

Substituting the values of k_f= 0.58W/m. K, $k_s = 0.21$W/m. K and $N_u = 1.84$ into Eqn. C.6 gives $\gamma = 0.37$.

The outer radius of the tubes was determined as:

$$R_o = \left(\frac{k_s t(T_m - T_i)}{\tau_o \rho_p L_F}\right)^{0.5} \qquad \text{C.7}$$

where: τ_o is the nondimensional time variable which was expressed as:

$$\tau_o = \left(\frac{F_o}{2\beta}\right) + \frac{1}{4}\left[(1 + F_o)\ln(1 + F_o) - F_o\right] \qquad \text{C.8}$$

F_o is the amount of PCM solidified at the tube inlet at the end of the discharge period and its value is usually between 0 and 10 for latent heat storage case. Substituting the values of $F_o =$ 5.9 and $\gamma = 0.37$ into Eqn. E.8 gives $\tau_o = 9.83$ and $R_o = 9$mm and, taking the ratio of the inner and outer radius of the tubes as 1.2, $R_i = 7.5$mm.

The number of tubes was determined from the length of the pipe as:

$$n_t = \left(\frac{NTU\dot{m}_f C_{pf}}{2\pi h R_i L}\right) \qquad \text{C.9}$$

h is the heat transfer coefficient of the air: $h = \frac{k_f Nu}{R_o}$ C.10

Substituting the values of Nu = 1.84, k_f=0.58W/m.K, $\dot{m}_f$=0.0041kg/s, C_{pf}=4.18kJ/kg.K, R_i= 7.5mm and R_o=9mm into Eqn. C.9 and C.10 gives n_t=5.